Antiproliferative Effects of 15-Lipoxygenase Metabolites on Chronic Myeloid Leukemia Cell Line - K-562: Studies on Molecular Mechanisms

Thesis submitted for the degree of

DOCTOR OF PHILOSOPHY

by

S. VIJAYA KUMAR MAHIPAL

Department of Animal Sciences
School of Life Sciences
University of Hyderabad
Hyderabad-500 046, INDIA

August, 2005
Enrolment No. 2KLAPH02


Dedicated
to
Lord Shiva
and
Peddamma & Pedananna

University of Hyderabad
(A Central University established in 1974 by Act of Parliament)
HYDERABAD – 500 046, INDIA

DECLARATION

I hereby declare that the work embodied in this thesis entitled "***Antiproliferative Effects of 15-Lipoxygenase Metabolites on Chronic Myeloid Leukemia Cell Line - K-562: Studies on Molecular Mechanisms"*** has been carried out by me under the supervision of Prof. P. Reddanna and this has not been submitted for any degree or diploma of any other University earlier.

Prof. P. Reddanna
(Research Supervisor)

S. Vijaya Kumar Mahipal
(Research Scholar)

University of Hyderabad
(Central University established in 1974 by Act of Parliament)
HYDERABAD – 500 046, INDIA

CERTIFICATE

This is to certify that ***Mr. S. Vijaya Kumar Mahipal*** has carried out the research work embodied in the present thesis under my supervision and guidance for a full period prescribed under the Ph. D. ordinance of this University. We recommend his thesis "***Antiproliferative Effects of 15-Lipoxygenase Metabolites on Chronic Myeloid Leukemia Cell Line - K-562: Studies on Molecular Mechanisms***" for submission for the degree of Doctor of Philosophy of this University**.**

Prof. P. Reddanna _____
Supervisor

Head _____
Department of Animal Sciences

Dean _____
School of Life Sciences

Acknowledgements

I express my deepest sense of gratitude to my mentor, ***Prof P. Reddanna*** *for giving me an opportunity to work under his able guidance, providing the lab facilities and constant support through out my work. It gives me immense pleasure to admit that Prof.P.Reddanna, a man of integrity, patience and perseverance has been a constant source of inspiration throughout my doctoral discourse.*

Words fail to express my gratitude and heartfelt indebtedness both on personal and professional fronts to ***Prof. Aparna Dutta Gupta****, Head, Department of Animal Sciences for her encouragement and the moral support she gave me throughout my research work.*

I would like to thank members of doctoral committee, late. ***Prof. Radha Krishna Murthy****,* ***Prof. Aparna Dutta Gupta*** *and* ***Dr. Manjula Sritharan*** *for their valuable suggestions and guidance. My special thanks to Prof. Appa Rao Podile for all his support and personal rapport I had shared with him through out and the faculty members of school of life sciences who taught us during our post graduation and also extended their support during my thesis work.*

I would like to thank the ***Prof. Aparna Dutta Gupta,*** *Head, Department of Animal Sciences and the* ***Prof. A. S. Raghavendra****, Dean, School of Life Sciences for providing the necessary facilities for the research work.*

My heartfelt thanks to Dr. Madhava Reddy and Dr. Subhashini, senior colleagues in the labs, whose help and encouragement were instrumental in carrying out my thesis work.

My special thanks to senior colleagues, Dr. G. V. Reddy, Dr. Sreenivas Reddy, Dr. Maya and Dr. Sunitha for their help and support.

I wish to thank friendly and cooperative lab mates Aparna, Sreekanth, Roy, Sreedevi, Anil, Bharat, Smitha, Arunasree, Ramakrishna, Chandramohan Reddy,

Nishanth and Satya Sai Kumar for their help and creating cheerful work atmosphere.

I thank all my teachers since my childhood whose guidance and encouragement at each step was instrumental in shaping my career.

I fall short of words to thank my best friends, Ramakrishna Reddy, Sudheer, Ravi, Mallikarjun Reddy and Shiva Ram for being there with me althrough and for their help and encouragement. I wish them all success and happiness in their lives.

I would like to thank my seniors and close friends Pavan, Vijaya Bhasker Reddy, Sadanand and Dr. Haffiz for their concern and encouragement.

I thank all my friends Apparao, Sudar, Sravan, Sadanand, Vijayanthi, Sireesha, Madan, Padmaja, Sunil for their timely help and support.

I thank Ms. Akhila, Suresh, Ajay from Dr. Reddy's Research Foundation and Krishnaveni and Abira from CDFD for their timely help.

I am gratified by the tremendous and instantaneous help offered by Mr. Shiva Kumar. Assistance from the non-teaching staff of school of life sciences, Mr. Jagan, Mr Ankineedu garu, Mr. Joseph and Mr. Gopi and lab assistants Mr. Nagesh and Mr. Balram is greatly appreciated.

I acknowledge HBL-NIFE Systems Pvt Ltd, Hyderabad and CSIR, New Delhi for the financial assistance.

I thank my dad, grandmother, aunts, uncles for their blessings and affection and I also thank my brothers Kalyan, Vijay and Rajeev for their love and support.

Finally, I express my gratitude to the almighty and my mother for their celestial blessings, providing me the moral strength to lead the life against all odds and I owe all my success to them.

CONTENTS

LIST OF FIGURES

Abbreviations

AA	:	arachidonic acid
Ac-DEVD-AFC	:	N-acetyl-(Asp-Glu-Val-Asp)-trifluoromethylcoumarin
AP-1	:	activator protein-1
COX	:	cyclooxygenase
DAPI	:	4', 6-diamidino-2-phenylindole
DCFH-DA	:	2', 7'-Dichlorofluorescein Diacetate
DPI	:	diphenylene iodonium
EDTA	:	ethylene diamine tetra acetic acid
FACS	:	fluorescence activated cell sorter
FBS	:	fetal bovine serum
g	:	gram
h	:	hour(s)
HPLC	:	high-performance liquid chromatography
13-(*S*)-HODE	:	13-(*S*)-hydroxyoctadecadienoic acid
13-(*S*)-HPODE	:	13-(*S*)-hydroperoxyoctadecadienoic acid
15-(*S*)-HETE	:	15-(*S*)-hydroxyeicosatetraenoic acid
15-(*S*)-HPETE	:	15-(*S*)-hydroperoxyeicosatetraenoic acid
kDa	:	kilodalton
l	:	litre
LA	:	linoleic acid
LC-MS	:	liquid chromatography-mass spectrometry
L-NMMA	:	N^G-Monomethyl-L-arginine
LOX	:	lipoxygenase
mg	:	milligram
min	:	minutes
ml	:	milliliter
mM	:	millimolar
MTT	:	[3-(4, 5-dimethylthiazol-2-yl)-2, 5-diphenyl tetrazolium bromide]
NAC	:	N-acetyl cysteine
-κB	:	nuclear factor-kappa B
nm	:	nanometers
NSAIDs	:	non-steroidal anti-inflammatory drugs
PAGE	:	polyacrylamide gel electrophoresis
PARP	:	poly (ADP) ribose polymerase
PBS	:	phosphate buffered saline
PI	:	propidium iodide
Tris	:	tris-(Hydroxymethyl) aminoethane
UV	:	ultraviolet
µM	:	micro molar
^{0}C	:	degree centigrade/ degree celsius

Introduction

Introduction

1.1. Arachidonic acid metabolism

Arachidonic acid (AA), (5Z, 8Z, 11Z, 14Z- eicosa-5, 8, 11, 14-tetraenoic acid), a polyunsaturated fatty acid (PUFA) is found *in vivo* esterified to cell membrane glycerophospholipids. Activation of phospholipases, like cytosolic phospholipases-A_2, releases free AA from the phospholipid pools and makes it available for oxidative metabolism by three distinct enzymatic pathways. The three major metabolic enzymatic pathways involve the isoforms of cyclooxygenase (COX), lipoxygenase (LOX) and monooxygenase cytochrome P450 (CYP) and additional pathways (Fig. 1) that inactivate and remove eicosanoids (oxygenated metabolites of arachidonic

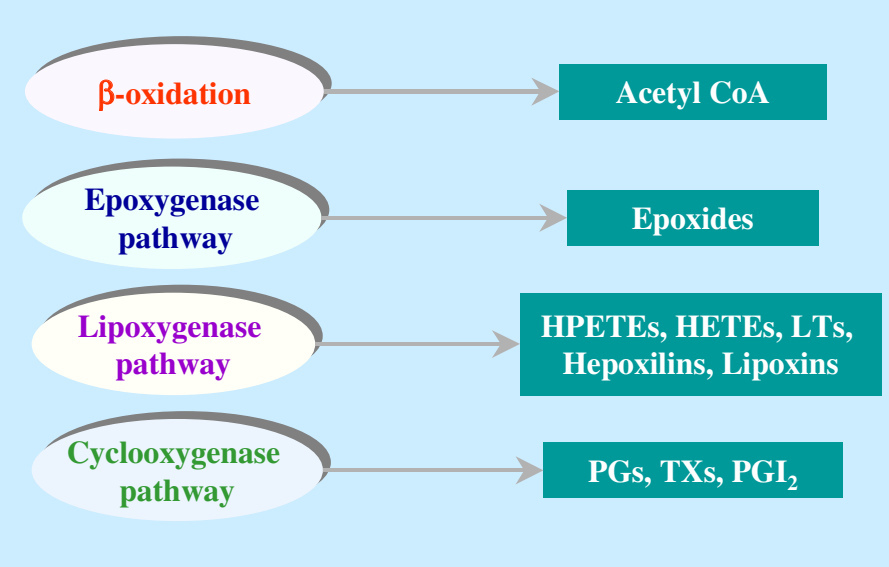

Fig. 1. Arachidonic acid metabolism

acid) to terminate their function of signal mediators. The COXs metabolize AA to prostaglandin H_2 (PGH_2), which serves as the precursor of prostaglandins, thromboxanes and prostacyclin (Smith et al., 1996). The LOXs convert AA to labile hydroperoxy intermediates that go on to form the

hydroxyeicosatetraenoic acids (HETEs), leukotrienes, and lipoxins (Brash, 1999). The eicosanoid derivatives of COXs and LOXs have been shown to play important functional roles in a variety of fundamental biological processes such as inflammation, cellular proliferation and intracellular signaling. Cytochrome P450s metabolize AA to *cis*-epoxyeicosatrienoic acids (14,15-, 11,12-, 8,9-, and 5,6-EETs), which can be formed as either the *R, S* or the *S, R* enantiomers. EETs derived through cytochrome P450 have been shown to have potent effects such as peptide hormone secretion, vascular and bronchial smooth muscle tone, and ionic transport (Zeldin, 2001).

1.2. Lipoxygenases

Lipoxygenases (linoleate: oxygen oxido reductase, EC 1.13.11.12) are a group of closely related non-heme iron containing dioxygenases. These enzymes catalyze the addition of molecular oxygen into polyunsaturated fatty acids (PUFAs) containing cis, cis 1-4 pentadiene structures to give their hydroperoxy derivatives.

1.2.1. Occurrence

Lipoxygenases (LOXs) are essentially ubiquitous among eukaryotic organisms and have been demonstrated to exist in many tissues of numerous fungi, higher plants and animals (Gerwick, 1994; De Petrocellis and Di Marzo 1994; Funk, 1996; Yamamoto et al., 1997; Grechkin, 1998). Polyunsaturated fatty acids containing a series of *cis* double bonds act as suitable substrates for LOXs. Linoleic and α-linolenic fatty acids, present mostly in vegetable oils, are essential fatty acids in humans. These substrates are not present in most bacteria (except for cyanobacteria and some marine species (Gerwick and

Bernart, 1993; Watanabe et al., 1997). Yeast and insects, in general do not contain LOXs but arachidonic acid-derived LOX product, hydroxyeicosatetraenoic acid (HETE), was found in a primitive insect *Thermobia domestica* (Ragab et al., 1991). Higher plants and animals contain

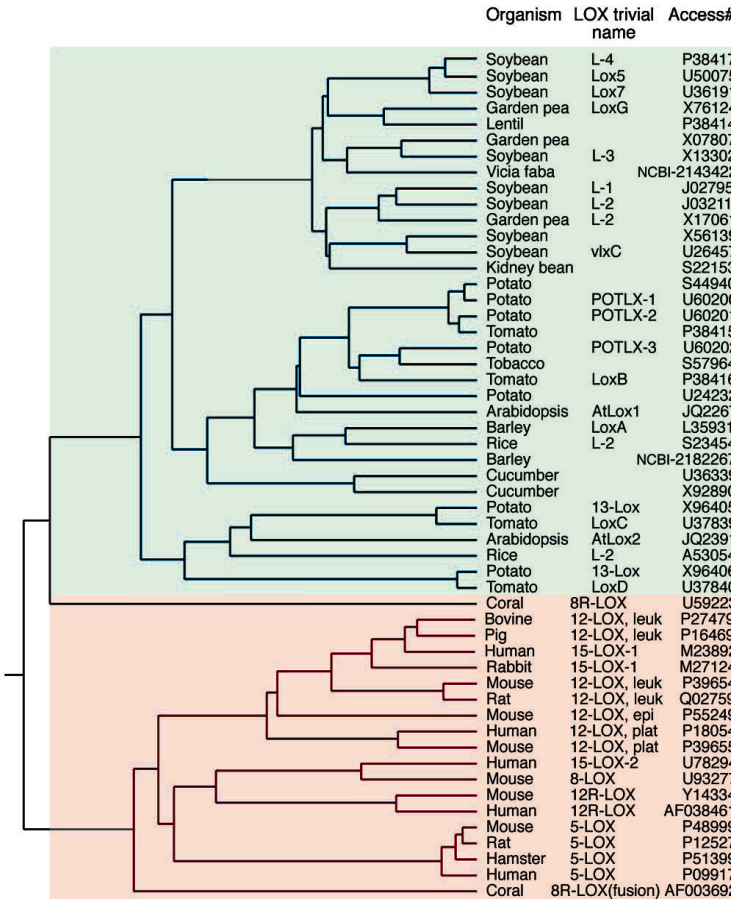

Fig. 2. Lipoxygenase phylogenetic tree
(*Source: Brash, A. R. (1999). J. Biol. Com., 274: 23679 – 23682*)

multiple LOXs with atleast eight identified in soybean, *Glycine max*, seven in mouse and five homologues are characterized in humans (Zimmerman and Vick, 1973; Krieg et al., 1998; Boeglin et al., 1998). High levels of LOX expression is observed in few plant and animal tissues, they constitute a major portion of the proteins in soybeans, and 15-lipoxygenase (15-LOX) represents one of the main proteins in rabbit reticulocytes during anemia (Sun et al.,

1998). The phylogenetic tree separates the plant and animal enzymes and forms several subgroups within each kingdom (Fig. 2). The formation of a particular LOX product is not necessarily associated with closely related sequences. For example, the soybean L-1 enzyme, a 15-LOX, has only 25% identity to any mammalian 15-LOX, and the two human 15-LOXs share only 35% identity with each other. By contrast, the close functional homologues across species, forming distinct subgroups, share 70–95% sequence identity.

1.2.2. Classification and Nomenclature

Lipoxygenases (LOXs) are classified according to their positional specificity of arachidonate oxygenation (Rapoport et al., 1979). 15-LOXs introduce molecular oxygen at carbon atom-15 of arachidonic acid where as 12-LOXs oxygenate the same substrate at C-12. Depending on their site of oxygen insertion on arachidonic acid (AA), these enzymes are designated as 5-, 8-, 9-, 11-, 12- and 15-LOXs. The prominent animal LOXs are 5-LOX, 8- LOX, 12-LOX and 15-LOX, while the plant LOXs are mostly 5-LOX and 15-LOX. The differing chain lengths of the most common substrates of plants (linoleate, linolenate, 18-carbon) and animals (arachidonate, 20-carbon) result in a plant 13-LOX corresponding to a mammalian 15-LOX; these LOXs "count" the substrate carbons from the tail end of the chain, and oxygenate at the ω-6 position. Things become more complex with the presence of more than one LOX, like 12-LOX, in the same species. The different types of mammalian 12-LOXs are hence named after the prototypical tissues of their occurrence (the platelet, leukocyte, or epidermal types of 12-LOXs) (Yamamoto et al., 1997). These are distinct enzymes by sequence, catalytic

activities, and function. LOXs (plant and animal), in general, form products with *S* stereochemistry. However, LOXs forming the mirror image *R* configuration products are also found among aquatic invertebrates (De Petrocellis and Di Marzo, 1994), plants (Gerwick, 1994), and recently in humans (Boeglin et al., 1998). *R*-LOXs contain the same conserved iron ligands and other sequence motifs common to plant or animal *S*-LOXs (Brash et al., 1996).

1.2.3. Enzyme Structure

Lipoxygenase proteins have a single polypeptide chain with a molecular mass of 75-80 kDa in animals and 94-104 kDa in plants. The proteins have an N-terminal β-barrel domain and a larger catalytic domain containing a single atom of non-heme iron (Fig. 3). The metal is liganded to conserved histidines and to the carboxyl group of a conserved isoleucine at the C-terminus of the protein. The enzymes are usually in the ferrous (inactive) form when isolated. Oxidation to the active ferric enzyme is required for catalysis. There are four available crystal structures, of which three are of the arachidonate 15-LOXs, soybean L-1, and rabbit reticulocyte 15-LOX (Boyington et al., 1993; Minor et al., 1996; Gillmor et al., 1997), and the fourth, soybean L-3, is a catalyst of nonspecific peroxidation (Skryzypczak-Jankun et al., 1997).

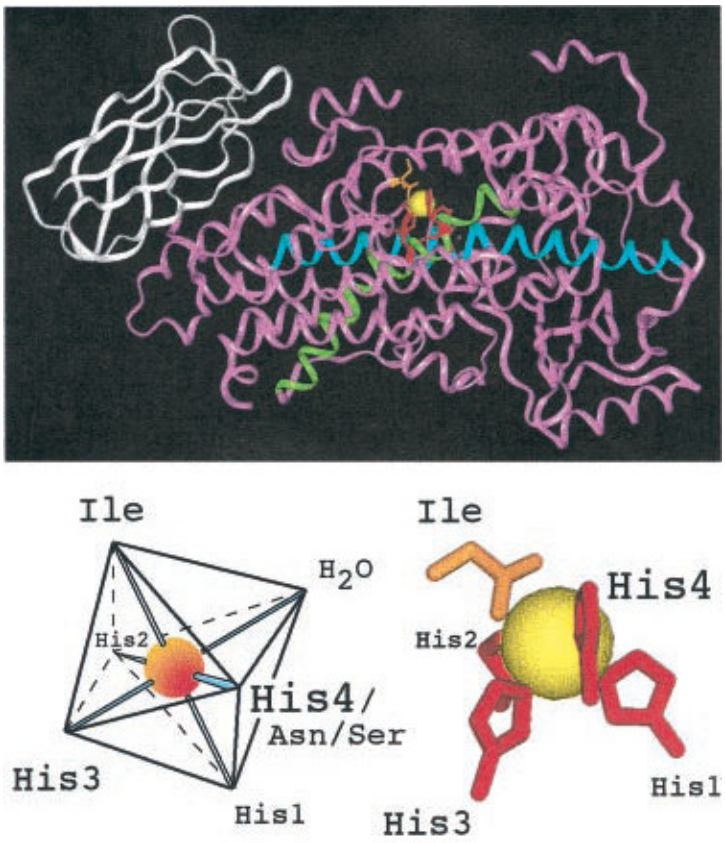

Fig. 3. Lipoxygenase crystal structure
(*Source: Brash, A. R. (1999). J. Biol. Com., 274: 23679 – 23682*)

1.2.4. The mechanism of the lipoxygenase reaction

In principle, the LOX reaction consists of three consecutive steps and all of them are stereochemically controlled (Fig. 4). 1). *Hydrogen abstraction*: The first step is hydrogen abstraction from a bis-allylic methylene to form a pentadienyl radical; this step is rate limiting for the overall LOX reaction (Rickert and Klinman, 1999). The LOXs select one of the bis-allylic methylenes from polyunsaturated fatty acids for hydrogen removal (regioselectivity) and also select either the pro-R or the pro-S hydrogen (enantioselectivity). 2) *Radical rearrangement*: In the second step, the pentadienyl radical is rearranged by electron redistribution either in the

direction of the methyl terminus ([+2]-rearrangement) or in the direction of the carboxyl terminus ([-2]-rearrangement) of the fatty acid. The positional specificity of the overall reaction depends on both the regiospecificity of

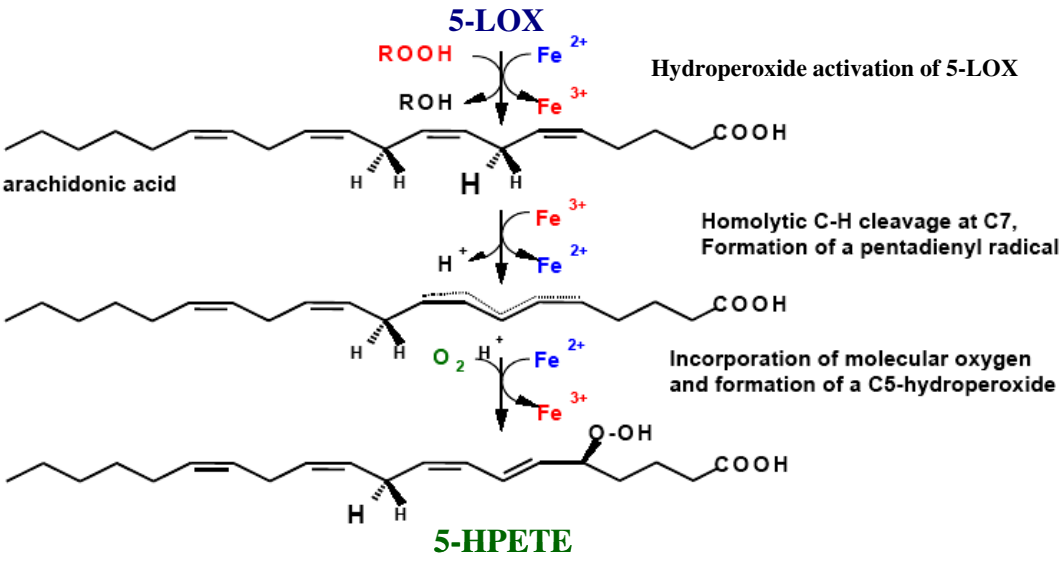

Fig. 4. Mechanism of lipoxygenase reaction

hydrogen removal and the direction of radical rearrangement (Kuhn et al., 1986). 3) *Oxygen insertion*: Molecular oxygen is introduced at either C-1 or C-4 of the rearranged pentadienyl radical system. This creates a new chiral center whose configuration (S- or R-) depends on the specificity of the LOX. For all LOXs investigated so far, hydrogen abstraction and oxygen insertion proceed in an antarafacial manner, meaning that hydrogen abstraction and oxygen insertion occur on opposite faces of the plane of the double bonds (Egmond et al., 1973; Maas and Brash, 1983).

1.3. 5-Lipoxygenase

The 5-LOX pathway is the source of potent pro-inflammatory mediators. The 5-LOX pathway is one of at least four LOX pathways of arachidonic acid metabolism (Brash, 1999) (Fig. 5). 5-LOX has been purified from various

leukocytes as monomers with estimated MWs between 72 kDa and 80 kDa. Mammalian 5-LOX cDNAs have been cloned from man, rat, mouse and

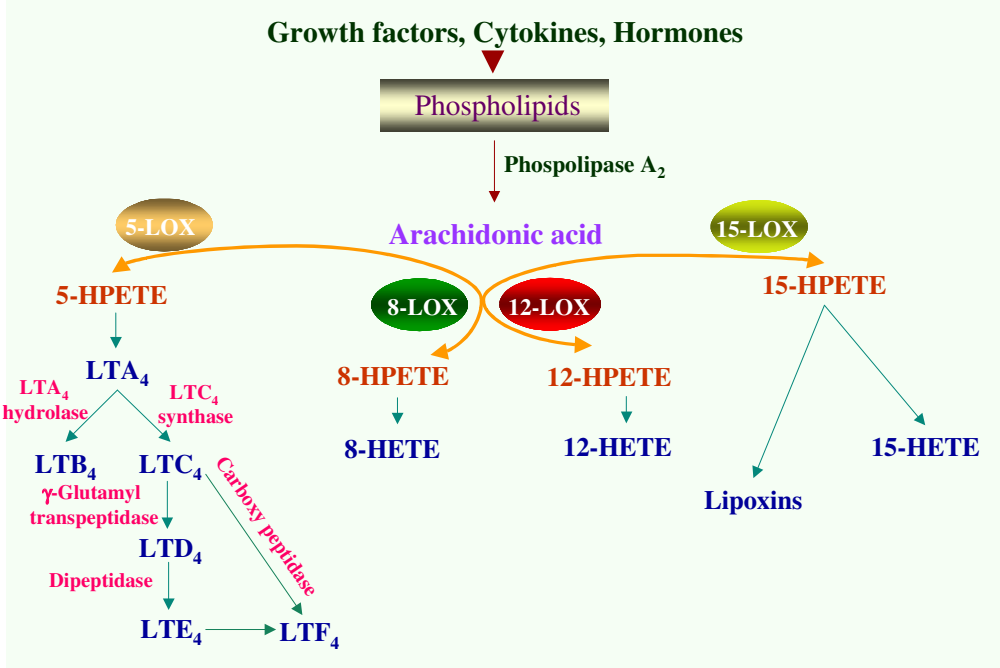

Fig. 5. Lipoxygenase pathways

hamster and the deduced amino acid sequences contain 672 or 673 amino acids with more than 90% identity (Prigge et al., 1996; Radmark, 2002). Northern blot of human RNAs showed a 2.7-kb species in extracts from human leukocytes, lung and placenta. In human brain tumors, a variety of 5-LOX transcripts of different sizes (2.7–8.6 kb) were found (Boado et al., 1992). The 5-LOX acts preferentially upon unesterified arachidonic acid, inserting molecular oxygen at the fifth carbon and forming the hydroperoxyl intermediate, 5-hydroperoxyeicosatetraenoic acid (Bigby et al., 1998; Funk, 2001). The same enzyme then catalyzes a dehydration reaction, forming the unstable epoxide intermediate, leukotriene LTA_4. In intact inflammatory cells, the presence of the 5-lipoxygenase activating protein (FLAP) is required to

make this enzyme active (Dixon et al., 1990). LTA_4 can then be further metabolized to LTB_4 by LTA_4 hydrolase or to LTC_4 by conjugation of glutathione at the sixth carbon by the action of LTC_4 synthase. Additional studies established that LTC_4 and its extracellular metabolites LTD_4 and LTE_4 are the constituents of slow-reacting substance of anaphylaxis, but they are now more properly termed cysteinyl leukotrienes. The cysteinyl leukotrienes have been recognized to mimic many of the clinical manifestations of asthma, including sustained bronchoconstriction, hypersecretion of mucus, and airway edema. LTE_4 gets further metabolized to inactive LTF_4 by the action of γ-glutamyl transpeptidase. Also LTF_4 was also shown to be found directly from LTC_4 by the action of carboxypeptidase (Reddanna et al., 2003) By contrast, LTB_4 induces chemotaxis, inflammatory cell stimulation, and a complex role in host defense, suggesting that it is a key component of the innate immune response (Bailie et al., 1996). The earliest investigations identified that 5-LOX activity was stimulated by calcium and ATP and requires phospholipids and also lipid hydroperoxide for conversion of inactive enzyme (ferrous form) to active enzyme (ferric form) for optimum activity (Samuelsson, 1983).

1.4. 8-Lipoxygenase

The recently identified mouse 8-LOX almost exclusively directs oxygen insertion into the 8(*S*) position of arachidonic acid and, with lower efficiency, into the 9(*S*) position of linoleic acid. The open reading frame of the 3.2 kb transcript encodes a protein of 677 amino acids with a calculated molecular weight of 76.23 kDa and a pI of 6.72 (Jisaka et al., 1997; Krieg et

al., 1998). The protein of 677 amino acids displays 78% sequence identity to human 15-LOX-2, which is considered to be its human orthologue (Brash et al., 1997). The 8-LOX gene, *Alox15b,* consisting of 14 exons and spanning 14.5 kb is located within a gene cluster of related epidermis-type LOXs at the central region of mouse chromosome 11. 8-LOX is predominantly expressed in stratifying epithelia of mice, constitutively in the hair follicle, forestomach, and footsole and inducible in the back skin with strain-dependent variations (Fürstenberger et al., 1991; Jisaka et al., 1997; Heidt et al., 2000). The expression is restricted to terminally differentiating keratinocytes, in particular the stratum granulosum and 8-LOX activity seems to be involved in terminal differentiation of mouse epidermis. Tumor-specific upregulation of 8-LOX expression and activity indicate a critical role of this enzyme in malignant progression during tumor development in mouse skin (Fischer et al., 1988; Nair et al., 2000). 8(*S*)-HETE is known to specifically bind to and activate the transcription factor peroxisome proliferator activator receptor-α (PPAR-α) and has indeed been shown to stimulate keratinocyte differentiation by inducing keratin 1 via a PPAR-α-dependent pathway (Muga et al., 2000; Yu et al., 1995).

1.5. 12-Lipoxygenase

The transformation of arachidonic acid to 12-(*S*)-hydroxy-5,8,10,14-eicosatetraenoic acid (12-(*S*)-HETE) was first demonstrated in human and bovine platelets (Hamberg and Samuelsson, 1974; Nugteren, 1975), and this was the first documented evidence of a LOX in the animal kingdom. There are three 12-(*S*)-LOX isoforms that are named after the cells where they were

originally discovered; platelet, leukocyte and epidermis (Yoshimoto and Takahashi, 2002). The open reading frames of cDNAs for the three isozymes predict 662 amino acids with molecular weights of approximately 75,000 Da. When the amino acid sequences of the murine enzymes are compared, the epidermal 12-(*S*)-LOX displays 60% identity with both platelet and leukocyte isozymes (Chen et al., 1994). At the genomic level, all of the 12-(*S*)-LOX genes have 14 exons and 13 introns that are organized in the same exon/intron format with boundaries in the same positions. The platelet-type 12-(*S*)-LOX gene (13–17 kb) is approximately twice the size of the genes for the other two isozymes (7.2–7.5 kb). All of the murine 12-(*S*)-LOX genes map to the central region of mouse chromosome 11 in a region of homology with human chromosome 17 (Funk, 1996). 12-(*S*)-LOX has been implicated in platelet activation, postsynaptic responses to histamine, and oxidation of low-density lipoprotein (LDL) leading to atherogenesis (Hamberg and Samuelsson, 1974; Yoshimoto and Takahashi, 2002). Recent studies revealed a critical role played by 12-(*S*)-HETE and 12-LOX in cancer growth and angiogenesis (Timar et al., 2000; Wong et al., 2001; Pidgeon et al., 2002). In addition to these findings patients with hypertension with sickle cell anemia were shown to have higher levels of platelet 12-LOX protein suggesting that 12-LOX-derived arachidonic acid metabolites may play a critical role in inflammation processes as well as blood vessel diseases (Yoshimoto and Takahashi, 2002).

1.6. 15-Lipoxygenase

15-LOX catalyzes the introduction of molecular oxygen at carbon 15 (C-15) of arachidonic acid resulting in the formation of

15-hydroperoxyeicosatetraenoic acid (15-(*S*)-HPETE). Two different 15-LOXs have been identified that differ in tissue distribution and substrate preference. 15-LOX-1 (reticulocyte-type) is expressed in reticulocytes, eosinophils, macrophages, tracheobronchial epithelial cells and skin (Funk, 1996). 15-LOX-2 (epidermis type) has limited tissue distribution with mRNA detected in prostate, lung, skin and cornea (Shappell et al., 1999). In terms of enzymatic characteristics, 15-LOX-1 preferentially metabolizes linoleic acid primarily to 13-hydroperoxyoctadecadienoic acid (13-(*S*)-HPODE), but also converts arachidonic acid to 15-(*S*)-HPETE. 15-LOX-2, on the other hand, converts arachidonic acid to 15-(*S*)-HPETE and metabolizes linoleic acid poorly (Brash et al., 1997).

1.6.1. Enzymatic properties of 15-LOX

As other LOXs, the reticulocyte-type 15-LOX is a single polypeptide (MW = 75 kDa) folded into a two-domain structure. It contains one non-heme iron per mole enzyme and four histidines (H361, H366, H541, H545) and the C-terminal isoleucine constituting the protein iron ligands. The reticulocyte-type 15-LOXs are characterized by a rather broad substrate specificity (Rapoport et al., 1979; Schewe et al., 1986). In addition to all major naturally occurring polyenoic fatty acids (such as arachidonic acid, eicosapentaenoic acid, linoleic acid and α-linolenic acid), ester lipids (phospholipids, cholesterol esters, mono-, di- and tri-acylglycerols) containing polyenoic fatty acids as well as more complex lipid–protein assemblies (biomembranes, lipoproteins) are all substrates for this isoform. The enzyme exhibits a dual positional specificity with arachidonic acid (Bryant et al., 1980) and undergoes

suicidal inactivation (Rapoport et al., 1984; Gan et al., 1995). The process of suicidal inactivation appears to be rather more complex and no single mechanism seems to give explanation in totality. The plausible molecular mechanisms include oxidation of a methionine residue to methionine sulfoxide at the active site by fatty acid hydroperoxide (Rapoport et al., 1984) or by covalent linkage of reaction intermediates similar to the observations made for porcine leukocyte-type 12-LOX (Kishimoto et al., 1996). However, mutation of oxidizable methionine to leucine didn't abrogate suicidal inactivation (Gan et al., 1995) and also suicidal inactivation of the enzyme occurred with linoleic acid as the substrate though there were no covalent linkages formed.

1.6.2. Regulation of cellular LOX activity

15-LOX expression and activity is strongly regulated (Kuhn et al., 1999) in various cell systems at transcriptional, translational and post-translational level.

1.6.2.1. Transcriptional regulation

In humans and rabbits elevated levels of 15-LOX expression is observed in reticulocytes, peripheral monocytes, lung, spleen, kidney, and liver during the time course of experimental anemia. The mechanism of 15-LOX induction during experimental anemia is unknown, but it might be possible that experimental anemia leads to the secretion of cytokines, which may switch on 15-LOX expression. Induction of 15-LOX expression is shown to be transcriptionally regulated by interleukins (Conrad, 1999). Expression of the 15-LOX was found to be up regulated, when the cells were treated with IL-4 or -13. Other cytokines, such as IFN γ, IL-6, IL-10, GM-CSF, etc. did not

exhibit this stimulatory effect. In general, the IL-4-induced signal transduction cascade involves the IL-4 cell surface receptor, the transcription factor STAT6 and functional binding sites for STAT6 are identified in the promoter region of the human 15-LOX gene (Conrad and Lu, 2000).

1.6.2.2. Translational regulation

In young rabbit reticulocytes, the 15-LOX mRNA is present but no functional enzyme is expressed (Thiele et al., 1982). Two regulatory proteins, hnRNPs K and E1 (Ostareck et al., 1997) have been identified to be capable of binding to repetitive sequences called 'differentiation control elements (DICE)' in the 3'-untranslated region of the 15-LOX mRNA preventing its translation (Ostareck-Lederer et al., 1994). Transfection of hnRNP K and hnRNP E1 into HeLa cells specifically silenced the translation of reporter mRNAs bearing the repetitive element of the rabbit 15-LOX mRNA in their 3'-untranslated regions.

1.6.2.3. Post-translational regulation

15-LOXs are not subjected to major post-translational modifications like glycosylation myristoylation or isoprenylation and regulation by phosphorylation/dephosphorylation cycle is also not observed. Ferrous LOXs are catalytically inactive and require activation by hydroperoxy fatty acids, which involves oxidation of the non-heme iron to a ferric form (De Groot et al., 1975). Other examples of post-translational regulation include regulation by nitric oxide (NO) (Wiesner et al., 1996; Holzhütter et al., 1997) and calcium-dependency for 15-LOX membrane association (Brinckmann et al., 1998).

1.6.3. Biological role of 15-LOXs

The unconventional ability to oxygenate biomembranes (Kuhn et al., 1990), lipoprotein lipids (Belkner et al., 1998) along with the free fatty acids facilitates 15-LOX to exhibit wide array of biological activities. 15-LOXs have been shown to play an important role in cell differentiation, atherogenesis inflammation, asthma and carcinogenesis.

1.6.3.1. Cell differentiation and maturation

In 1974, the first mammalian 15-LOX was detected in rabbit reticulocytes wit capability of inhibiting the cellular respiration (Rapoport et al., 1982; Schewe et al., 1986). The maturational degradation of mitochondria is a key process in late erythropoiesis and several lines of experimental evidences suggest the involvement of 15-LOX. During *in vitro* maturation of rabbit reticulocytes the appearance of the functional 15-LOX coincides in time with the onset of mitochondria degradation and 15-LOX inhibitors appear to slow down this process (Schewe et al., 1986; Grullich et al., 2001). 15-LOXs may also be important for the differentiation of other cell types like tracheobronchial cells (Hill et al., 1998) and macrophages (Miller et al., 2001).

1.6.3.2. Inflammation

5-LOX products, such as leukotriene B4, are important mediators of acute inflammation. However, tissue levels of 15-LOX products (15-(*S*)-HETE, 13-(*S*)-HODE) are also often elevated during inflammation, but the patho-physiological relevance of this increase remains unclear. 15(*S*)-HETE is the major eicosanoid in human proctocolitis (Donoiwitz, 1985; Zijlstra et al., 1991) and 15-(*S*)-HPETE induced inflammation in rabbit skin (Higgs et al.,

1981). 13-(*S*)-HODE (Henricks et al., 1991) and 5-Oxo-15-HETE, a more complex 15-LOX metabolite, have been shown to exhibit chemotactic activity (Schwenk et al., 1992). In recent years, several lines of experimental evidences suggested that 15-LOX products might exhibit anti-inflammatory properties (Holtzman et al., 1994; Smith et al., 1993; Takata et al., 1994 a & b). In experimental arthritis, 15-(*S*)-HETE exhibited anti-inflammatory activity by inhibiting leukotriene B4 formation and synovial cell proliferation (Herlin et al., 1990).

1.6.3.3. Bronchial asthma

A number of studies indicate a high level expression of the 15-LOX in human airways (Hunter et al., 1985; Sigal and Nadel, 1991, Holtzman, 1992). Large quantities of 15-(*S*)-HETE formed in airway epithelial cells are rapidly incorporated into the cellular phosphatidyl inositol pool and this process is up-regulated by IL-4 (Profita et al., 1999). Although the biological role of the 15-LOX pathways in airway epithelium is far from clear, there is circumstantial evidence relating an increased 15-LOX expression to bronchial asthma (Profita et al., 2000). *In vitro*, exogenous 15-(*S*)-HETE was reported to induce contraction of human bronchial smooth muscle cells at sub-micromolar concentrations (Salari and Schellenberg, 1991). However, inhaled 15-(*S*)-HETE was shown to exhibit no direct effects on airway caliber in either normal or in asthmatic individuals (Lai et al., 1990, a). On the other hand, the early allergic response was increased significantly by pre-inhalation of 15-HETE whereas the late allergic response was not influenced (Lai et al., 1990, b).

1.6.3.4. Atherogenesis

When specimens of human atherosclerotic lesions were incubated with exogenous arachidonic acid, formation of 15-(*S*)-HETE was observed suggesting the expression of a 15-LOX (Henriksson et al., 1985). Immunohistochemical staining, in situ hybridization, and reverse transcriptase polymerase chain reaction with atherosclerotic tissue of different mammals appeared to confirm these findings (Hiltunen et al., 1995). More detailed histochemical studies even suggested that the enzyme is expressed in foamy lesional macrophages and in a subset of smooth muscle cells (Yla-Herttuala et al., 1990; Hugou et al., 1995). Oxidative modification converts LDL to an atherogenic form that is rapidly taken up by macrophages or smooth muscle cells via scavenger receptor mediated pathways. Since this uptake is not feedback controlled, the cells may excessively take up lipids and develop into lipid laden foam cells. *In vitro* 15-LOXs are capable of oxidizing LDL to an atherogenic form (Kuhn et al., 1994; Neuzil et al., 1998). When transgenic mice overexpressing the human 15-LOX in vascular endothelium (Harats et al., 1995) were crossbred with LDL-receptor deficient mice, the double transgenics turned out to be more susceptible to atherosclerosis (Harats et al., 2000). In contrast to the data suggesting a pro-atherogenic activity of the enzyme, there are several observations suggesting an anti-atherogenic role such as transgenic rabbits, which overexpress the human reticulocyte 15-LOX in monocyte/macrophages, are protected from atherosclerosis (Shen et al., 1996). When these animals were fed a Western-type diet, the development of atherosclerotic lesions in the aorta was significantly reduced.

1.7. LOX metabolism, polyunsaturated fatty acids and carcinogenesis

Early tumorigenesis studies in animals showed that dietary fats enhance carcinogenesis through a structure containing polyunsaturated bonds (Broitman et al., 1977) and the ω-6 function (*e.g.,* arachidonic and linolenic acids) promote tumorigenesis, whereas, ω-3 polyunsaturated fatty acids (*e.g.,* those found in fish oil) have antitumorigenic effects in animal models (Singh et al., 1997; Chang et al., 1998; Hubbard et al., 1998). Later tumorigenesis studies demonstrated that polyunsaturated fatty acids must undergo oxidative metabolism to enhance tumorigenesis (Bull et al., 1984; Setty et al., 1987; Glasgow et al., 1992). The Lipoxygenases (LOXs) and Cyclooxygenases (COXs) mediate the oxidative metabolism of linoleic and arachidonic acids forming an array of biologically active metabolites, such as HODEs, HETEs, and prostaglandins. Various LOX products have been linked to tumorigenesis *in vitro* and *in vivo* in experimental models, and the modulation of LOX metabolism has anticarcinogenic effects in these models (Bortuzzo et al., 1996; Hussey and Tisdale, 1996). Therefore, the oxidative metabolism of ω-6 polyunsaturated fatty acids has been targeted for developing anticarcinogenic interventions, such as with the natural products curcumin and polyphenols, which modulate LOX activity and have promising results in preclinical carcinogenesis studies (Huang et al., 1991; Rao et al., 1995). Synthetic LOX inhibitors that were developed originally for treating inflammatory diseases (Drazen, 1997) also have antitumorigenic effects in preclinical models (Steele et al., 1999).

1.7.1. Procarcinogenic LOX metabolism of arachidonic acid

Several LOXs form different metabolites within the arachidonic acid pathway that appear to enhance tumorigenesis (Fig. 6). These LOXs and

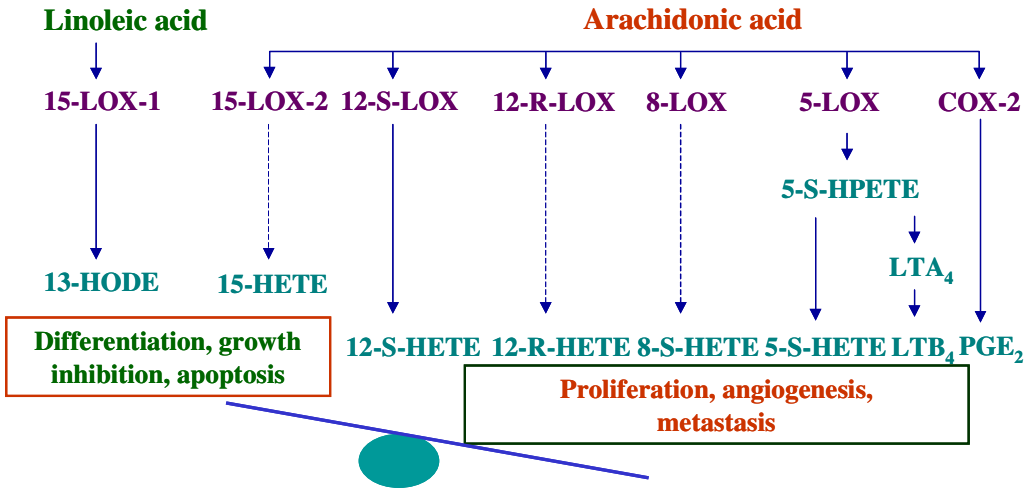

Fig. 6. Role of lipoxygenases and cyclooxygenases in carcinogenesis
(*Source: Shureiqi, I., and Lippman, S. M. (2001) Cancer Res., 61, 6307-6312*)

metabolites include 5-LOX and its products 5-(*S*)-HETE and LTB4; 8-LOX and 8-(*S*)-HETE; 12-(*S*)-LOX and 12-(*S*)-HETE; and 12-(*R*)-LOX and 12-(*R*)-HETE. Although 15-LOX-2 also metabolizes arachidonic acid to form 15-(*S*)-HETE, recent data suggest that it may be anticarcinogenic.

1.7.1.1. 5-LOX and its products 5-(*S*)-HETE and LTB_4

Several studies have suggested a link between 5-(*S*)-HETE, a 5-LOX product and carcinogenesis. Prostate, lung, and other cancer cell lines express 5-LOX and FLAP mRNA (Avis et al., 1996; Anderson et al., 1998). 5-LOX overexpression recently has been documented in human prostate cancer tissue (Gupta et al., 2001), and 5-(*S*)-HETE formation and inhibition respectively promote and inhibit the growth of prostate cancer cells (Ghosh and Myers, 1997). 5-(*S*)-HETE but not other HETE products (LTB_4, 12-, or 15-(*S*)-

HETE), inhibit apoptosis induction by MK-886 (a specific FLAP inhibitor) in prostate cancer cell lines (Ghosh and Myers, 1998).

1.7.1.2. 8-LOX and 8-(*S*)-HETE

Recent findings have suggested that 8-LOX enzyme activity increases dramatically in early stages of mouse skin tumorigenesis and that 8-LOX up-regulation in mice promotes skin carcinogenesis. Additionally 8-LOX has genotoxic effects that might contribute to the development of the phenotype of tumor cells.

1.7.1.3. 12-(*S*)-LOX and 12-(*S*)-HETE

Several lines of evidence indicate that the 12-(*S*)-LOX product 12-(*S*)-HETE contributes substantially to carcinogenesis (Tang and Honn, 1999). The expressions of platelet-type 12-(*S*)-LOX mRNA and protein have been detected in prostate, melanoma, and some other cancer cell lines (Gao et al., 1995; Timar et al., 2000). 12-(*S*)-LOX in tumor cells produces 12-(*S*)-HETE, and 12-(*S*)-HETE promotes tumorigenic events such as invasion and metastasis (Chopra et al., 1991; Hohn et al., 1992; Timar et al., 1992; Liu et al., 1995; Nie et al., 1998). These *in vitro* data have been supported by human and animal *in vivo* tumor studies. The degree of 12-(*S*)-LOX overexpression in human prostate cancer correlates with the tumor grade and stage (Gao et al., 1995) and identified even with angiogenesis (Nie et al., 1998).

1.7.1. 4. 12-(*R*)-LOX and 12-(*R*)-HETE.

Initially thought to involve only cytochrome P450, 12-(*R*)-HETE production also involves 12-(*R*)-LOX, which recently has been cloned from human skin (Boeglin et al., 1998). Very limited data regarding the relationship

between 12-(*R*)-HETE and tumorigenesis indicates that 12-(*R*)-HETE promotes the proliferation of colon cancer cell lines *in vitro* (Bortuzzo et al., 1996).

1.7.2. Anticarcinogenic LOX metabolism of arachidonic and linoleic acids

15-LOX-1 and 15-LOX-2 are two isoenzymes of 15-LOX that appear to exert important anticarcinogenic effects through the metabolism of polyunsaturated fatty acids. The preferred substrate for 15-LOX-1 is linoleic acid and that of 15-LOX-2 is arachidonic acid (Brash et al., 1997).

1.7.2.1. 15-LOX-1 and 13-*S*-HODE

Whereas several oxidative metabolites are formed from arachidonic acid, the main oxidative metabolite of linoleic acid in human cells is 13-(*S*)-HODE (Baer et al., 1991; Daret et al., 1989). 15-LOX-1 is the main enzyme for metabolizing linoleic acid into 13-(*S*)-HODE (Kuhn and Brash, 1990) and is the only 15-LOX isoenzyme found in the epithelium of the human colon (Ikawa et al., 1999). Several early studies suggested that 13-(*S*)-HODE enhances cell proliferation. 13-(*S*)-HODE potentiates the mitogenic response to EGF in fibroblasts (Glasgow and Eling, 1990) and Syrian hamster embryo cells (Glasgow et al., 1992). The transfection of C-erbB-2 (a protooncogene similar to EGF receptor) into normal fibroblasts increases 13-(*S*)-HODE production (Glasgow and Everhart, 1997). Therefore, it was proposed that the 15-LOX-1 product 13-(*S*)-HODE enhances colonic tumorigenesis (Ikawa et al., 1999) and that 13-(*S*)-HODE dehydrogenase counteracts this effect (Bronstein and Bull, 1993). These proposed effects, however, were inconsistent with other findings showing that 13-(*S*)-HODE did not enhance

EGF-dependent DNA synthesis in transformed Syrian hamster embryo cells that had lost tumor suppressor gene function (Hui et al., 1997). Recently it was found that 13-(*S*)-HODE levels and 15-LOX-1 expression are reduced in human colorectal cancers (Shureiqi et al., 1999). Several studies have also shown that 13-(*S*)-HODE is linked to cellular differentiation and apoptosis. 13-(*S*)-HODE attenuates ornithine decarboxylase activity in the rat colon (Bull et al., 1993) and reverses skin hyperproliferation in guinea pigs (Miller and Ziboh, 1990). Human osteosarcoma cells with enzymatically active 15-LOX-1 expression after transient transfection with human 15-LOX-1 grow slower by 50% than do osteosarcoma cells without enzymatically active 15 LOX-1 expression (Sigal et al., 1990). 13-hydroperoxyoctadecadienoic acid, the immediate and transient precursor of 13-(*S*)-HODE, induces apoptosis in human T cells (Sandstrom et al., 1995). The induction of differentiation causes the expression of 15-LOX-1 in Caco-2 colon cancer cells and human tracheobronchial epithelial cells, and 13-(*S*)-HODE induces cell cycle arrest in colorectal cancer cells (Shureiqi et al., 1999). Recently it has been found that NSAIDs induce 15-LOX-1 expression in colorectal cancer cells and that 15-LOX-1 up-regulation is critical to NSAID induction of apoptosis (Shureiqi et al., 2000, a) and also these effects of NSAIDs were independent of COX-2 inhibition (Shureiqi et al., 2000, b). 15-LOX-1 is down regulated *in vitro* and *in vivo* in human esophageal cancers, and NSAIDs restore 15-LOX-1 to induce apoptosis in human esophageal cancer cells (Shureiqi et al., 2001).

1.7.2.2. 15-LOX-2 and 15-*S*-HETE.

The 15-LOX-2 enzyme converts arachidonic acid mainly into 15-(*S*)-HETE. 15-LOX-2 is expressed mainly in human tissues like cornea, prostate, lung, and skin (Brash et al., 1997). 15-LOX-2 expression is reduced in human prostate carcinomas (Shappell et al., 1999) and high-grade prostatic intraepithelial neoplasia (Jack et al., 2000). There are conflicting *in vitro* data, however, regarding the role of 15-(*S*)-HETE in carcinogenesis. Some studies suggest that 15-(*S*)-HETE might have antitumorigenic effects, particularly by antagonizing other LOX products, such as LTB_4 (Vanderhoek et al., 1980, a; Vanderhoek et al., 1985) and possibly 12-(*S*)-HETE (Vanderhoek, 1980, b). 15-(*S*)-HETE reduced 5-LOX activity in rat basophilic leukemia cells (Kang and Vanderhoek, 1995; Montero et al., 1999). Other studies have suggested that 15-(*S*)-HETE may suppress apoptosis (Tang et al., 1996; Herrmann et al., 1997), has no effect on apoptosis in cancer cells (Bortuzzo et al., 1996; Desplat et al., 1999), or inhibition of proliferation in PC3 prostate carcinoma cells possibly through activation of PPAR-γ (Shappell et al., 2001). Although the evidences suggest that 15-(*S*)-HETE has an antitumorigenic role, further studies are needed to confirm this role.

1.8. Apoptosis

Cell death can follow two distinct pathways, apoptosis or necrosis. Necrosis appears to be the result of acute cellular dysfunction in response to severe stress conditions or after exposure to toxic agents, and is a relatively passive process associated with rapid cellular ATP depletion. Morphologically, necrosis is characterized by a dramatic increase in cell

volume and rupture of the plasma membrane, with spilling of the cellular contents into the intercellular milieu (Gores et al., 1990). This release of the dying cells' contents into the extracellular space can cause further tissue damage by affecting neighboring cells or by attracting proinflammatory cells to the lesion (Haslett, 1992). Apoptosis is a form of cell death that occurs during several pathological situations in multicellular organisms and constitutes a common mechanism of cell replacement, tissue remodeling, and removal of damaged cells (Delong, 1998). Cell shrinkage, chromatin condensation, internucleosomal DNA fragmentation (Kerr et al., 1972; Wyllie et al., 1980), and formation of ''apoptotic bodies'' are all characteristic features of apoptosis. Several protease families are implicated in apoptosis, the most prominent being caspases. Caspases are aspartic acid-specific cysteine proteases, which exist as zymogens in the soluble cytoplasm, mitochondrial intermembrane space, and nuclear matrix of virtually all cells (Nicholson and Thornberry, 1997). At least three models for caspase activation have been proposed (Fig. 7).

Apoptosis induced by ligation of cell surface receptors like the Fas or TNF-R, dubbed ''death receptors,'' represents a pathway, referred as "extrinsic death pathway", almost exclusively controlled by caspases. In these scenarios, ligand binding of the receptor causes the assembly of a series of proteins called the death-inducing signaling complex (DISC), which then activates an apical caspase, procaspase- 8 (Peter and Krammer, 1998). The ensuing events present the strongest evidence that caspases act in cascades, with caspase-8 causing activation of caspase-3, which can activate other

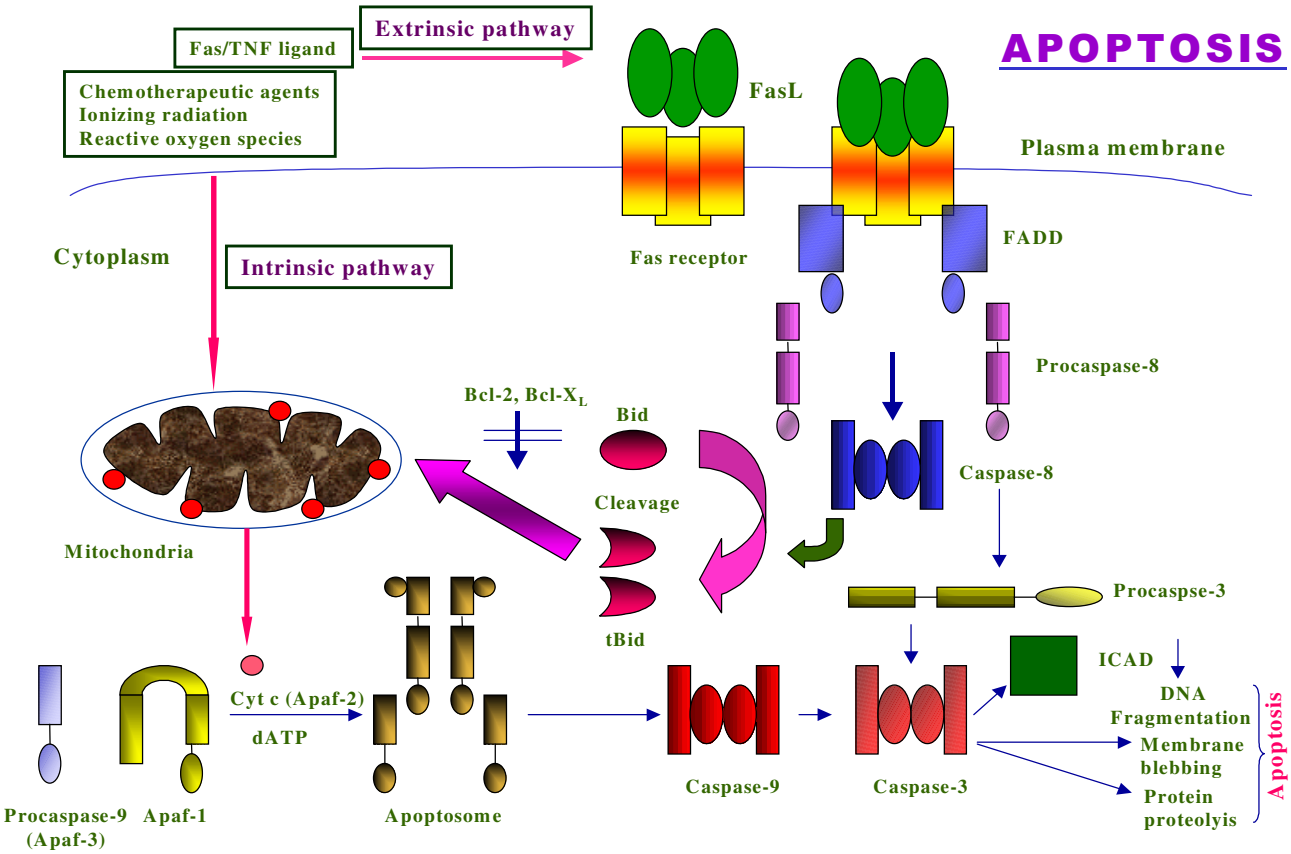

Fig.7. An overall view of major apoptotic pathways

(*Source: Katoch et al., Ind. J. Exp. Biol., 2002*)

caspases and ultimately cleave a variety of cellular proteins. One of these proteins is a caspase-dependent endonuclease, which is freed from its inhibitor by caspase-3, and subsequently cuts DNA into oligonuclesomal (180 bp) fragments (Liu et al., 1998; Sakahira et al., 1998).

A different model for caspase activation has been proposed for the numerous agents that trigger apoptosis without involving cell surface receptors. This pathway, "named intrinsic death pathway", focuses on mitochondria and contends that mitochondrial dysfunction occurs during apoptosis and causes the release of cytochrome *c* from mitochondria into the cytosol, where it binds to apoptotic protease activating factor 1 (Apaf-1), a mammalian homologue of the pro-apoptotic nematode protein, ced-4 (Zou et

al., 1999). Apoptotic protease activating factor 1 (Apaf-1) contains binding sites for cytochrome *c* and dATP and oligomerizes with other Apaf molecules. This complex, termed the apoptosome, recruits and binds pro-caspase-9 by using the caspase recruitment domain (CARD) of Apaf-1 (Saleh et al., 1999). Mature caspase-9 then activates the more distal caspases-3 and -7.

Finally, a third pathway, which is capable of activating the caspase cascade, is initiated by cytotoxic cells (Yang et al., 1998). Perforin and granzyme B cooperate to induce apoptosis in tumor cells and in cells infected with intracellular pathogens. Perforin permeabilizes cells, allowing granzyme into the cytosol where it activates caspase-3, either by direct cleavage or via recruitment of the mitochondrial pathway of caspase activation. Regardless of the mechanism, upon activation, caspases cleave numerous cellular proteins including poly(ADP-ribose) polymerase (PARP) and fodrin (Nicholson and Thornberry, 1997). In fact, more than a hundred cellular proteins have now been identified as potential caspase substrates during apoptosis, and most events in apoptosis appear to require a caspase mediated proteolytic step.

Although caspase activation via death receptors or granzyme B has been reported to proceed without mitochondrial participation, recent reports suggest that amplification of these pathways does involve mitochondria. The common partaker is Bid, a proapoptotic Bcl-2 family member, which is cleaved by both caspase-8 (Lou et al., 1998) and granzyme B (Alimonti et al., 2001). The truncated version of Bid (tBid) translocates to mitochondria and causes cytochrome *c* release and caspase-9 activation.

1.9. Oxidative stress & apoptosis

Reactive oxygen species (ROS) is a collective term used for all those species that contain chemically reactive oxygen and ROS encompass a variety of partially reduced metabolites of oxygen [e.g., superoxide anions ($O_2^{\cdot-}$)], hydroxyl radical (OH^-) and hydrogen peroxide (H_2O_2), possessing higher reactivities than molecular oxygen (Thannickal and Fanburg, 2000). They are generated intracellularly through a variety of processes, for example as by products of normal aerobic metabolism or as second messengers in various signal transduction pathways. They can also be derived from exogenous sources, either being taken up directly by cells from the extracellular milieu or produced as consequence of the cell's exposure to some environmental insult. Transient fluctuations in ROS serve important regulatory functions, but when present at high and/or sustained levels, ROS can cause severe damage to DNA, protein and lipids. The cell is endowed with an extensive antioxidant system to combat ROS, either directly by interception or indirectly through reversal of oxidative damage. When ROS overcome the cellular defense systems and redox homeostasis is altered, the result is oxidative stress. Oxidative stress is implicated in the pathogenesis of a wide variety of diseases including atherosclerosis, diabetes, pulmonary fibrosis, neurodegenerative disorders, arthritis and is believed to be a major factor in aging (Finkel and Holbrook, 2000).

1.9.1. Sources of ROS/RNI production

Both ROS and RNI can be generated at many different organelles in response to various stimuli. Major sources of ROS production include the

mitochondrion, endoplasmic reticulum, plasma membrane and cytosol, while RNI are usually formed in the cytosol or at the mitochondrion.

The mitochondrion, organelle in eukaryotes responsible for aerobic respiration, is the major site of generation of free radicals. Under physiological conditions, electrons (1-2 %) carried by the electron transport chain leak out of the pathway and pass directly to oxygen generating superoxide radical ($O_2^{\bullet -}$). Complex I, NADH - ubiquinone oxidoreductase and complex III, ubiquinol – cytochrome *c* oxidoreductase are the two sites where superoxide is produced (Beyer, 1992).

Another oxidase gaining prominence in studies of apoptosis is NADPH oxidase, found at the plasma membrane of phagocytes. The leukocyte NADPH oxidase, which reduces molecular oxygen to superoxide consists of five protein components. Assembly and activation of this oxidase occurs in response to a range of stimuli during immune responses. Evidence is mounting that a similar NADPH-like oxidase is expressed in a variety of cells throughout the body. Activation of this enzyme and subsequent superoxide production is necessary for apoptosis in a variety of systems (Finkel, 2000; Tamariello et al., 2000). Other sources of $O_2^{\bullet -}$ include enzymes such as cytochrome *P*450 in the endoplasmic reticulum (ER), lipoxygenases, cyclooxygenases and xanthine oxidase. The dismutation of $O_2^{\bullet -}$ by superoxide dismutase (SOD) results in the generation of H_2O_2, which can then react with Fe^{2+} to form hydroxyl radicals via the Fenton reaction.

Reactive nitrogen intermediates (RNI) are now also recognized as important radicals. Nitric oxide (NO) is formed endogenously from the

oxidation of L-arginine to L-citrulline by a family of NADPH dependent enzymes, the NO synthases. Three major isoforms of this enzyme exist, neuronal NOS (nNOS, NOS1), endothelial NOS (eNOS, NOA3) and inducible NOS (iNOS, NOS2). Inducible NOS (iNOS) is expressed in cells of the immune system and other cells in response to various stimuli (Nathan, 1997). NO exists in different chemical forms (NO^{-}, $NO^{\bullet}$ and NO^{+}) and thus has a wide ranging degree of chemical reactivity and exhibits variety of biological roles (Stamler et al., 1992).

1.9.2. Relevance of oxidative stress to apoptosis

The role of oxidative stress in apoptosis has been shaped by several independent observations (Zamzami et al., 1995; Stridh et al., 1998). For many years, direct treatment of cells with oxidants, like hydrogen peroxide or redox-active quinones, was thought to exclusively cause necrosis, but other studies have shown that lower doses of these agents can trigger apoptosis (Hampton and Orrenius, 1997). In addition to this direct evidence, many groups have suggested that intracellular ROS generation may constitute a conserved apoptotic event, and cite ROS production as a critical determinant of toxicity associated with exposure to ionizing radiation and chemotherapeutic drugs (Zamzami et al., 1995). Depletion of glutathione (GSH) pools has also been suggested to be part of the cell death effector machinery, and accompanies ROS production during apoptosis in relevant systems (Macho et al., 1997). Furthermore, oxidative modification of proteins and lipids observed in cells undergoing apoptosis in response to non-oxidative stimuli and the ability of various cellular antioxidants like catalase and N-acetyl cysteine (NAC) to

block apoptosis induced by diverse agents other than oxidants suggest a central role for oxidative stress in apoptosis (Buttke and Sandstrom, 1994). Reciprocally, broad-spectrum anti-apoptotic proteins like Bcl-2 and the baculovirus protein p35 have been ascribed an antioxidant function (Jacobson, 1996, Sah et al., 1999), again indicating that ROS generation may be a requisite apoptotic event.

1.9.3. Models for oxidative stress-induced apoptosis

Several mechanisms for ROS induction of apoptosis have been proposed; however, an integrated model is yet to be established. Several related reports favor a scheme in which ROS, H_2O_2 being one example, act upon mitochondria, causing a disruption of mitochondrial membrane potential and the release of cytochrome *c* (Stridh et al., 1998). Once cytochrome *c* is in the cytosol, it binds to Apaf-1 as an essential component of the apoptosome. Assembly of the apoptosome complex initiates the caspase cascade by first activating caspase-9. An alternative model for ROS-induced apoptosis involves upregulation of the Fas/Fas L system. The observation that various chemotherapeutic drugs cause intracellular ROS production and Fas upregulation has perpetuated this paradigm (Cabaner et al., 1999); however, other studies contend that H_2O_2-induced apoptosis is Fas-independent (Dumont et al., 1999). A central role for FasL induction has also been introduced into this debate, by a study demonstrating upregulation of the ligand by reactive oxygen intermediates during activation-induced cell death (Bauer et al., 1998). Other studies have shown caspase-3 activation by H_2O_2; however, this could be a result of either Fas- or mitochondrially mediated

pathways (Matsura et al., 1999). Finally, transcription factors can be modulated by oxidative stress. Nuclear translocation of p^{53} is caused by H_2O_2 (Uberti et al., 1999), and the ubiquitous transcription factors, NF-κB and AP-1, are activated by ROS (Pinkus et al., 1996). Once activated, these transcription factors might drive transcription of pro-apoptotic genes or perhaps cause expression of inhibitors of survival-related proteins. Intracellular ROS production has also been noted during Fas-induced apoptosis (Bauer et al., 1998; Cabaner et al., 1999). Taken together, these data suggest that some of the above-mentioned mechanisms for ROS-induced apoptosis may be linked.

1.9.4. Antioxidants and protection against apoptosis

The primary antioxidant defense system that prevents oxidative damage directly by intercepting ROS before they can damage intracellular targets consists of superoxide dismutase (SOD), glutathione peroxidase (GPx), catalase and thirodoxin reductase. Four classes of SOD have been identified that include Mn-SOD, Cu, Zn-SOD, Ni-SOD and extracellular SOD. All four SOD enzymes destroy the free radical superoxide by converting it to H_2O_2. H_2O_2 is one of the major ROS in the cell. While low levels of H_2O_2 result in apoptosis, high levels can lead to necrosis or caspase independent apoptosis (Hampton and Orrenius, 1997; Creagh et al., 2000). The primary defense mechanisms against H_2O_2 are catalase (Michiels et al., 1994) and GPx through the glutathione (GSH) redox cycle (Reed, 1990). Catalase disintegrates H_2O_2 to water and molecular oxygen. Overexpression of catalase in cytosolic or mitochondrial compartments has been demonstrated to protect cells against

oxidative injury (Bai et al., 1999). In addition, catalase-overexpressing thymocytes are resistant to apoptosis (Tome et al., 2001). These studies demonstrate the cytotoxic effects of H_2O_2 and also emphasize the importance of catalase.

The GSH system is probably the most rapid and abundant weapon against ROS accumulation and GSH (γ-glu-cys-gly) regulates the redox state of many other cellular substances. The system consists of GSH, glutathione peroxidase and glutathione reductase. Glutathione peroxidase catalyses the reduction of H_2O_2 and other peroxides and converts GSH to its oxidized form, GSSG. GSSG is then reduced back to GSH by glutathione reductase. Decrease in GSH levels and concomitant increase in ROS during the apoptotic process has been reported (Tan et al., 1998). Decreases in intracellular GSH content is observed during Fas-induced apoptosis in Jurkat cells (van den Dobbelsteen et al., 1996). This drop in GSH was not due to an inhibition of synthesis, oxidation of GSH to glutathione disulfide (GSSG), or a deficit in the GSH salvage pathway, but to an increased rate of GSH efflux.

Scope
&
Objectives

2. Scope and Objectives

Lipoxygenases (LOXs) (linoleate: oxygen oxido reductase EC 1.13.11.12), the lipid peroxidizing enzymes, have been shown to mediate plethora of physiological processes such as erythrocyte, keratinocyte and eye-lens cell development, mobilization of fatty acids for β-oxidation (Brash et al., 1999; Kuhn et al., 2002). The pathological conditions include inflammation, asthma, atherogenesis and carcinogenesis. The role of various LOXs in regulating carcinogenesis was very well documented. Indeed 5-LOX, 8-LOX and 12-LOX were shown to have a procarcinogenic role where as the two isoforms of 15-LOX, 15-LOX-1 and 15-LOX-2, were shown to be anti-carcinogenic (Shureiqi et al., 2001). 15-LOX-2 was shown to be anti-carcinogenic, however, the role of 15-LOX-1 in mediating the anti-carcinogenic effects is quite controversial. There are contradictory reports regarding the role of 15-LOX-1 in controlling carcinogenesis. It was shown that 15-LOX-1 is expressed at higher levels in colorectal carcinoma tissues and tumors associated with prostate than their corresponding normal tissues (Ikawa et al., 1999; Kelavkar et al., 2000). However, Shureiqi et al., (1999) reported the opposite, higher expression of 15-LOX-1 in normal tissues compared to the tumors. Moreover, it was found that in colorectal carcinomas, nonsteroidal anti-inflammatory drugs (NSAIDs) and histone deacetylase (HDAC) inhibitors induce the expression of 15-LOX-1 and this up regulation of 15-LOX-1 is critical for subsequent induction of apoptosis (Shureiqi et al., 2000 b; Kamitani et al., 2000; His et al., 2004). On the other hand, 15-LOX-2 expression and the production of its metabolite 15-(*S*)-HETE were found to be

reduced in prostate carcinomas (Shappell, et al., 2001) suggesting an anticarcinogenic role for 15-LOX-2. Even though several reports implicate a role for 15-LOXs in regulating cancers and induction of apoptosis, the molecular mechanisms mediating these effects are still unknown. These effects are also observed to be cell type or tissue specific or being observed only under certain conditions. Further more the intricate details of the apoptotic cascades mediated by 15-LOXs and their metabolites are not very well explored.

Our group has earlier shown that 15-LOX-2 metabolites, 15-(*S*)-HPETE and 15-(*S*)-HETE, exert differential effects on BHK-21 cell proliferation (Kiran Kumar et al., 1993). While 15-(*S*)-HPETE inhibited the proliferation of these cells more potently, 15-(*S*)-HETE at the same concentration didn't show significant effect. It is now well established that the effects of LOX metabolites are mediated through induction of apoptosis in a variety of cell lines including neuronal and leukemic cell types *in vitro* (Maccarrone et al., 2000). There fore the current study is designed to understand the molecular mechanisms mediating 15-LOX metabolite-induced apoptosis, taking a human erythroleukemic cell line (K-562) as a model cell line.

The specific objectives of the study include:

- To study the antiproliferative and growth inhibitory effects of 15-LOX-1 (13-(*S*)-HPODE and 13-(*S*)-HODE) and 15-LOX-2 (15-(*S*)-HPETE and 15-(*S*)-HETE) metabolites on chronic myeloid leukemia cell line - K-562.

- To study the upstream and downstream signaling events involved in 15-LOX metabolite-induced cell death.

- To understand the mechanism of action of 15-LOX metabolite-induced cell death.

Materials & Methods

3. Materials and Methods

3.1 Materials

Cell lines used in this study, U-937 (human histiocytic leukemia), HL-60 (human promyelocytic leukemia), Jurkat (human peripheral blood T cell leukemia) and K-562 (chronic myeloid leukemia) cell lines were obtained from National Center for Cell Science (NCCS), Pune, India. Arachidonic acid (AA) and linoleic acid (LA) were procured from Cayman chemical company (Ann Arbor, Michigan, U.S.A). Phosphate buffered saline (PBS), RPMI medium and fetal bovine serum (FBS) were purchased from GIBCO Ltd. (BRL Life Technologies, Inc., Grand Island, NY). MTT [3-(4, 5-dimethylthiazol-2-yl)-2, 5-diphenyl tetrazolium bromide], DAPI (4', 6-diamidino-2-phenylindole), proteinase K, RNase A, propidium iodide (PI), N-acetyl cysteine (NAC), reduced glutathione (GSH), catalase, soybean lipoxygenase and superoxide dismutase were from Sigma Chemical Co (St.Louis, MO). Nitrocellulose membranes and the enhanced chemiluminescence (ECL) kit were from Amersham Biosciences (Indianapolis, IN). Mouse monoclonal antibodies against cytochrome *c* were from Santa Cruz (CA, USA). Polyclonal antibodies of poly (ADP) ribose polymerase (PARP) were from R&D systems, USA and polyclonal antibodies for caspase-3 were purchased from Cell Signaling Technology Inc (Beverly, MA, USA). DCFH-DA was purchased from Molecular Probes, USA. Ac-DEVD-AFC, Ac-DEVD-CHO and Z-VAD-FMK were from BD Biosciences. Diphenylene iodonium (DPI), verapamil and L-NMMA were procured from Calbiochem (San Diego, USA). All other chemicals, which have not been mentioned here, were of fine grade and high quality and were procured from international or local companies.

3.2. Preparation and separation of 15-LOX metabolites - HPLC analysis

The commercially procured soybean LOX was employed for the preparation of hydroperoxides and hydroxides of AA [15-(*S*)-HPETE & 15-(*S*)-HETE] and LA [13-(*S*)-HPODE & 13-(*S*)-HODE] as per the method described earlier (Reddy et al., 1992; Sailesh et al., 1994)**.** Soybean LOX was incubated with either arachidonic acid or linoleic acid in 0.1 M Tris, pH 9.3 buffer for 3 min and the reaction was terminated by acidifying the reaction mixture to pH 3.0 with 6 N HCl. The products formed were extracted with equal volumes of hexane: ether (1:1) twice and the organic solvent was evaporated under inert conditions. The dried products were then dissolved in straight phase HPLC mobile phase consisting of hexane: propane-2-ol: acetic acid in 1000:15:1 ratio and separated on the straight phase HPLC system at a flow rate of 1 ml/min. To obtain corresponding hydroxides, these products were dissolved in methanol and reduced with sodium borohydride ($NaBH_4$) for 2 min and then separated on HPLC as mentioned above.

The compounds were separated on straight phase HPLC (Shimadzu model equipped with SPD 6AV detector and CR4A chromatopac), using CLC-SIL (25 x 0.4 cm) column and the solvent system mentioned above. The samples were monitored at 235 nm and peaks were analyzed on a Shimadzu 1601 model UV/VIS scanning spectrophotometer. Peaks showing conjugated diene spectra were collected and identified based on co-chromatography with the standards and LC-MS analysis.

3.3. LC-MS analysis

HPLC purified samples were subjected to LC-MS analysis on LC-MSD (1100 Series LC-MSD, Agilent Technologies). Samples were analysed through Flow Injection Analysis in the negative ion mode employing electron spray ionization (ESI). Acetonitrile: Water (70: 30) was used as the mobile phase at a flow rate of 0.4 ml/min.

3.4. Cell culture and treatment

The human chronic myeloid leukemia (K-562) cells and other leukemic cell lines (U-937, HL-60 & Jurkat) were grown in suspension in RPMI 1640 medium supplemented with 10% heat inactivated fetal bovine serum (FBS), 100 IU/ml penicillin, 100 μg/ml streptomycin and 2 mM L-glutamine. Cultures were maintained in a humidified atmosphere with 5 % CO_2 at 37°C. The cultured cells were subcultured twice each week, seeding at a density of about 2 x 10^5 cells/ml. For treatment exponentially growing K-562 cells were collected and resuspended in fresh culture medium with 1% FBS. The HPLC purified 15-LOX metabolites [15-(*S*)-HPETE, 15-(*S*)-HETE, 13-(*S*)-HPODE and 13-(*S*)-HODE] dissolved in ethanol were used for the treatments. The final concentration of the vehicle never exceeded 0.1%. Wherever any inhibitor was used in this study, toxic profiling in terms of dosage and time were done and the non-toxic and efficient doses were employed for further studies.

3.5. Cell viability and cytotoxicity

15-LOX metabolite induced growth inhibitory effects were assessed using the 3-(4, 5-dimethylthiazol-2-yl)-2, 5-diphenyl tetrazolium bromide

(MTT) assay as described by Mosmann (Mosmann, 1983). For MTT assay, 5 x 10^3 exponentially growing cells were plated in 100 µl of the growth medium in the presence or absence of 1-20 µM of hydroperoxy [15-(*S*)-HPETE and 13-(*S*)-HPODE] and 10-160 µM of hydroxy [15-(*S*)-HETE and 13-(*S*)-HODE] 15-LOX metabolites in 96 well plates and cultured at 37 °C in 5 % CO_2 for 3-24 h. The cells were then incubated with 20 µl of MTT (5 mg/ml) at 37 °C for 4 h. After dissolving the crystals in a triplex solution containing 12 % SDS, 5 % isobutanol and 12 mM HCl, the plates were read in a microtiter plate reader at 570 nm. Each concentration was tested in three independent experiments run in four replicates. Standard errors of means were calculated and data were presented as the % growth vs control. The concentration of the compound that inhibited cell growth by 50 % (IC_{50}) was determined from these cell survival plots.

3.6. Morphological differentiation and analysis of nuclear morphology

K-562 cells were incubated with 10 µM of 15-(*S*)-HPETE for 3 h or 40 µM of 15-(*S*)-HETE for 6 h, examined for morphological differentiation by phase contrast microscopy and photographed with Nikon F-601 AF Camera. The treated cells were harvested, washed with ice cold PBS, fixed in a solution of methanol: acetic acid (3:1) for 30 min and then stained with DAPI (1 µg/ml) to study their nuclear morphology by fluorescence microscopy (Olympus BH2RFC). Apoptotic cells were defined based on morphological changes like membrane blebbing, formation of apoptotic bodies and nuclear changes such as chromatin condensation and fragmentation. Apoptotic cells

were observed and photographed under high magnification (400X). Each experiment was repeated atleast three times and photographs included in the results are representative of one of those experiments.

3.7. DNA fragmentation assay

Cells were treated with 15-LOX-2 metabolite treatments [with 5 μM, 10 μM of 15-(*S*)-HPETE for 3 h and with 20 μM, 40 μM 15-(*S*)-HETE for 6 h] and used for the isolation of the DNA. DNA laddering was detected by isolating fragmented DNA using the SDS/ Proteinase K/ RNase A extraction method, which allows the isolation of only fragmented DNA without contaminating genomic DNA **(**Hermann, 1994**).** Five million cells were pelleted, washed in cold PBS and lysed in a buffer containing 50 mM Tris-HCl (pH 8.0), 1 mM EDTA, 0.2 % Triton X-100 for 20 min at 4^0 C. After centrifugation at 14,000 g for 15 min, the supernatant was treated for 1 h at 37^0 C with RNase A (0.5 mg/ml) and then with proteinase K (0.5 mg/ml) for 1 h at 50^0 C. DNA was extracted with buffered phenol and precipitated with ethanol and DNA was resolved on 1 % agarose gel in TBE (44.6 mM Tris, 44.5 mM boric acid and 1 mM EDTA). DNA fragmentation was visualized upon staining gel with ethidium bromide (0.5 mg/ml) and exposed to UV light.

3.8. Quantification of apoptosis by flow cytometry

To quantitate apoptosis, flow cytometric analysis using propidium iodide was performed. Cells that were less intensely stained than G1 cells (sub- G0/G1 cells) in flow cytometric histograms were considered apoptotic cells. The method for DNA labeling was done as described previously (Madhava Reddy et al., 2003) with minor modifications. After treatment, cells

were prepared as single cell suspension in 200 µl PBS, fixed with 2 ml of ice-cold 70 % ethanol, and maintained at 4^0 C overnight. The cells were harvested by centrifugation at 500xg for 10 min, resuspended in 500 µl PBS supplemented with 0.1 % Triton X-100 and RNase A (50 µg/ml), incubated at 37^0 C for 30 min, and stained with 50 µg/ml propidium iodide (PI) in the dark at 4^0 C for 30 min. The red fluorescence of individual cells was measured with a FACSCalibur flow cytometer (Becton Dickinson, San Jose, CA, USA). A minimum of 10,000 events were counted per sample.

3.9. Preparation of whole cell extracts and immunoblot analysis

The cell lysis was carried out based on a method described earlier **(**Sambrook et al., 1989**)**. To prepare the whole cell extract, cells were washed with PBS and suspended in a lysis buffer (20 mM Tris, 1 mM EDTA, 150 mM NaCl, 1 % NP-40, 0.5 % sodium deoxy cholate, 1 mM β-glycerophosphate, 1 mM sodium orthovanadate, 1 mM PMSF, 10 µg/ml leupeptin, 20 µg/ml aprotinin). After 30 min of shaking at 4^0C, the mixtures were centrifuged (10,000xg) for 10 min, and the supernatants were collected as the whole-cell extracts. The protein content was determined according to the Bradford method (Bradford, 1976). An equal amount of total cell lysate was resolved on 8-12 % SDS-PAGE gels along with protein molecular weight standards, and then transferred onto nitrocellulose membranes. Membranes were stained with 0.5 % Ponceau *S* in 1 % acetic acid to check the transfer. The membranes were blocked with 5 % w/v nonfat dry milk and then incubated with the primary antibodies (for Caspase-3 and PARP) in 10 ml of antibody-diluted buffer (1X Tris-buffered saline and 0.05 % Tween-20 with 5 % milk) with gentle

shaking at 4^0C for 8-12 h and then incubated with peroxidase conjugated secondary antibodies. Signals were detected either by using peroxidase substrate -TMB/H_2O_2 or with ECL Western blotting detection kit according to manufacturer's recommendations (Amersham Biosciences, Indianapolis, IN). The blots were probed with β-actin antibodies to confirm equal loading.

3.10. Detection of cytochrome *c* release using Western blot analysis

After exposure to 10 μM 15-(*S*)-HPETE or 40 μM 15-(*S*)-HETE for various time periods, cells were collected and washed once with PBS and subsequently with buffer A (0.25 M sucrose, 30 mM Tris-HCl, pH 7.9, 1 mM EDTA). Cells were then resuspended in buffer A containing 1 mM PMSF, 1 mg/ml leupeptin, 1 mg/ml pepstatin, 1 mg/ml aprotinin and homogenized with a glass dounce homogeniser. After centrifugation for 10 min at 21,000x g, protein concentration of the supernatant was determined using the Bradford method. 30 μg of cytosolic protein extract was then used for Western blot analysis as described above. Cytochrome *c* was detected using the mouse monoclonal antibody directed against human cytochrome *c*.

3.11. Measurement of reactive oxygen species (ROS)

ROS production upon treatment with 15-LOX-2 metabolites was measured using the dye 2', 7'-Dichlorodihydrofluorescein diacetate (DCFH-DA). DCFH-DA, a nonfluorescent cell-permeant compound, is cleaved by endogenous esterases once inside the cell and the de-esterified product becomes the fluorescent compound 2'7'-dichlorofluorescein upon oxidation by ROS (Bass et al., 1983; Cathcart et al., 1983). Prior to the treatments, cells were then incubated with 10 μM DCFH-DA at 37^o C for 15 min and then

washed twice in PBS supplemented with 10 mM glucose. Washed cells were resuspended in the same buffer and treated with either 10 μM 15-(*S*)-HPETE or 40 μM 15-(*S*)-HETE for various time periods and ROS measurement was carried out on FACSCalibur flow cytometer. Data were collected using the data acquisition program CELLQuest (Becton Dickinson, San Jose, CA). DCF data was collected with the following excitation and emission wavelengths: λ_{exc} = 488 nm, λ_{em} = 525 nm. 10,000 cells were analyzed per sample.

3.12. Estimation of the cellular glutathiones (GSH & GSSG)

After the treatments with 15-(*S*)-HPETE (10 μM) or 15-(*S*)-HETE (40 μM), equal number of cells were collected and washed twice with phosphate buffered saline, lysed and protein concentrations were estimated. The cell lysates were then incubated with sulfosalicylic acid (10 % w/v) for 10 min to precipitate the proteins and centrifuged at 10,000xg for 5 min to remove denatured proteins. GSH was determined by enzymatic method described elsewhere (Tietze, 1969). Briefly, 25 μl of the cell extract was incubated in 1 ml of a reaction mixture containing 0.1 M sodium phosphate buffer (pH. 7.5), 5 mM EDTA, 0.6 mM DTNB, 0.2 mM NADPH and 1 Unit/ml glutathione reductase at 25°C and then the increase in absorbance at 412 nm was monitored for 4 min. For determination of GSSG, the same DTNB recycling assay was performed after using 2-vinylpyridine to remove the reduced GSH. Briefly, 2 μl of 2-vinylpyridine and 6 μl of triethanolamine were simultaneously mixed with 100 μl of the sample, followed by incubation in the dark at room temperature for 1 h before initiation of the recycling assay.

The kinetics of the reaction was monitored for 4 min. The increment in absorbance at 412 nm was converted to GSH concentration using a standard curve with known amounts of GSH.

3.13. Caspase-3 activity assay

After the stipulated treatments, $2x10^6$ cells were lysed in 100 µl of CHAPS lysis buffer by three to four freeze thaw cycles. The extracts were centrifuged at 12,000xg and resulting supernatants were used for the assay. The assay was performed according to the manufacturer's protocol (BD biosciences, USA). The assay buffer contained 20 mM PI PES, 100 mM NaCl, 10 mM DTT, 1 mM EDTA, 0 .1 % (w/ v) CHAPS, 10 % sucrose, pH-7 .2. 50 µg of the protein and 8 µM of the substrate were added to 1 ml of the assay buffer and incubated for 1 h at 37°C. Measurements were done on spectrofluorimeter with an excitation wavelength of 400 nm and an emission wavelength of 480- 520 nm.

3.14. Antioxidant enzyme assays

$5x10^6$ cells were treated with 10 µM of 15-(*S*)-HPETE or 40 µM of 15-(*S*)-HETE for stipulated time periods, centrifuged at 700xg and the cell pellet was collected. Pellet was washed twice with ice cold PBS. Cells were lysed in 200 µl of lysis buffer containing 10 mM Tris, pH 7.5, 150 mM NaCl, 0.1 mM EDTA, 0.5 % Triton-X-100, incubating on ice for 10 min. Cell lysates were spun at 12,000xg for 10 min and supernatants were collected. These cell lysates were used for the assay of all the antioxidant enzymes.

3.14.1. Assay of superoxide dismutase (SOD)

The instability of its substrate dictates an indirect assay for this enzyme. The method used depends upon the ability of superoxide dismutase to compete with the ferricytochrome *c* for superoxide anions generated by the xanthine oxidase system and thus to inhibit the reduction of cytochrome *c* (Beauchamp and Fridovich, 1971). The standard assay was performed in 1 ml of solution containing 1x 10^{-5} M ferricytochrome *c*, 5x10^{-5} M xanthine, 1x10^{-4} M EDTA, 50 µl of sample and 0.05 M potassium phosphate, pH 7.8 at 25° C. Sufficient xanthine oxidase (6x10^{-9} M) was added to produce a rate of reduction of cytochrome *c* of 0.025 absorbance per min at 550 nm. Under these specified conditions, one unit of superoxide dismutase is that amount which halved the rate of reduction of cytochrome *c*.

3.14.2. Assay of catalase

Catalase activity was assayed by the method described by Beers and Sizer (Beers and Sizer, 1952) in which the disappearance of peroxide is followed spectrophotometrically at 240 nm. The incubation mixture contained 0.05 M potassium phosphate, pH 7.0, 0.02 M hydrogen peroxide and a sample of 50 µl of the supernatant fluid in a final volume of 1 ml. The decrease in absorbance was recorded at 240 nm for 2 min. One unit of catalase was defined as the amount of enzyme, which decomposed one µmol of H_2O_2 per minute at 25°C and pH. 7.0.

3.14.3. Assay of glutathione peroxidase (GPx)

The GPx activity was measured by a modification of the procedure described by Paglia and Valentine (Paglia and Valentine, 1967). The standard

assay mixture (1 ml) contained 0.1 M potassium phosphate pH. 7, 1 mM GSH, 0.2 mM NADPH, 1.4 IU GSH-reductase, 0.25 mM H_2O_2 or 1.2 mM cumene hydroperoxide and a sample of 50 µl of cell lysate. When hydrogen peroxide was used as the substrate, 1 mM sodium azide was added to the reaction mixture in order to inhibit catalase activity. The use of two substrates permitted the measurement of two isozymes: a selenium dependent GPx (Se-GPx) which reacts with a wide variety of hydroperoxides including both hydrogen peroxide and organic hydroperoxides and a non-selenium dependent GPx, which doesn't use hydrogen peroxide as a substrate but reacts with organic hydroperoxides. GPx activity was calculated with an extinction coefficient of 6.22 $mM^{-1}.cm^{-1}$. One unit of GPx activity was defined as one nmole of NADPH oxidized per min.

3.15. Electrophoretic Mobility Shift Assay (EMSA)

The EMSA analysis was carried out according to the method described elsewhere (Chaturvedi et al., 1997). After the treatment, $3x10^6$ cells were used for the preparation of nuclear extraction. The cells were washed with PBS (1X) and harvested by centrifugation at 2000 rpm for 5 min in 200 µl of ice cold lysis buffer (20 mM Tris-HCl, pH 7.5, 10 mM magnesium acetate, 1% NP-40, 1mM PMSF, and incubated for 5 min on ice with 3-4 vortexings of 10 sec each. The nuclei were then harvested by centrifugation at 1600 rpm. The nuclear pellet was resuspended in 50 µl of nuclear extraction buffer (420 mM NaCl, 10 mM HEPES, 10 mM $MgCl_2$, 1 mM EDTA, 0.1 mM DTT and 25% glycerol) and incubated on ice for 30 min with intermittent vortexing of 10 sec each. The sample was then centrifuged at 13,000 rpm for 30 min at

4^{o} C. The supernatant collected was used for the assay after protein estimation using Bradford assay. 8 μg of nuclear extracts were incubated with ^{32}P labeled double stranded oligonucleotides [AP-1 (5' CTGAATCAACTGCTTCAA 3') or NF-κB (5' AGT TGA GGG GAC TTT CCC AGG C 3')] for 30 min at 37^{o} C and the DNA-protein complex formed was separated from free oligonucleotides on 6.6 % native acrylamide gel. The specificity of binding was also examined by competition with unlabeled oligonucleotide.

3.16. Statistical analysis

Data were presented as the mean ± SE of three independent experiments. Statistical analysis of differences was carried out by one-way analysis of variance (ANOVA) using Student-Newman-Keuls method. A *P*-value of less than 0.05 was considered as significant.

Results

4. Results

In order to understand the role of 15-LOX-1 and 15-LOX-2 pathways on the growth and multiplication of cancer cells, the effects of 13-(*S*)-HPODE and 13-(*S*)-HODE (15-LOX-1 metabolites) and 15-(*S*)-HPETE and 15-(*S*)-HETE (15-LOX-2 metabolites) on chronic myeloid leukemia cell line were analyzed. The 15-LOX-1 and 15-LOX-2 metabolites were synthesized by incubating the commercially available soybean 15-LOX with LA and AA respectively as per the methods described in the methodology and the generated products were separated on HPLC and analyzed by MS analysis. These products were then employed to test their effects on chronic myeloid leukemia cell line-K-562.

4.1. HPLC and LC-MS analysis

The 15-LOX-1 [13-(*S*)-HPODE and 13-(*S*)-HODE] and 15-LOX-2 [15-(*S*)-HPETE and 15-(*S*)-HETE] metabolites were extracted and separated on HPLC as per the procedure. When the collected peaks were rerun on HPLC, 13-(*S*)-HPODE was eluted as a single peak at 20^{th} min (Fig. 8 A), 13-(*S*)-HODE was eluted at 18^{th} min (Fig. 8 B), 15-(*S*)-HPETE has given a single peak at 16.21 min (Fig. 8 C) and 15-(*S*)-HETE has given a single peak at 11^{th} min (Fig. 8 D) under similar conditions. This is in accordance with their polarities. 13-(*S*)-HPODE and 15-(*S*)-HPETE, the hydroperoxy metabolites of 15-LOX, being polar to hydroxy metabolites [13-(*S*)-HODE and 15-(*S*)-HETE] were eluted at a later time point compared to their respective hydroxy metabolites.

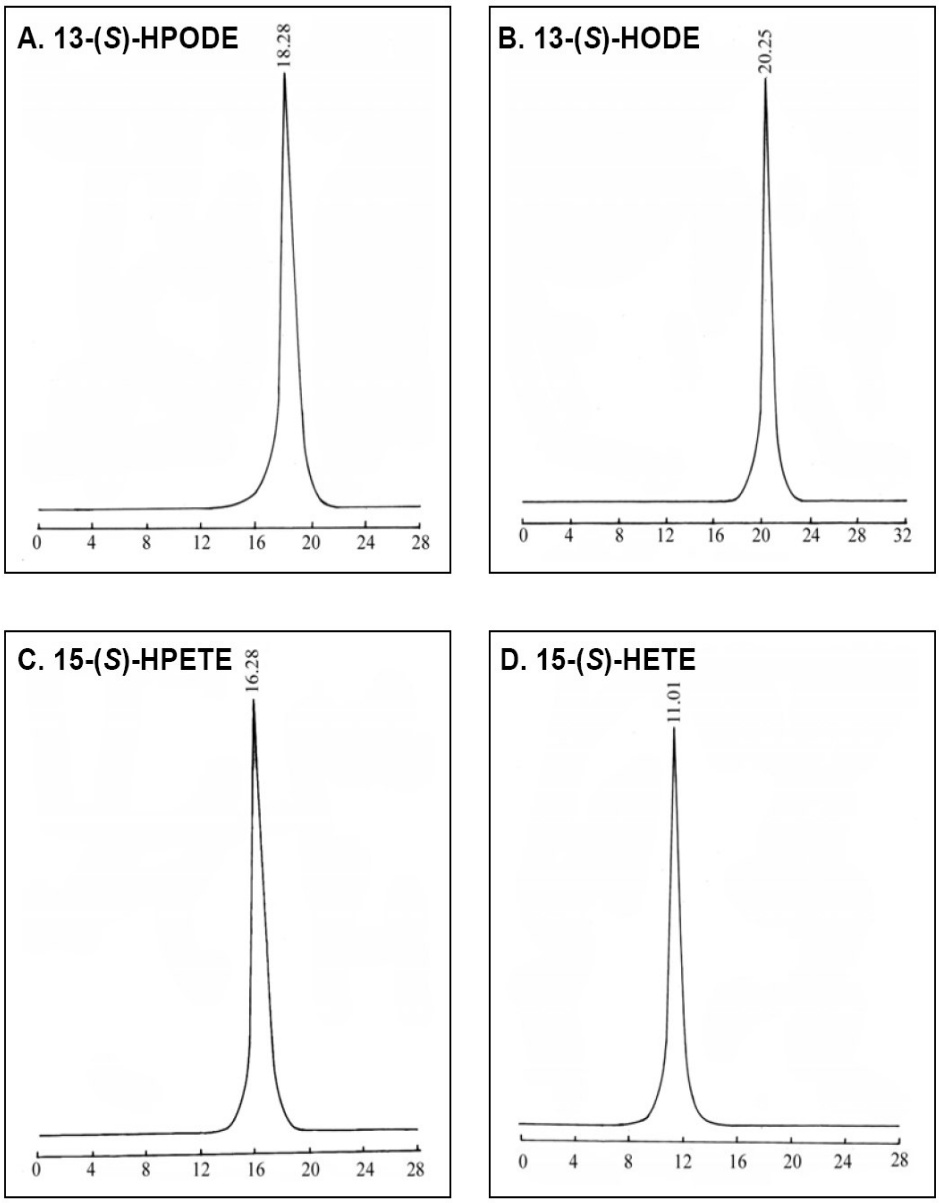

Fig. 8. HPLC chromatograms of 15-LOX-1 (13-(*S*)-HPODE and 13-(*S*)-HODE) and 15-LOX-2 (15-(*S*)-HPETE and 15-(*S*)-HETE) metabolites. **A**. 13-(*S*)-HPODE; **B**. 13-(*S*)-HODE; **C**. 15-(*S*)-HPETE; **D**. 15-(*S*)-HETE.

When these peaks were pooled and monitored on UV-VIS spectrophotometer, they gave characteristic conjugated diene spectra with a peak at 235 nm (approximated) (Fig. 9 A & B). When these peaks were

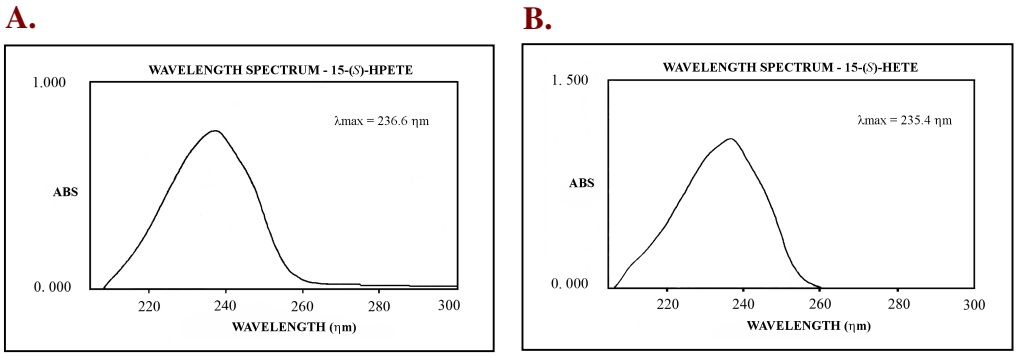

Fig. 9. Wave Length Spectra of 15-(*S*)-HPETE and 15-(*S*)-HETE. Peaks collected after HPLC separation were scanned over a wavelength range of 190 nm – 300 nm. HPLC purified fractions, when wavelength scanned, have shown characteristic conjugated diene spectra with their characteristic peak maxima. A. 15-(*S*)-HPETE, B. 15-(*S*)-HETE

subjected for mass- spectral analysis, both 15-(*S*)-HPETE and 15-(*S*)-HETE have shown characteristic mass spectra (Fig. 10 A & B). 15-(*S*)-HPETE has shown majorily a mass fragment with m/z 335.2 ($M\text{-}H^+$) including other mass fragments with m/z values 336.2 ((M^-), 318.2, 317.2, 281.2, 255.2. (Fig. 10 A) and 15-(*S*)-HETE has shown mass fragments with m/z values 319.2 ($M\text{-}H^+$) and 320.2 (M^-) (Fig. 10 B). Similar analyses were performed with 13-(*S*)-HPODE and 13-(*S*)-HODE and their identity was confirmed. The mass spectrum of 13-(*S*)-HPODE has shown a base peak with an m/z value of 311.1 ($M\text{-}H^+$) along with other mass fragments 294.2 and 293.2 (Fig. 10 C). 13-(*S*)-HODE has shown a characteristic mass spectrum containing a mass peak with an m/z value of 296.2 (M^-), base peak with an m/z value of 295.2 ($M\text{-}H^+$) and other mass fragments include 279.2 and 255.2 (Fig. 10 D).

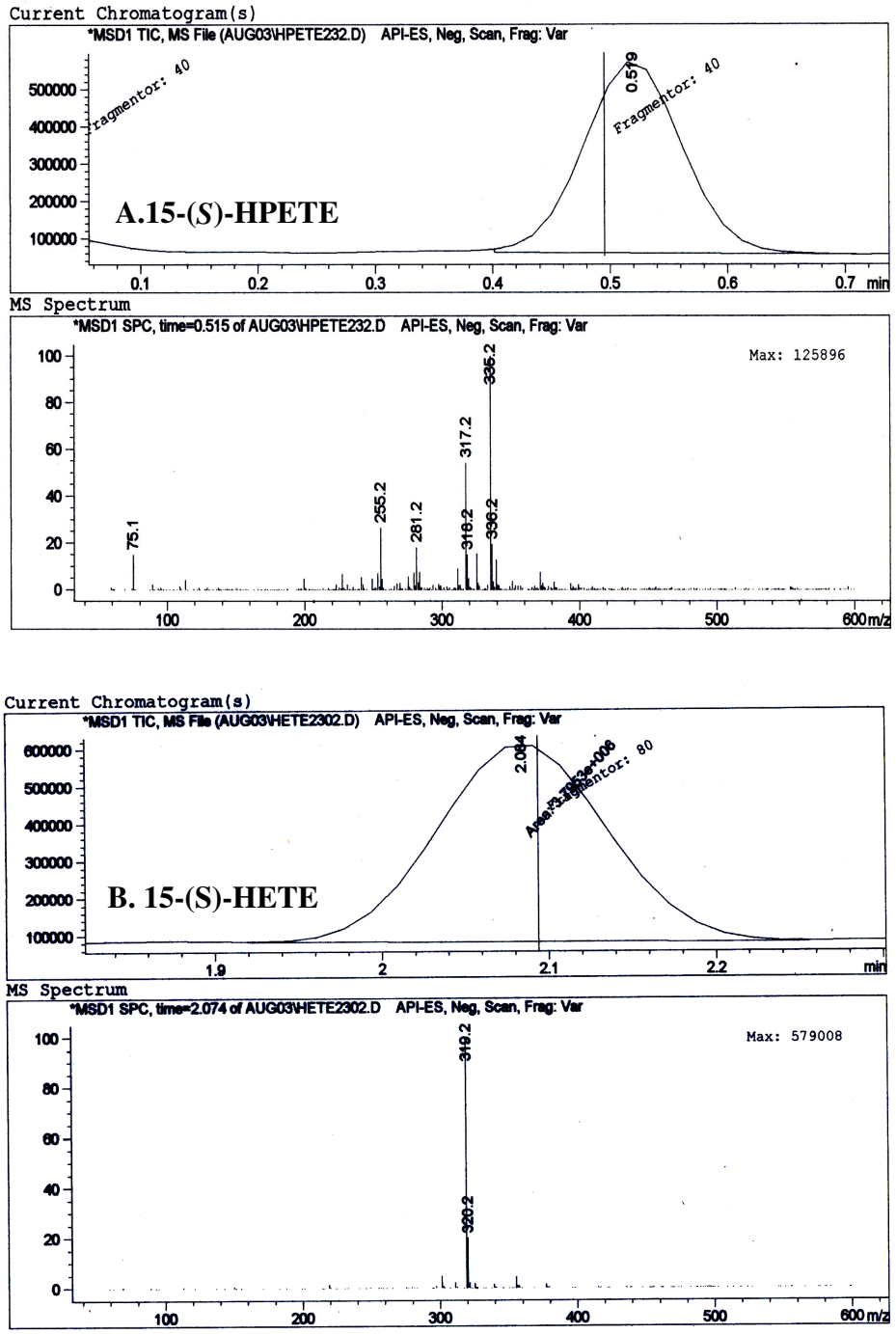

Fig. 10 A & B. LC-MS analysis of 15-LOX-2 metabolites of arachidonic acid (15-(*S*)-HPETE and 15-(*S*)-HETE). HPLC purified 15-LOX metabolites of arachidonic acid were subjected to LC-MS analysis under negative ion mode employing electron spray ionization (ESI). **A**. LC-MS chromatogram of 15-(*S*)-HPETE shows characteristic mass peak with an m/z of 336.2 (M^-) and a base peak with an m/z value of 335.2 ($M\text{-}H^+$). **B**. Mass spectrum of 15-(*S*)-HETE shows a characteristic mass peak with an m/z value of 320.2 (M^-) and a base peak with an m/z value of 319.2 ($M\text{-}H^+$).

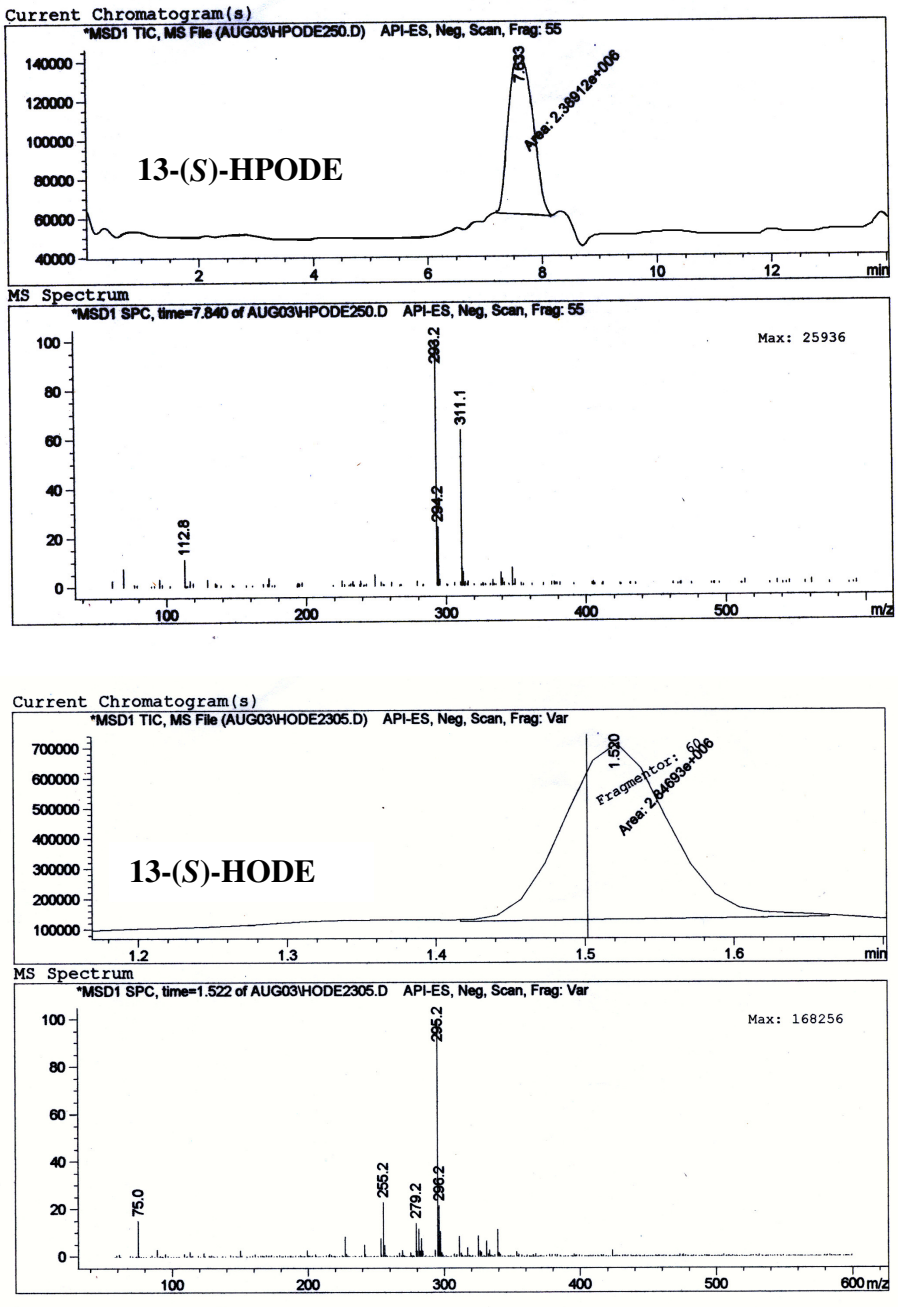

Fig. 10 C & D. LC-MS analysis of 15-LOX-1 metabolites of linoleic acid (13-(*S*)-HPODE and 13-(*S*)-HODE). HPLC purified 15-LOX metabolites of linoleic acid were subjected to LC-MS analysis under negative ion mode employing electron spray ionization (ESI). **C**. Mass spectrum of 13-(*S*)-HPODE showing a base peak of m/z value 311.1 ($M\text{-}H^+$) and other mass fragments with m/z values, 294.2 and 293.2. **D**. Mass spectrum of 13-(*S*)-HODE showing mass peak with an m/z value, 296.2 (M^-) and a base peak with an m/z value, 295.2 ($M\text{-}H^+$).

Since soybean LOX is known to generate mostly *S*-stereospecific metabolites, the LOX metabolites obtained in the present study were considered as of *S*-configuration.

4.2. Effects of 15-LOX metabolites on the growth of K-562 cell line

To test the 15-LOX metabolite-induced growth inhibition and apoptosis in K-562 cells, we first assessed the effect of 15-LOX metabolites on the survival and proliferation of these cells by MTT assay. Cells were cultured in RPMI 1640 + 10 % FBS and incubated in 1 % FBS containing medium with 1- 20 μM 15-(*S*)-HPETE and 13-(*S*)-HPODE, 1-160 μM 15-(*S*)-HETE and 13-(*S*)-HODE for 3-24 h and after the incubation, the cytotoxicity and cell proliferation were evaluated by the MTT assay. Under these experimental conditions, 15-(*S*)-HPETE and 13-(*S*)-HPODE inhibited the growth of K-562 cells rapidly by 3 h with IC_{50} values of 10 μM & 15 μM respectively (Fig. 11A & C). However, 15-(*S*)-HETE showed maximum cytotoxicity at much higher concentrations than its corresponding hydroperoxide 15-(*S*)-HPETE, with an IC_{50} value of 40 μM by 6 h (Fig. 11 B). 13-(*S*)-HODE, the hydroxymetabolite of LA, on the otherhand, showed effect only beyond 40 μM i.e at 80 μM and 160 μM concentrations. (Fig. 11 D). These results were also confirmed by trypan blue dye exclusion assay (data not shown). Further studies to elucidate the mechanism behind 15-LOX metabolite mediated cell death were carried out with 15-LOX-2 metabolites, 15-(*S*)-HPETE and 15-(*S*)-HETE with the above mentioned doses and time periods.

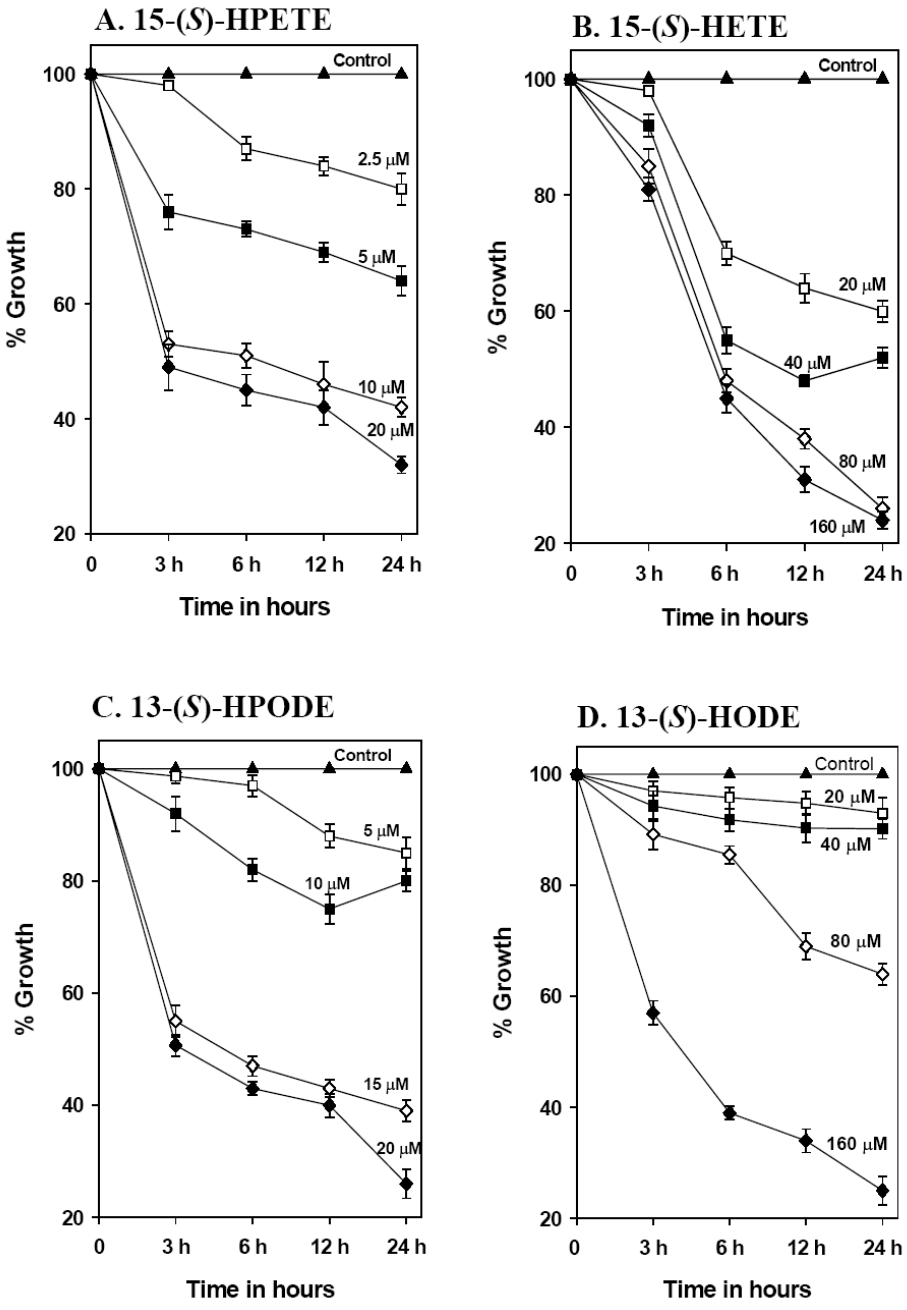

Fig. 11. Effects of 15-LOX-1 (13-(*S*)-HPODE and 13-(*S*)-HODE) and 15-LOX-2 (15-(S)-HPETE and 15-(S)-HETE) on the growth of human chronic myeloid leukemia-K-562 cell line. Cells (5 X10^3) were treated with various concentrations (as indicated in the figure) of **A**. 15-(*S*)-HPETE, **B**. 15-(*S*)-HETE, **C**. 13-(*S*)-HPODE and **D**. 13-(*S*)-HODE and the cell viability was measured by MTT assay at 3, 6, 12 and 24 h post treatment. The values represent the mean ± S.E from three independent experiments.

4.3. Phase contrast microscopy

Phase contrast microscopy pictures of K-562 cells, treated with 15-(*S*)-HPETE (10 µM for 3 h) and 15-(*S*)-HETE (40 µM for 6 h) were taken to observe the altered morphological features. Cells grown in the absence of 15-LOX-2 metabolites were round in shape with characteristic features of lymphoid cells (Fig. 12 A). However, treatments with 10 µM 15-(*S*)-HPETE (Fig. 12 B) and 40 µM 15-(*S*)-HETE (Fig. 12 C) showed altered cellular morphology with cytoplasmic shrinkage and membrane blebbing. Many cells

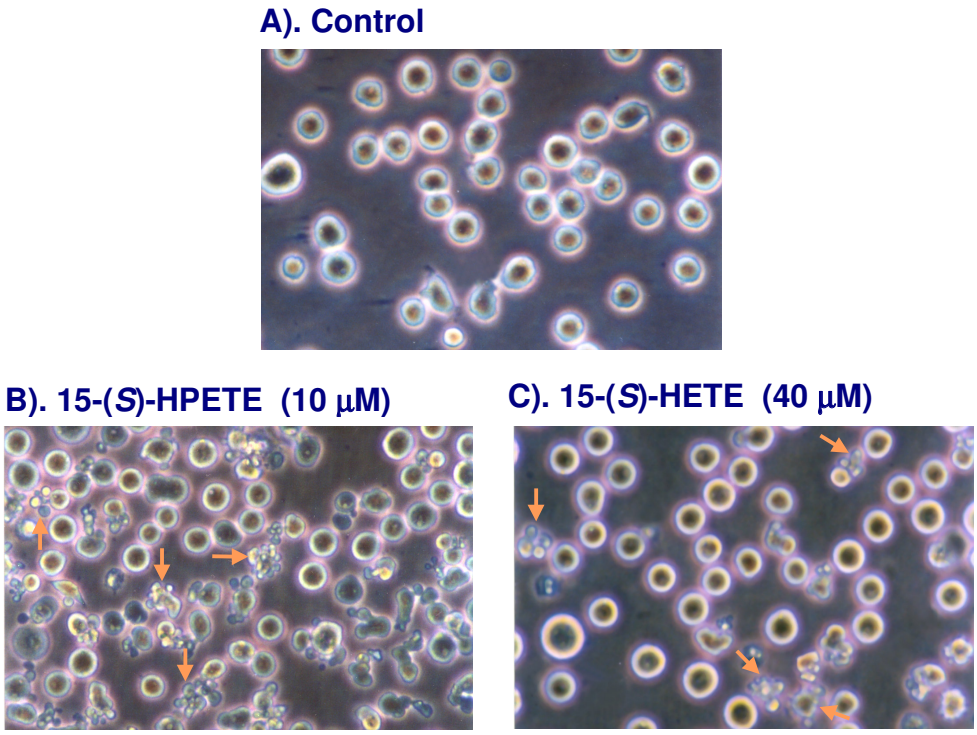

Fig. 12. Phase contrast microscopic analysis of 15-LOX-2 metabolite treated K-562 cells. K-562 cells were treated with 10 µM 15-(*S*)-HPETE for 3 h or with 40 µM 15-(*S*)-HETE for 6 h and photographed. Arrows indicate a typical apoptotic cell with apoptotic bodies (Magnification - 400X). **A**. K-562 cells treated with 0.1 % absolute ethanol (control); **B**. K-562 cells treated with 15-(*S*)-HPETE (10 µM) for 3 h; **C**. K-562 cells treated with 15-(*S*)-HETE (40 µM) for 6 h.

displayed protuberances of the plasma membrane that would eventually separate into membrane-bound apoptotic bodies. Apoptotic body formation was also clearly evident in the treatments.

4.4. Fluorescence microscopic studies

A distinguishing feature of apoptosis is the condensation and fragmentation of nuclear chromatin, which can be monitored by fluorescence microscope when stained with specific DNA binding fluorescent dyes like DAPI. K-562 cells were exposed to 15-(*S*)-HPETE (10 µM for 3 h) and 15-(*S*)-HETE (40 µM for 6 h), and then assessed for morphological signs of apoptosis by staining with DAPI. Nuclear condensation and fragmentation, hallmarks of apoptosis, were clearly observed in cells treated with 15-LOX-2 metabolites (Fig. 13 B & C). Chromatin of apoptotic cells was segregated and compacted into sharply delineated masses, very close to the nuclear envelope, where as control cells have shown intact nuclei (Fig. 13 A).

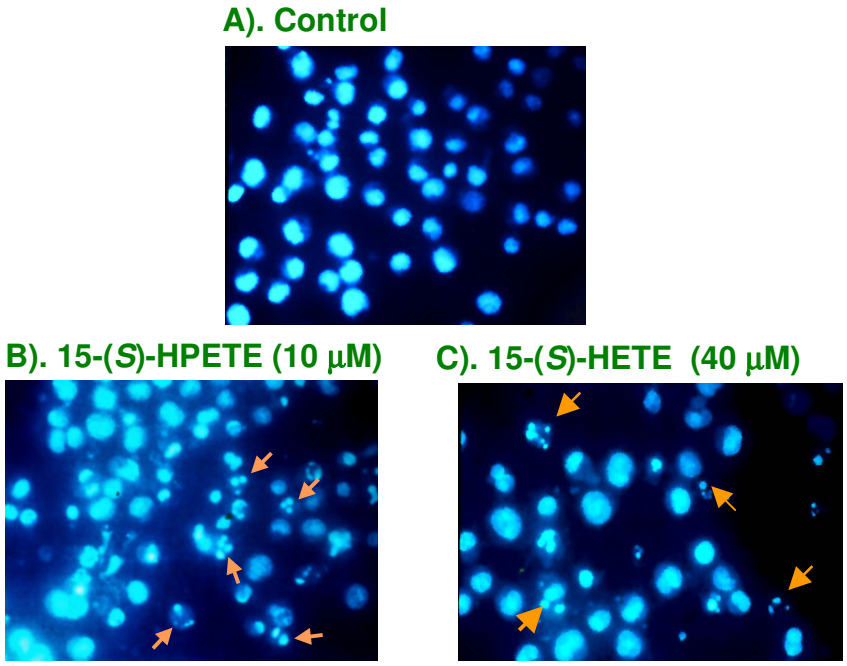

Fig. 13. Fluorescence microscopic analysis of 15-LOX-2 metabolite treated K-562 cells. Nuclear morphology of K-562 cells was observed under a fluorescence microscope (Olympus BH2RFC) after treatment with 10 µM 15-(*S*)-HPETE for 3 h and with 40 µM 15-(*S*)-HETE for 6 h and stained with DAPI. The arrows indicate the apoptotic nuclei with fragmentation and condensation (Magnification - 400X). **A**. Control (vehicle treated); **B**. K-562 cells treated with 15-(*S*)-HPETE (10 µM) for 3 h; **C**. K-562 cells treated with 15-(*S*)-HETE (40 µM) for 6 h.

4.5. Flow cytometric analysis of 15-LOX-2 metabolite-induced apoptosis

The induction of apoptosis in 15-LOX-2 metabolite treated cells was further verified and quantified by flow cytometric analysis of DNA content. Loss of DNA is a typical feature of apoptotic cells. In the present study, K-562 cells treated with 15-(*S*)-HPETE (5 µM, 10 µM for 3 h) and 15-(*S*)-HETE (20 µM and 40 µM for 6 h) were taken for FACS analysis. Fig. 14, illustrates the DNA content histograms obtained after PI staining of permeabilized cells that

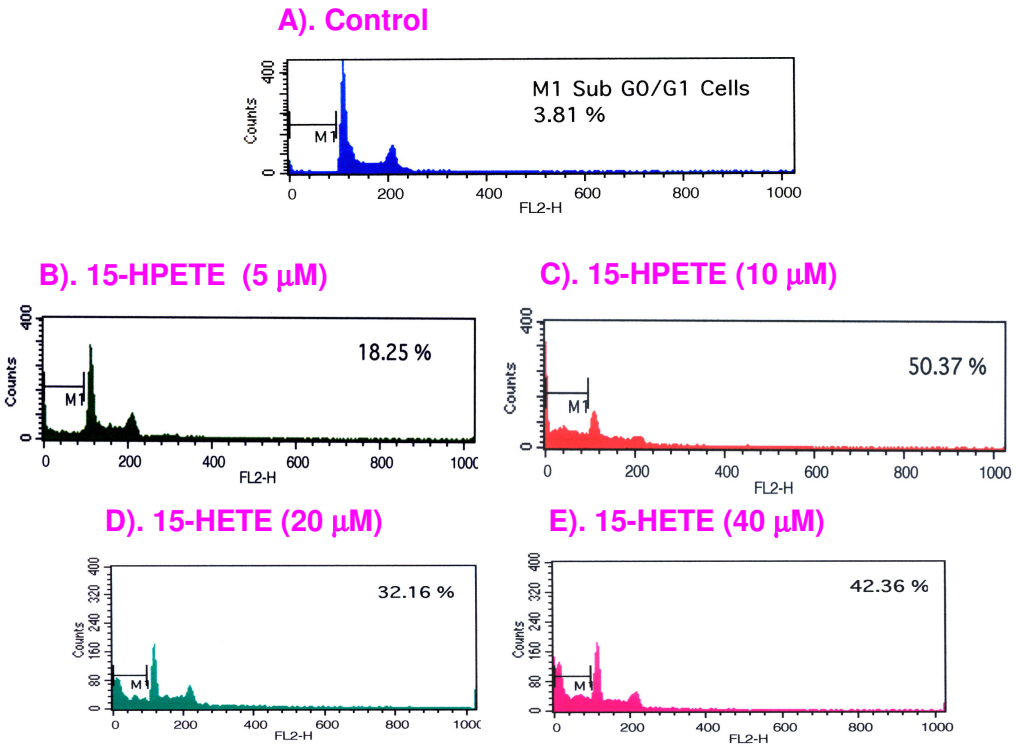

Fig. 14. Flow cytometric analysis of DNA content in K-562 cells treated with 15-(*S*)-HPETE and 15-(*S*)-HETE for induction of apoptosis. K-562 cells (1.3 x 10^6 cells) treated with 5 µM and 10 µM 15-(*S*)-HPETE for 3 h and with 20 µM and 40 µM 15-(*S*)-HETE for 6 h respectively were fixed in 1 ml of 70 % ethanol with 0.5 % Tween-20 at 4° C for 30 min and suspended in PBS. The cells were then stained with propidium iodide (PI) solution for 1 h and analyzed for DNA content by flow cytometry. Data represent the results from one of three similar experiments. **A**. Control (vehicle treated); **B**. K-562 cells treated with 15-(*S*)-HPETE (5 µM); **C**. K-562 cells treated with 15-(*S*)-HPETE (10 µM); **D**. K-562 cells treated with 15-(*S*)-HETE (20 µM); **E**. K-562 cells treated with 15-(*S*)-HETE (40 µM).

were treated with 15-LOX-2 metabolites. Typical sub-diploid apoptotic peaks were observed in K-562 cells treated with 15-(*S*)-HPETE (5 µM, 10 µM for 3 h) and 15-(*S*)-HETE (20 µM and 40 µM for 6 h). The FACS analysis of control cells, on the other hand, showed prominent G1, followed by S and G2/M phases. Only around 4 % of these cells showed hypodiploid DNA (sub G0/G1 peak) (Fig. 14 A). This value of 4 % hypodiploid DNA in control cells increased to 18.25 % and 50.37 % incase of 5 and 10 µM 15-(*S*)-HPETE (Fig. 14. B & C) treated cells and to 32.16 % and 42.36 % incase of 20 µM and 40 µM 15-(*S*)-HETE (Fig. 14. D & E) treated cells respectively. These studies thus reveal increase of hypodiploid apoptotic cells in response to 15-LOX-2 metabolite treatment in a concentration-dependent manner and the decrease of the cells in other phases of cell cycle.

4.6. 15-(*S*)-HPETE and 15-(*S*)-HETE treatment evoke cytochrome *c* release

One of the major apoptotic pathways is activated by the release of apoptogenic protein, cytochrome *c* from mitochondria into the cytosol. The release of cytochrome *c*, one of the most important respiratory-chain proteins, from the mitochondria into the cytosol is the hallmark of cells undergoing apoptosis (Liu et al., 1996; Martinou et al., 2000). To specify the molecular basis of apoptosis, the release of cytochrome *c* into the cytosol was analysed in K-562 cells treated with 15-LOX-2 metabolites by Western blot analysis employing cytochrome *c* antibodies. As shown in Fig. 15 A, the levels of cytochrome *c* in the cytosol were elevated within 1 h after treatment with 10 µM 15-(*S*)-HPETE (lanes 2 & 3) and the levels were further increased at later time points (2 h & 3 h). In case of 15-(*S*)-HETE treatment,

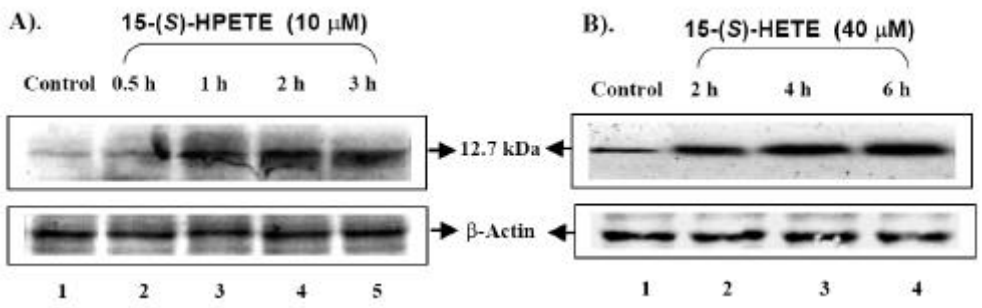

Fig. 15. Effect of 15-(*S*)-HPETE and 15-(*S*)-HETE on cytochrome *c* release. Equal quantities of protein (30 μg) from the K-562 cells treated with 10 μM 15-(*S*)-HPETE (**A**) and 40 μM 15-(*S*)-HETE (**B**) for the indicated times were analyzed by 15 % SDS-PAGE and immunoblotted with anti-cytochrome *c* antibody. β-Actin was used as control for equal loading of protein.

the same time dependent increase in the level of cytochrome *c* in the cytosol (lanes 2, 3, 4) in comparison to the control (lane 1) was observed in the Western blot analysis, but only at higher concentration (40 μM) (Fig. 15 B).

4.7. Caspase-3 activation in response to 15-(*S*)-HPETE and 15-(*S*)-HETE treatment

Cytochrome *c* leakage into the cytosol results in the activation of caspases (Li et al., 1997), a family of cysteine aspartate proteases, which cleave the cellular proteins and eventually steer a cell to undergo apoptosis. As 15-LOX-2 metabolite treatment of K-562 cells resulted in the leakage of cytochrome *c*, we examined for the activation of caspase-3. Indeed caspase-3 was activated during 15-LOX-2 metabolite-induced apoptosis as shown by Western blot analysis and caspase-3 activity assay. Western blot analysis carried out with antibodies specific to cleaved caspase-3, has clearly shown time dependent activation of caspase-3 in cells treated with both 10 μM 15-(*S*)-HPETE (Fig. 16 A) and 40 μM 15-(*S*)-HETE (Fig. 16 B).

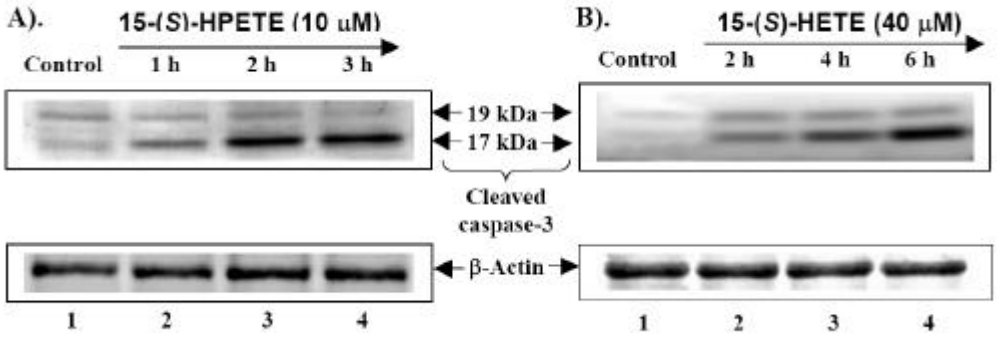

Fig. 16. Caspase-3 activation during 15-LOX-2 metabolite-induced apoptosis. Cells were treated with either 15-(*S*)-HPETE (10 μM) (**A**) or 15-(*S*)-HETE (40 μM) (**B**) for indicated time periods. After the treatments cell extracts were resolved on 12 % SDS-PAGE and probed with caspase-3 antibodies that specifically detect cleaved caspase-3 fragments. β-Actin was probed to confirm equal loding.

In order to quantify the caspase-3 activity, a fluorometric assay was carried with caspase-3 substrate, Ac-DEVD-AFC. As shown in Fig. 17 A, 10 μM 15-(*S*)-HPETE has resulted in almost 5-fold (5 ± 0.34, n=3, $P < 0.05$)

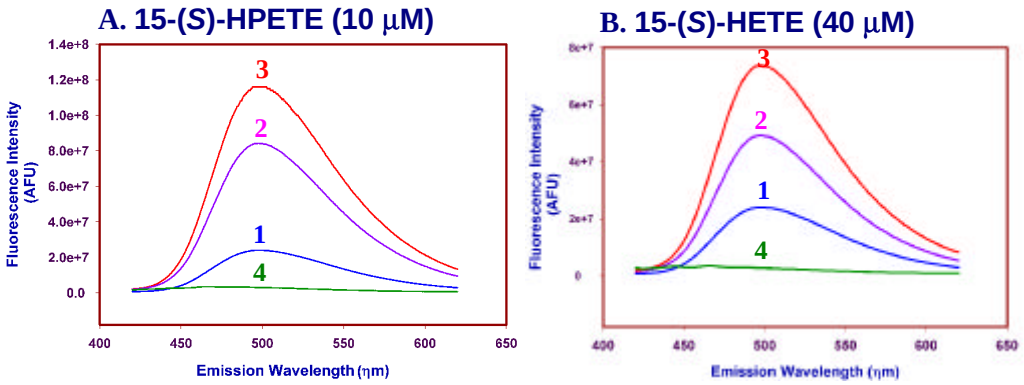

Fig. 17. Flurometric analysis of 15-LOX-2 metabolites-induced caspase-3 activation. K-562 cells after treatement with either 10 μM 15-(*S*)-HPETE (for 1, and 2 h) or 40 μM 15-(*S*)-HETE (for 2 and 4 h) were lysed and assayed for caspase-3 activity with a fluorescence caspase –3 substrate – Ac-DEVD-AFC. Ac-DEVD-CHO, a specific inhibitor for caspase-3 was used as an assay control. **A**. 15-(*S*)-HPETE (10 μM) treatments, 1. Control (vehicle treated); 2. 10 μM 15-(*S*)-HPETE – 1 h; 3. 10 μM 15-(*S*)-HPETE – 2 h; 4. 10 μM 15-(*S*)-HPETE – 2 h + Ac-DEVD-CHO (1 μg/ml). **B**. 15-(*S*)-HETE (40 μM) treatments, 1. Control (vehcle treated); 2. 40 μM 15-(*S*)-HETE – 2 h; 3. 40 μM 15-(*S*)-HETE – 4 h; 4. 40 μM 15-(*S*)-HETE – 4 h + Ac-DEVD-CHO (1 μg/ml).

increase in caspase-3 activity by 2 h post treatment (Fig. 17 A-2) compared to control (Fig. 17 A-1). Cells treated with 40 μM 15-(*S*)-HETE have shown 3.5 to 4 fold (3.5 ± 0.4, n=3, P <0.05)) increase in caspase-3 activity by 4 h (Fig. 17 B-3) when compared to control (Fig. 17 B-1). Ac-DEVD-CHO (1 μg/ml), a caspase-3 specific inhibitor, when added to the assay mixtures, completely inhibited the caspase-3 activity in both the treatments (Fig. 17 A & B-4).

4.8. Z-VAD-FMK, a broad-spectrum caspase inhibitor, prevents 15-LOX-2 metabolite-induced apoptosis

15-LOX-2 metabolite-induced apoptosis was completely abrogated when pretreated with 25 μM Z-VAD-FMK (a broad-spectrum caspase inhibitor) for 2 h (Fig. 18 A). As depicted in Fig. 18 B, upon treatment with 10 μM 15-(*S*)-HPETE and 40 μM 15-(*S*)-HETE, apoptosis from 6.2 % ± 1.2 in control raised to 43.5 % ± 3.4 (n=3, $P < 0.05$) and 37 % ± 2.5 (n=3, $P < 0.05$) respectively. Where as pretreatment with 25 μM Z-VAD-FMK resulted in the complete protection of cells from 15-LOX-2 metabolite-induced apoptosis (Fig. 18 B). As a result there were only 7.5 % ± 1.3 and 5.9 % ± 1.2 cells undergoing apoptosis with exposure to 10 μM 15-(*S*)-HPETE and 40 μM 15-(*S*)-HETE respectively, in the presence of Z-VAD-FMK. The above results clearly show that caspase-3 activation is an essential event in 15-LOX-2 metabolite-induced apoptosis.

A

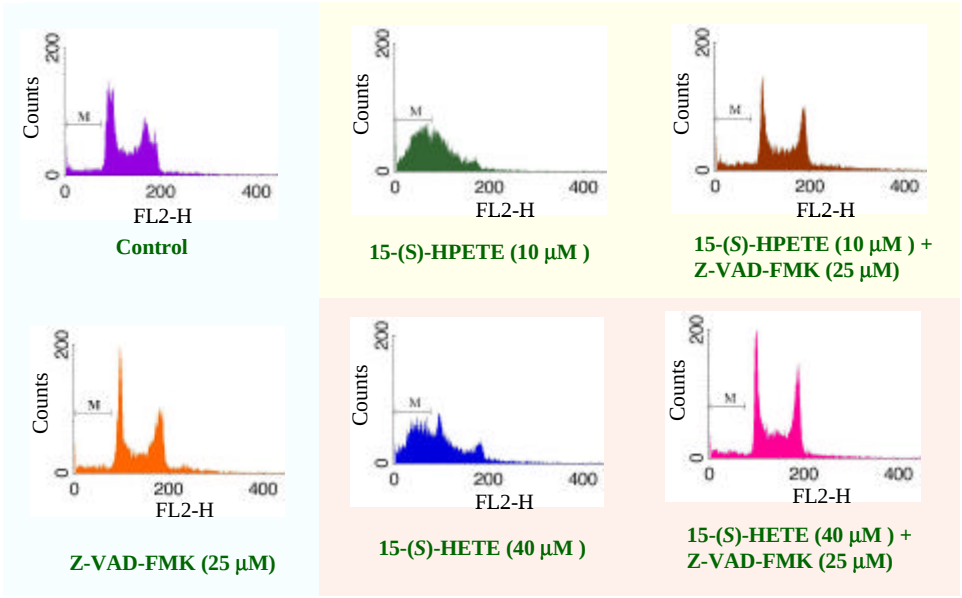

B

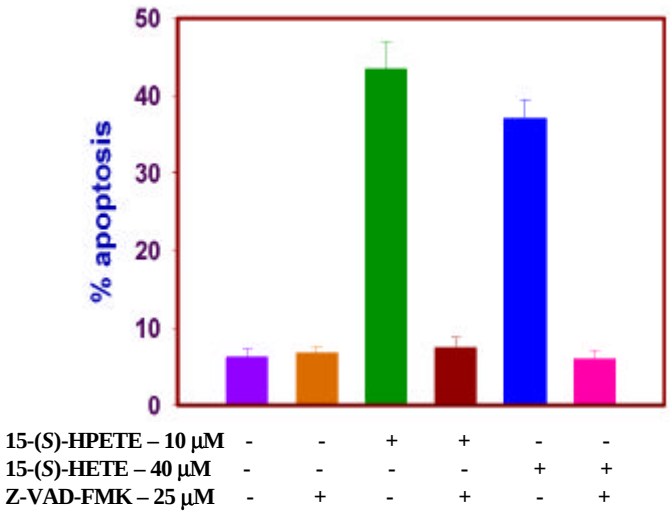

Fig. 18. Protective effect of Z-VAD-FMK, a broad spectrum caspase inhibitor, on 15-LOX-2 metabolite-induced apoptosis. K-562 cells were preincubated with a cell permeable caspase inhibitor, Z-VAD-FMK (25 µM) for 1 h and then treated with either 10 µM 15-(*S*)-HPETE for 3 h or with 40 µM 15-(*S*)-HETE for 6 h and scored for apoptosis induction on flow cytometer using propidium iodide staining. **A**. Flow cytometric histograms of control and treated samples as indicated. **B**. Quantitative comparison of the induction of apoptosis by 15-(*S*)-HPETE and 15-(*S*)-HETE treated samples and the prvention of apoptosis in Z-VAD-FMK pretreated cells.

4.9. PARP cleavage in response to 15-LOX-2 metabolite treatment

Activated capsase-3 cleaves many vital cellular proteins including nuclear poly (ADP-ribose) polymerase (PARP), which has been implicated in many cellular processes such as apoptosis and DNA repair (Casciola-Rosen et al., 1996). PARP is a 116 kDa protein and is cleaved by

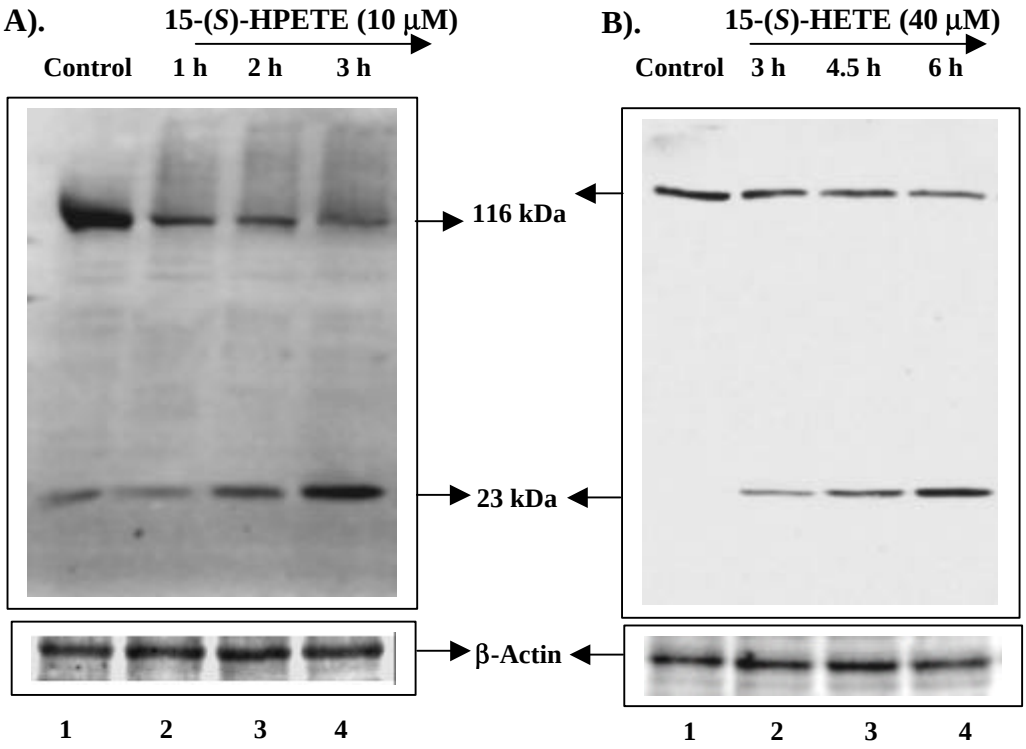

Fig. 19. Detection of PARP cleavage by Western blot analysis. K-562 cells (3.5 x 10^6) were seeded in 60 mm dishes and treated with 10 µM 15-(*S*)-HPETE (**A**) and 40 µM 15-(*S*)-HETE (**B**) for indicated time periods. 50 µg of total protein extract was separated on 12 % SDS-polyacryamide gel and electroblotted onto a nitrocellulose membrane. Intact PARP (116 kDa) and the cleavage product of PARP (23 kDa) were detected using a goat polyclonal anti-PARP antibody. β-Actin was used control for equal loading.

caspases to generate 89 and 23 kDa fragments during apoptosis. To determine whether PARP is cleaved in 15-LOX-2 metabolite induced cell death, we treated K-562 cells with 10 µM 15-(*S*)-HPETE and 40 µM 15-(*S*)-HETE as indicated and PARP cleavage was monitored with PARP antibodies, which specifically recognize the 23 kDa fragment of the cleaved PARP and

uncleaved 116 kDa PARP. Fig. 19 A & B, illustrate the gradual increase in the proportion of the 23 kDa cleavage product and simultaneous decrease in the proportion of 116 kDa uncleaved PARP, with increasing time periods after 15-LOX-2 metabolite treatment. In the control cells, however, very minute or no 23-kDa fragment of PARP was detected, except the uncleaved 116-kDa protein (lane 1).

4.10. 15-LOX-2 metabolites induced DNA fragmentation in K-562 cells

In addition to morphological evaluation, apoptosis induction by 15-LOX-2 metabolites was ascertained by using an assay developed to measure DNA fragmentation, a biochemical hallmark of apoptosis. During

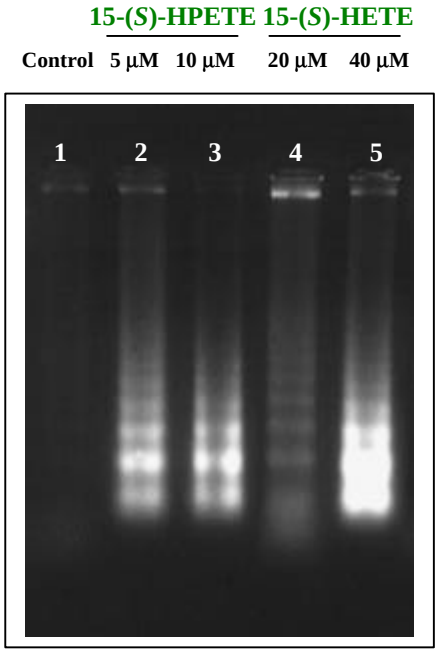

Fig. 20. Analysis of DNA fragmentation in K-562 cells treated with 15-LOX-2 metabolites. After treatment of the cells with various concentrations of 15-(*S*)-HPETE for 3 h and 15-(*S*)-HETE for 6 h, DNA was isolated and separated on 1.5% agarose gels. DNA was stained with ethidium bromide and visualized under UV light. Lane. 1: Vehicle treated control; lanes. 2-3: Cells treated with 15-(*S*)-HPETE; lanes. 4-5: Cells treated with 15-(*S*)-HETE.

later stages of apoptosis, internucleosomal cleavage of cellular DNA by endonucleases to 180 bp or oligomers of 180 bp fragments could be detected

by agarose gel electrophoresis of nuclear DNA. As illustrated in Fig. 20, agarose gel electrophoresis of DNA extracted from K-562 cells treated with 15-(*S*)-HPETE (5 µM, 10 µM for 3 h) and 15-(*S*)-HETE (20 µM and 40 µM for 6 h) show a progressive increase in the non-random fragmentation into a ladder of 180-200 bp (lanes 2-5). Such a pattern corresponds to internucleosomal cleavage, reflecting the endonuclease activity, characteristic of apoptosis. Control cells did not show any internucleosomal DNA fragmentation (lane 1).

4.11. Reactive oxygen species (ROS) mediate 15-LOX-2 metabolite - induced cell death

As ROS have been implicated in rapid induction of cell death in several studies, a possible correlation between ROS and 15-LOX-2 metabolite-induced apoptosis was examined through DCFH-DA analysis. As shown in Fig. 21 A, there was a massive outburst of ROS within minutes of post treatment as evidenced by the shift in DCF fluorescence towards right with increasing time periods after treatment with 10 µM 15-(*S*)-HPETE (2 and 3). This shift accounts for 6.29 folds over control in 30 min (2) and 8.95 folds over control in 60 min (3). 15-(*S*)-HETE (40 µM), however resulted in the ROS production (61% in 60 min, 82 % in 1.5 h compared to control) (3 & 4 in Fig. 21 B) that is lesser compared to 15-(*S*)-HPETE but a significant increase and accumulation of ROS was observed (Fig. 21 B). This differential ability of induction of ROS by the hydroperoxy (15-(*S*)-HPETE) and hydroxy (15-(*S*)-HETE) metabolites might play a key role in their difference in growth inhibitory effects and induction of apoptosis.

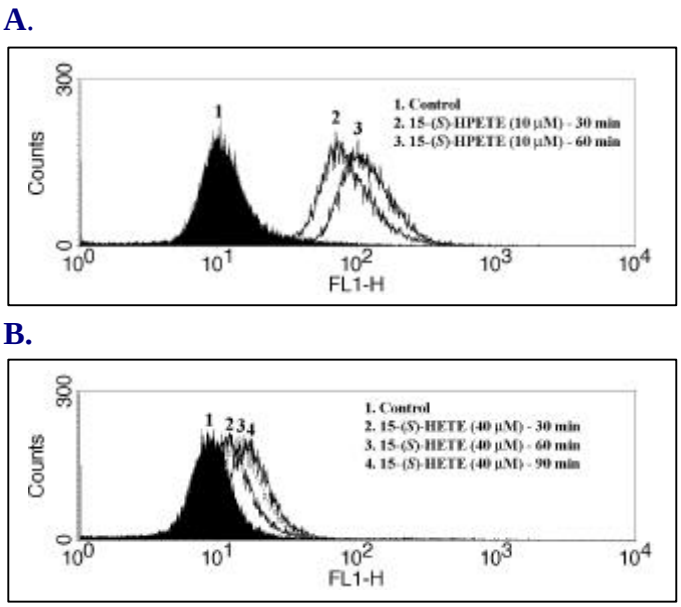

Fig. 21. DCFH-DA analysis of 15-(*S*)-HPETE and 15-(*S*)-HETE induced ROS generation in K-562 cells. K-562 cells were incubated with 10 μM DCFH-DA for 15 min and then washed and incubated in PBS (containing 10 mM glucose) with either 10 μM 15-(*S*)-HPETE or 40 μM 15-(*S*)-HETE for indicated time periods. DCF fluorescence was detected by flow cytometry after stipulated treatments using 530 nm emission filter. **A**. 1. Vehicle treated control; 2. 10 μM 15-(*S*)-HPETE –30 min; 3. 10 μM 15-(*S*)-HPETE – 60 min; **B**. 1. Vehicle treated control; 2. 40 μM 15-(*S*)-HETE –30 min; 3. 40 μM 15-(*S*)-HETE – 60 min; 4. 40 μM 15-(*S*)-HETE – 90 min

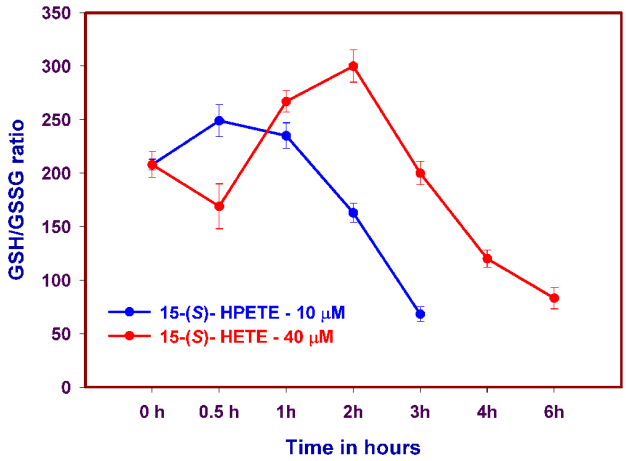

Fig. 22. Effect of 15-LOX-2 metabolites on glutathione depletion, as represented by GSH/GSSG ratio. GSH and GSSG levels were measured after treating K-562 cells with 15-(*S*)-HPETE (10 μM) and 15-(*S*)-HETE (40 μM) for indicated time periods. The cell lysates were treated with 10% sulfosalicylic acid (w/v) and the protein free extracts were used to measure GSH and GSSG levels by DTNB recycling assay. Significance over control was established at $^{(*)}$ $P < 0.05$.

We further tested, whether the ROS production in case of 15-LOX-2 metabolite treatment is associated with changes in cellular glutathione content. These studies revealed a drastic depletion of cellular GSH (reduced form of glutathione) content without any significant change in the levels of oxidized glutathione (GSSG) and thus resulting in a decrease in GSH/GSSG ratio (Fig. 22). To determine the role of ROS generation and glutathione depletion associated with it in 15-LOX-2 metabolite-induced apoptosis, K-562 cells were pretreated with 50 μM NAC (a glutathione precursor and an antioxidant) for 3 h followed by exposure to 10 μM 15-(*S*)-HPETE or 40 μM 15-(*S*)-HETE and analyzed for ROS production and inhibition of apoptosis. NAC pretreatment resulted in reduction of cellular ROS levels by 52 % incase of 15-(*S*)-HPETE (Fig. 23 A) and by 63 % incase of 15-(*S*)-HETE (Fig. 23 B) and reduced apoptotic induction by 63.2% and 47% incase of 15-(*S*)-HPETE (Fig. 23 A) and 15-(*S*)-HETE (Fig. 23 B) respectively. Apoptosis induced by 10 μM 15-(*S*)-HPETE (Fig. 25 A**,** page. 70) and 40 μM 15-(*S*)-HETE (Fig. 25 B, page. 70) was reduced by 66.8% and 55% respectively, when the cells were pretreated with 200 μM GSH. These studies unequivocally demonstrate the role of ROS and depletion of reduced glutathione in 15-LOX-2 metabolite-induced apoptosis. As shown in Fig. 26 A & 26 B (page. 71), these antioxidants inhibit the activation of caspase-3 and thereby abrogating the subsequent induction of apoptosis. The above studies thus clearly suggest a critical role for ROS in the activation of caspase-3 through cytochrome *c* leakage by perturbing mitochondrial permeability transitions.

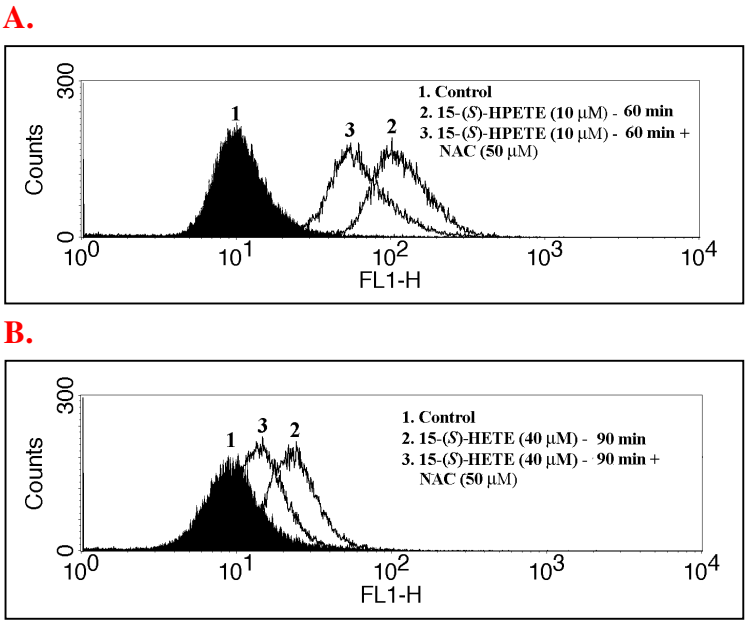

Fig. 23. DCFH-DA analysis of ROS production in K-562 cells pretreated with N-Acetyl cysteine (NAC– glutathione precursor). K-562 cells were pretreated with 50 µM NAC for 3 hr followed by treatment with 15-LOX-2 metabolites. **A**: 1. Vehicle treated control; 2. 10 µM 15-(*S*)-HPETE – 60 min; 3. 10 µM 15-(*S*)-HPETE – 60 min + 50 µM NAC; **B**: 1. Vehicle treated control; 2. 40 µM 15-(*S*)-HETE – 90 min; 3. 40 µM 15-(*S*)-HETE – 90 m in + 50 µM NAC. Data presented represent one of the three independent experiments.

4.12. 15-LOX-2 metabolites activate NADPH Oxidase to generate ROS and subsequently induce apoptosis

To find the possible involvement of NADPH oxidase activation in ROS production, we studied the effect of DPI pretreatment, a pharmacological inhibitor of NADPH oxidase on 15-LOX-2 metabolite-induced apoptosis. Pretreatment of K-562 cells with 10 µM DPI for 1 h followed by treatments with 10 µM 15-(*S*)-HPETE for 1 h or 40 µM 15-(*S*)-HETE for 1.5 h, resulted in the reduction intracellular ROS levels and shift in the DCF fluorescence towards control as shown in Fig. 24 A & B. DPI pretreatment inhibited of ROS production induced by 15-(*S*)-HPETE by 85 % and that of 15-(*S*)-HETE by 76 %. These results substantially demonstrate that NADPH oxidase is the site of ROS production by 15-(*S*)-HPETE and 15-(*S*)-HETE, though the

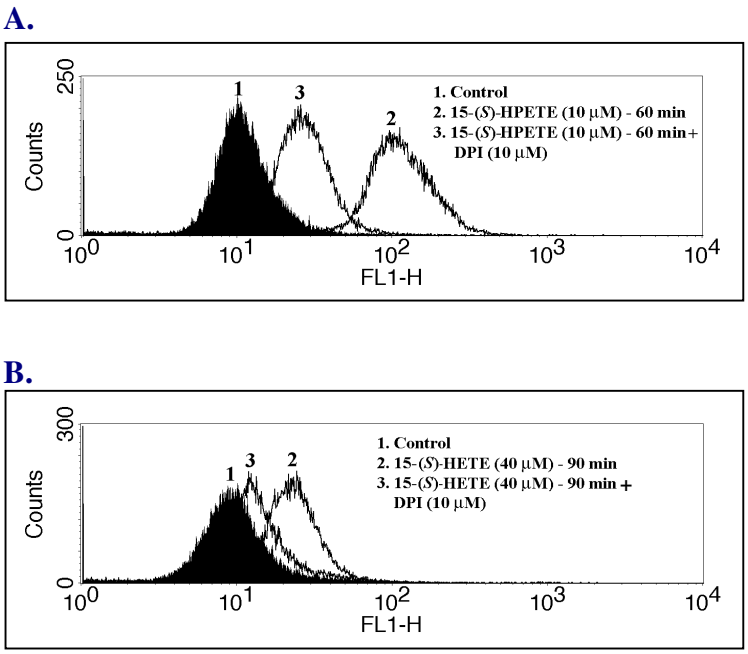

Fig. 24. Inhibition of ROS production in K-562 cells by DPI, an NADPH oxidase inhibitor. K-562 cells were pretreated with 10 µM DPI, an NADPH Oxidase inhibitor for 1 h and followed by the treatment with 15-LOX-2 metabolites and analysed for ROS production. **A**: 1. Vehicle treated control; 2. 10 µM 15-(*S*)-HPETE – 60 min; 3. 10 µM 15-(*S*)-HPETE + 10 µM DPI. and **B**: 1. Control, 2. 40 µM 15-(*S*)-HETE – 90 min 3. 40 µM 15-(*S*)-HETE – 90 min + 10 µM DPI. Data presented represent one of the three independent experiments.

degree of NADPH activation varied with hydroperoxy and hydroxy metabolites. This differential ability of these metabolites to activate NADPH oxidase might have resulted in varying levels of ROS production in K-562 cells. Consequently, we sought to examine whether the inhibition of intracellular ROS production by DPI could abrogate 15-LOX-2 metabolite-induced apoptosis. When the cells pretreated with 10 µM DPI were analyzed by propidium iodide staining, a dose dependent decrease in the hypodiplod DNA content was observed as illustrated in Fig. 25 A & B. As depicted in Fig. 26 A & B, the abrogation of apoptosis by DPI pretreatment was preceded by concomitant inhibition of caspase-3 activation. As DPI, an NADPH oxidase inhibitor, was also shown to inhibit inducible nitric oxide synthase (iNOS)

(Stuehr et al., 1991), to determine the role of iNOS, we examined the effects of L-NMMA, a more specific inhibitor of iNOS on 15-LOX-2 metabolite-induced apoptosis. The results presented in Fig. 25 A & B, 26 A & B (page. 71) clearly showed that L-NMMA could neither rescue cells from cell death

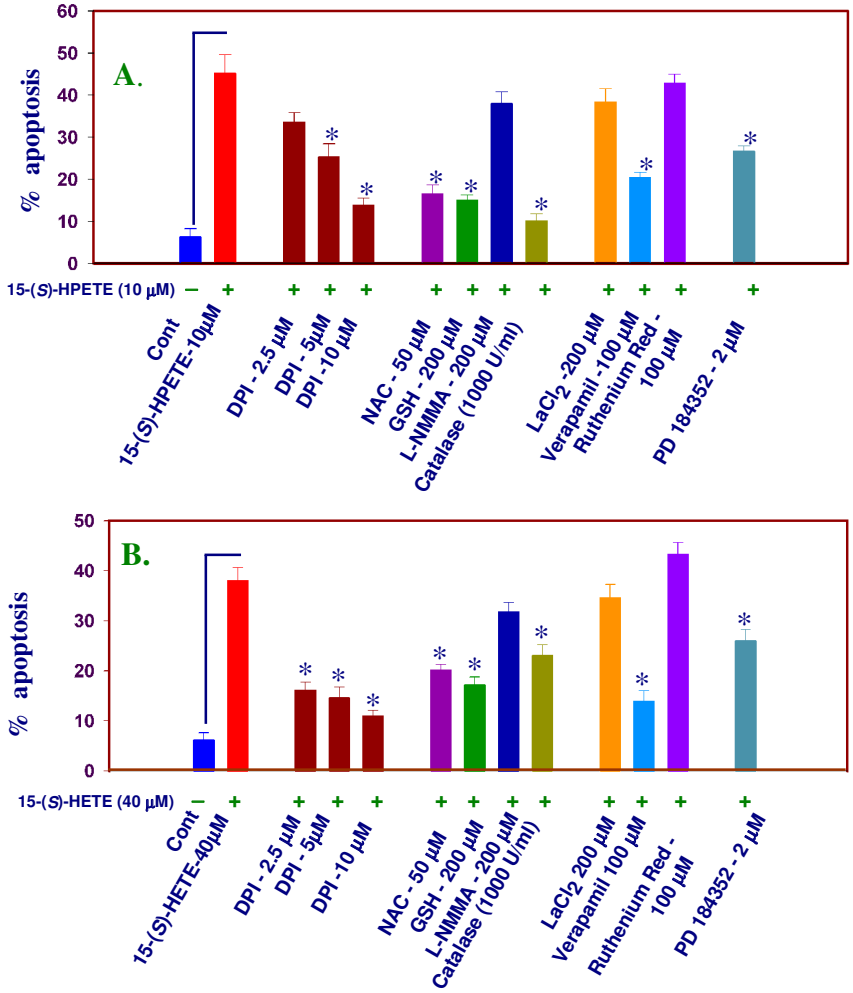

Fig. 25. Inhibitory effects of NADPH Oxidase inhibitor (DPI), ROS inhibitors (NAC, GSH, catalase), calcium channel blockers (lanthanum chloride ($LaCl_2$), ruthenium red, verapamil), iNOS inhibitor (L-NMMA), MEK inhibitor (PD-184352) on 15-LOX-2 metabolite-induced apoptosis as analysed upon propidium iodide staining by flow cytometer. K-562 cells were pretreated with various classes of inhibitors - 10 µM DPI (1 h) / 50 µM NAC (3 h) / 200 µM GSH (3 h) / 200µM L-NMMA/ 1000 U/ml catalase (1 h) / 200 µM lanthanam chloride (3 h) / 100 µM verapamil(3 h) / 100 µM ruthenium red (3 h) / 2 µM PD- 184352 (1 h) and followed by 15-LOX-2 metabolite treatment. **A**. K-562 cells treated with various inhibitors and/or 10 µM 15-(*S*)-HPETE as shown in the figure, **B**. K-562 cells treated with various inhibitors and/or 40 µM 15-(*S*)-HETE. Data represent mean ± SE from three independent experiments and the significant difference was established at $^{(*)}$ P <0.05 compared with 15-(*S*)-HPETE and 15-(*S*)-HETE alone treated samples.

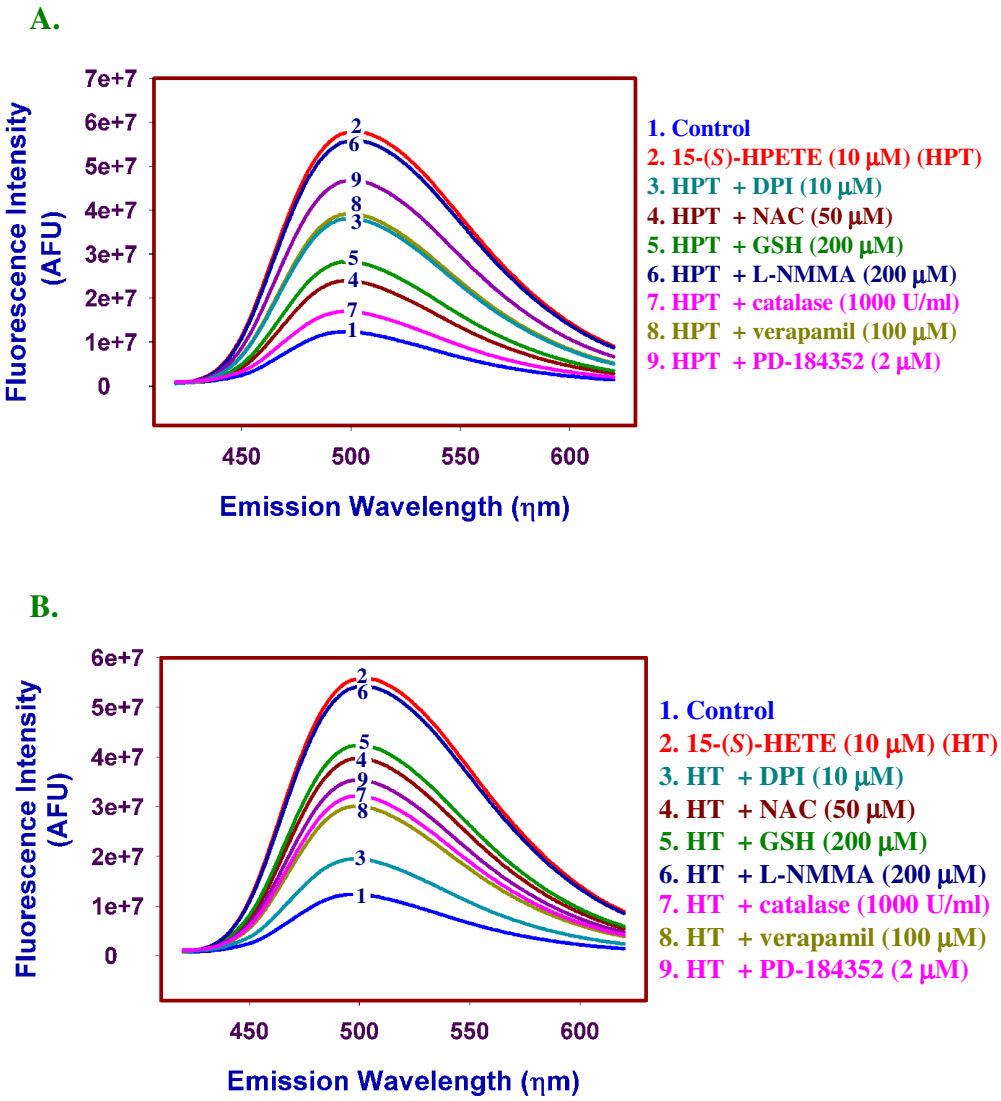

Fig. 26. Inhibitory effects of 10 µM DPI (1 h) / 50 µM NAC (3 h) / 200 µM GSH (3 h) / 200 µM L-NMMA / 1000 U/ml catalase (1 h) / 100 µM verapamil(3 h) / 2 µM PD-184352 (1 h) on 15-LOX-2 metabolites induced caspase-3 activity. K-562 cells were treated with various classes of inhibitors followed by 15-LOX-2 metabolites as shown in the figure. **A**. K-562 cells treated with various inhibitors and/or 15-(*S*)-HPETE (10 µM); **B**. K-562 cells treated with various inhibitors and/or 15-(*S*)-HETE (40 µM). Data represent one of the three independent experiments carried out.

nor inhibit caspase-3 activation, excluding the role of iNOS in 15-LOX-2 metabolite induced apoptosis. These data further substantiates that NADPH oxidase is the site for ROS production that led to the induction of apoptosis and DPI could prevent these effects.

4.13. Role of Calcium channel blockers in 15-LOX-2 metabolite-induced apoptosis

The association and mutual influence of Ca^{2+} and ROS generation has been well documented (Supiniski et al., 1999; Lee et al., 2000) and the release of calcium from endoplasmic stores has been suggested to play an important role in LOX metabolite-induced apoptosis (Maccarrone et al., 2000). To examine the role of Ca^{2+} in the rapid induction of apoptosis by 15-LOX-2 metabolites, K-562 cells were pretreated with 200 µM lanthanum chloride ($LaCl_2$), a store operated Ca^{2+} channel blocker, 100 µM verapamil, an L-type voltage dependent Ca^{2+} channel blocker, 100 µM ruthenium red, an endoplasmic reticulum calcium channel blocker for 3 h followed by 10 µM 15-(*S*)-HPETE for 3 h or 40 µM 15-(*S*)-HETE for 6 h. Following the completion of the above treatments, the cells were analysed for apoptotic induction by propidium iodide staining. Both $LaCl_2$ and ruthenium red did not show any significant inhibition of 15-LOX-2 metabolite-induced apoptosis (Fig. 25 A & B, page. 70). Whereas pretreatment with 100 µM verapamil resulted in the reduction of apoptosis by 55 % from 10 µM 15-(*S*)-HPETE treated samples (Fig. 25 A) and by 63 % incase of 40 µM 15-(*S*)-HETE treatment (Fig. 25 B). This inhibition of apoptosis by verapamil was also observed to be associated with inhibition of caspase-3 activation as shown in Fig. 26 A & B, page. 71). However, pretreatment with any of these inhibitors including verapamil did not show any effect on ROS production (data not shown) suggesting that either ROS might precede Ca^{2+} influx or Ca^{2+} might

independently act at mitochondrial level by bringing in permeability changes, leakage of cytochrome *c* and subsequent caspase-3 activation.

4.14. Effect of 15-LOX-2 metabolites on antioxidant enzymes

Rapid accumulation of intracellular ROS will result in impairment of cellular antioxidant defense system, turn detrimental to the cell survival and ultimately concedes the cell to undergo cell death. To determine the effect of 15-LOX-2 metabolite generated ROS on various antioxidant enzymes, cells were treated with either 10 µM 15-(*S*)-HPETE or 40 µM 15-(*S*)-HETE for indicated time periods and enzyme activities were measured in the cell extracts. 15-(*S*)-HPETE (10 µM) has drastically decreased catalase activity where as 15-(*S*)-HETE (40 µM) did not significantly inhibit catalase activity (Fig. 27). These results suggest a possible accumulation of H_2O_2 in K-562

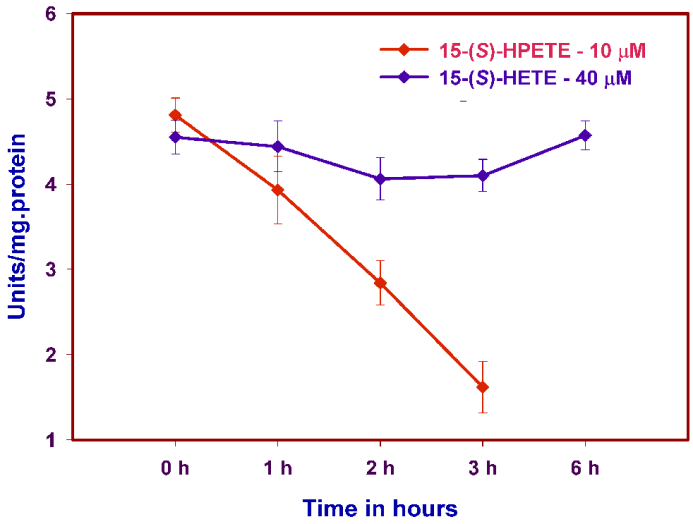

Fig. 27. Effect of 15-LOX-2 metabolites on catalase activity. K-562 cells were treated with either 10 µM 15-(*S*)-HPETE or 40 µM 15-(*S*)-HETE for indicated time periods and cells were lysed, catalase activity was assayed and the values are represented as units/ mg.protein. One unit of catalase was defined as the amount of enzyme, which decomposed one µmol of H_2O_2 per minute at 25°C and pH. 7.0. The values represent the mean ± S.E from three independent experiments and the significant difference was established at $^{(*)}$ P <0.05 compared with the control group (0.1 % EtOH).

cells treated with 15-(*S*)-HPETE as result of inactivation of catalase, thus leading to the rapid induction of apoptosis. To test this possibility, we pretreated the K-562 cells with 1000 U/ml of catalase for 1 h, followed by 15-LOX-2 metabolites and subjected these cells for cell death analysis by PI staining. The data presented in Fig. 25 A & B (page. 70) illustrates that catalase pretreatment almost completely abrogated (by 80 %) apoptosis induced by 15-(*S*)-HPETE (10 μM) and by 55 % incase of 15-(*S*)-HETE (40 μM) substantiating the hypothesis that accumulation of H_2O_2 might result in the induction of apoptosis. Corroborating this data, pre-incubation of the cells with catalase, inhibited caspase-3 activation by 71 % and by 42 % incase of 15-(*S*)-HPETE and 15-(*S*)-HETE respectively (Fig. 26 A & B, page. 71). Other antioxidant enzymes like superoxide dismutase and glutathione peroxidase were unaffected by 15-LOX-2 metabolites. Recent studies have shown that accumulation of ROS (H_2O_2) leads to the activation of extracellular signal regulated kinase (ERK) and its pertinence to induction of apoptosis through activation of transcription factors like AP-1 (Kitamura et al., 2002). The preliminary data presented in Fig. 25 A & B show that PD-184352, a MEK inhibitor, inhibits the apoptotic induction by 41% and 31% incase of 15-(*S*)-HPETE (10 μM) and 15-(*S*)-HETE (40 μM) treatments respectively, suggesting a possible role for ERK signaling in inducing apoptosis.

4.15. Cellular glutathione peroxidase levels and induction of apoptosis by 15-LOX-2 metabolites

The 15-(*S*)-HPETE, within in the cell gets eventually converted to 15-(*S*)-HETE by cellular GPx, but in view of their differential ability to induce

ROS and apoptosis, it is conceived that cellular GPx levels play a critical role in 15-LOX-2 metabolite induced apoptosis. In order to test the role of GPx, the enzyme activity levels were measured in K-562 and other leukemic cell lines like U-937, HL-60 and Jurkat. These studies revealed very low levels of GPx activity in K-562, Jurkat and the highest levels in U-937 cells (Fig. 28).

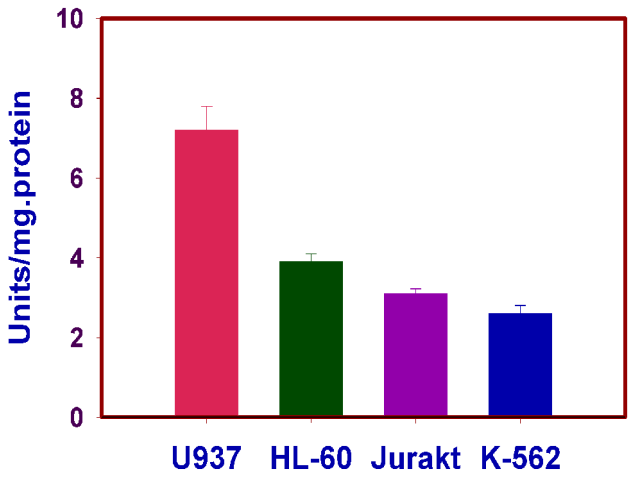

Fig. 28. Analysis of glutathione peroxidase levels in various cancer cell lines as indicated and the activity is represented as Units/mg.protein. One unit of GPx activity was defined as one nmole of NADPH oxidized per min. The values represent the mean ± S.E. from three independent experiments.

To ascertain the importance of these varying levels of GPx on growth inhibitory effects of 15-LOX-2 metabolites, we treated Jurkat and U-937 cells with different concentrations of 15-(*S*)-HPETE and 15-(*S*)-HETE and analyzed by MTT assay. Interestingly, as Fig. 29 illustrates [data with only 10 µM 15-(*S*)-HPETE and 40 µM 15-(*S*)-HETE (these are the IC_{50} values observed with K-562 cell line) were presented], U-937 cell line with high levels of GPx was found to be highly resistant and Jurkat with low levels of GPx was more sensitive to 15-LOX-2 metabolite treatment. Jurkat with

similar levels of GPx as of K-562 cell line has shown growth inhibitory effects comparable to that of K-562 cell line upon 15-LOX-2 metabolite treatment. These results clearly suggest that cellular GPx levels play an important role in 15-LOX-2 metabolite-induced apoptosis.

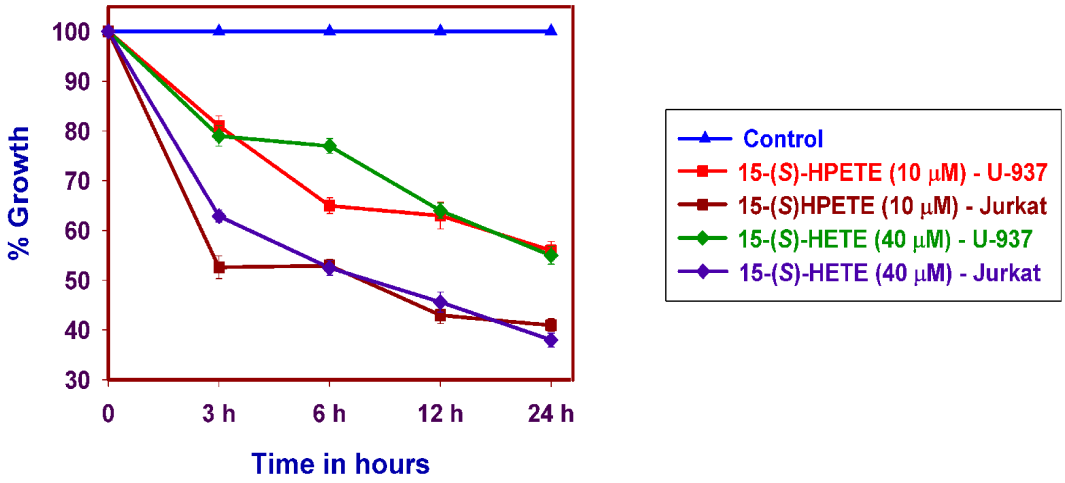

Fig. 29. Growth inhibitory effects of 15-LOX-2 metabolites on U937 & Jurkat cell lines. 5 x 10^3 cells were treated with 10 µM 15-(*S*)-HPETE and 40 µM 15-(*S*)-HETE for 3, 6, 12, 24 h and analysed by MTT assay as described in methodology. Data presented represent the mean ± SE from three independent experiments and the significance over control was established at $^{(*)}$ P <0.05.

4.16. Effect of 15-LOX-2 metabolites on transcription factors AP-1 and NF-kB

Activator protein (AP-1) and nuclear factor-kB (NF-kB) are two important transcription factors that are sensitive to redox changes and get translocated to nucleus during oxidative stress and bring in transcriptional changes (Morel and Barouki, 1999). Several studies have shown a critical role played by these transcription factors in mediating induction of apoptosis (Baeuerie and Baltimore, 1996; Ameyar et al., 2003). To examine the activation of these transcription factors during 15-LOX-2 metabolite-induced apoptosis, nuclear extracts were isolated from the cells treated with either 5 µM, 10 µM, 20 µM 15-(*S*)-HPETE or with 10 µM, 20 µM, 40 µM 15-(S)-

HETE for 1 h and electrophoretic mobility shift (EMSA) analysis was carried out. As illustrated in Fig. 30 A, 15-(S)-HPETE (lanes 6 and 7) and 15-(*S*)-HETE (lanes 8, 9, 10) have shown significant activation of AP-1 in a dose

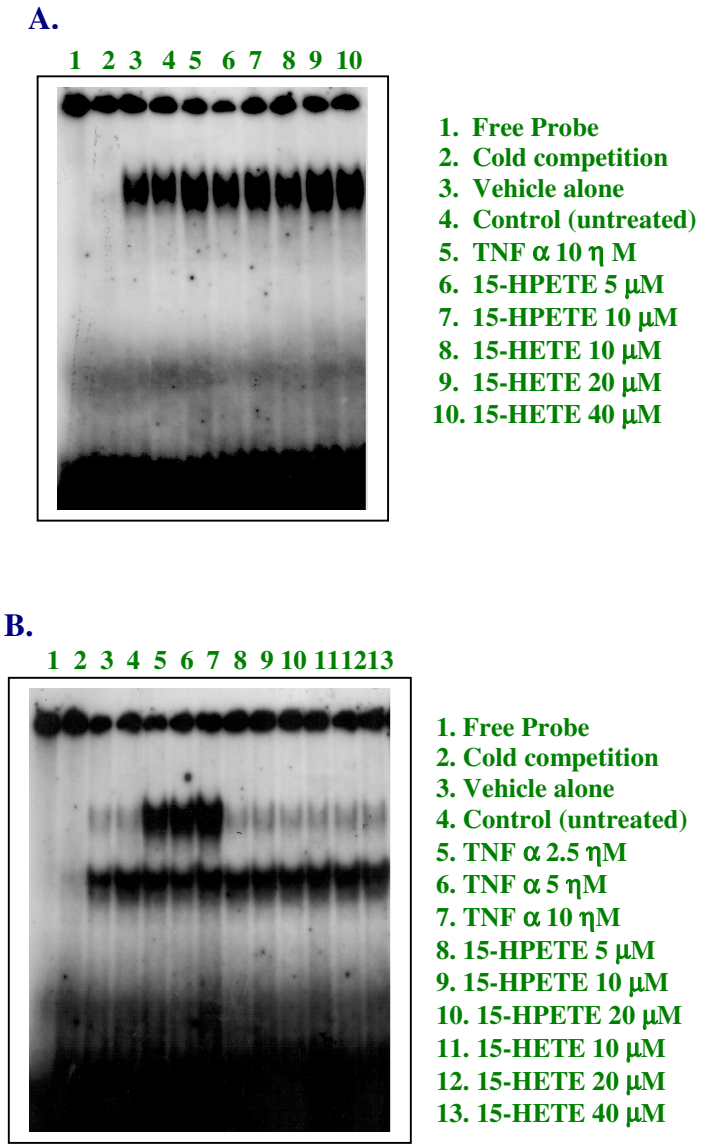

Fig. 30. EMSA analysis of Activator Protein-1 (AP-1) (A) and Nuclear Factor-κB (NF-κB) (B). K-562 cells were treated as indicated. After the treatments, nuclear extracts were isolated from treated cells and EMSA analysis was carried out as mentioned in the methodology.

dependent manner, compared to control (untreated, lane 4) and vehicle treated (lane 3) samples. However, activation of another redox sensitive transcription factor NF-kB was not observed in response to 15-LOX-2 metabolite treatments. As shown in Fig. 30 B 15-(*S*)-HPETE (lanes 8, 9 and 10) and 15-(*S*)-HETE did not show any significant change in the activation of NF-kB compared to the control (lane 4) and vehicle treated (lane 3) samples. These results clear indicate that AP-1 but not NF-kB get activated during 15-LOX-2 metabolite-induced apoptosis.

Discussion

5. Discussion

Lipoxygenases (linoleate: oxygen oxido reductase EC 1.13.11.12) are a group of closely related non-heme iron containing dioxygenases. These enzymes catalyze the addition of molecular oxygen into polyunsaturated fatty acids (PUFAs) containing cis, cis 1-4 pentadiene structures to give their hydroperoxy derivatives. Lipoxygenases (LOXs) are essentially ubiquitous among eukaryotic organisms and have been demonstrated to exist in many tissues of numerous higher plants and animals. LOX reactions may initiate the synthesis of a signaling molecule or be involved in inducing structural or metabolic changes in the cell. LOXs are classified according to their positional specificity of arachidonate oxygenation (Yamamoto et al., 1997). Depending on the site of oxygen insertion on AA, these enzymes are designated as 5-, 8-, 12- and 15-LOXs. While the predominant animal LOXs are 5-LOX, 8- LOX, 12-LOX and 15-LOX, the plant LOXs include 5-LOX and 15- LOX (Brash, 1999).

LOXs are implicated in plethora of physiological and pathological conditions. They have been shown to mediate mobilization of fatty acids for β-oxidation during embryonic development, involve in erythrocyte, keratinocyte maturation and lens epithelial cell development. In plants, LOXs favour seed germination, participate in the synthesis of traumatin, jasmonic acid, and respond to abiotic stress (Brash, 1999). Mammalian LOXs are implicated in the pathogenesis of several inflammatory disorders such as arthritis, psoriasis and bronchial asthma (Kuhn et al., 2002). They are also shown to play role in atherosclerosis, brain aging, HIV infection and kidney

diseases. Besides mediating various allergic disorders, LOXs have also been shown to mediate either regression or progression of carcinogenesis. Several LOXs form different metabolites within the arachidonic acid pathway that appear to enhance tumorigenesis. These LOXs and metabolites include 5-LOX and its products 5-(*S*)-HETE and LTB4; 8-LOX and 8-(*S*)-HETE; 12-(*S*)-LOX and 12-(*S*)-HETE; and 12-(*R*)-LOX and 12-(*R)*-HETE. 5-LOX overexpression and 5-(*S*)-HETE formation recently has been documented in prostate, lung, and other cancer cell lines. 5-LOX activation and inhibition respectively promote and inhibit the growth of prostate cancer cells (Ghosh and Myers, 1997). The expression of platelet-type 12-(*S*)-LOX mRNA and protein have been detected in prostate, melanoma (Gao et al., 1995; Timar et al., 2000), and 12-(*S*)-LOX overexpression was identified with tumor metastatic potential, skin tumorigenesis, and angiogenesis in human prostate cancers and enhanced angiogenic response in normal endothelial cells (Chopra et al., 1991; Hohn et al., 1992; Timar et al., 1992; Liu et al., 1995; Nie et al., 1998).

15-LOX-1 and -2 are two isoenzymes of 15-LOX that appear to exert important carcinogenic effects through the metabolism of polyunsaturated fatty acids. 15-LOX-1 preferentially acts on linoleic acid (18:2, ω-6) and converts it primarily to 13-hydroperoxyoctadecadienoic acid (13-(*S*)-HPODE), which will eventually be reduced to 13-hydroxyoctadecadienoic acid (13-(*S*)-HODE). In contrast, 15-LOX-2 preferentially acts on arachidonic acid (20:4, ω-6) to convert it to 15-hydroperoxyeicosatetraenoic acid (15-(*S*)-HPETE) that will be subsequently reduced to stable 15-hydroxyeicosatetraenoic acid (15-(*S*)-HETE). Several studies have suggested that 15-LOX-1 and its product

13-(*S*)-HODE enhance cell proliferation and play a procarcinogenic role (Glasgow and Eling, 1990; Ikawa et al., 1999). These proposed effects, however, were inconsistent with other findings showing that 13-(*S*)-HODE did not enhance EGF-dependent DNA synthesis in transformed Syrian hamster embryo cells that had lost tumor suppressor gene function (Hui et al., 1997). Recently it has been found that NSAIDs induce 15-LOX-1 expression in colorectal cancer cells and that 15-LOX-1 up-regulation is critical to NSAID-induced apoptosis and also these effects of NSAIDs were independent of cyclooxygenase-2 (COX-2) inhibition (Shureiqi et al., 2000 a & b). The 15-LOX-2 enzyme, expressed mainly in human tissues like cornea, prostate, lung, and skin, converts arachidonic acid mainly into 15-(*S*)-HETE (Brash et al., 1997). 15-LOX-2 expression is reduced in human prostate carcinomas (Shappell et al., 1999) and high-grade prostatic intraepithelial neoplasia (Jack et al., 2000). 15-(*S*)-HETE was shown to have antitumorigenic effects, particularly by antagonizing other procarcinogenic LOX products, such as LTB_4 and possibly 12-(*S*)-HETE (Vanderhoek et al., 1980 b).

Other studies, including our earlier studies have suggested that 15-(*S*)-HETE might or might not suppress apoptosis depending on the cancer cell type under study (Kiran Kumar et al., 1993). However, 15-(*S*)-HETE was shown to inhibit proliferation of PC3 prostate carcinoma cells, possibly through activation of PPAR-γ (Shappell et al., 2001). Recently LOX products have also been shown to induce apoptosis in human T cells, neutrophils, PC12h cells and Jurkat cells (Maccarrone, et al., 2001). These contradictory reports present a complex picture on the effects of various LOXs and in

particular 15-LOXs. The mechanistic aspects mediating these effects are still unclear. In this context, the present study is taken up to study the anticarcinogenic effects and to understand the molecular mechanisms mediated by 15-LOX metabolites in detail on chronic myeloid leukemia cell line - K-562.

5.1. Differential effects of 15-LOX-1 and 15-LOX-2 metabolites on the growth of chronic myeloid leukemia cell line - K-562

In the current study, we analysed the anticarcinogenic effects of metabolites of 15-LOX-1 (13-(*S*)-HPODE & 13-(*S*)-HODE) and 15-LOX-2 (15-(*S*)-HPETE & 15-(*S*)-HETE) on chronic myeloid leukemia (K-562) cells. While hydroperoxy LOX metabolites, 15-(*S*)-HPETE and 13-(*S*)-HPODE inhibited the growth of K-562 cells rapidly by 3 h with IC_{50} values of 10 μM & 15 μM respectively, 15-(*S*)-HETE, the hydroxy metabolite of arachidonic acid, showed maximum cytotoxicity at much higher concentrations than its corresponding hydroperoxide, 15-(*S*)-HPETE, with an IC_{50} value of 40 μM by 6 h. However, 13-(*S*)-HODE, the hydroxy metabolite of linolenic acid showed effect only beyond 40 μM i.e at 80 μM and 160 μM concentrations. Both 15-(*S*)-HPETE and 15-(*S*)-HETE have shown rapid growth inhibitory effects on K-562 cell line, the former being more potent than the latter. Among 15-LOX-1 metabolites, 13-(*S*)-HPODE showed potent growth inhibitory effects but the hydroxy metabolite, 13-(*S*)-HODE did not show significant effect even at concentrations as high as 80 μM. These results are in agreement with several other earlier reports wherein 50 μM of 13-(*S*)-HODE did not inhibit the proliferation of Caco-2 or DLD-1 colorectal carcinoma cells (Nixon

et al., 2004) and LNCaP, PC3 and DU145 prostatic cancer cell lines (Tang et al., 2002). Further studies to elucidate the molecular mechanisms associated with 15-LOX metabolite mediated cell death were carried out with 15-LOX-2 metabolites, 15-(*S*)-HPETE and 15-(*S*)-HETE with the above mentioned doses (IC_{50} values) and time periods standardized through MTT assay.

5.2. 15-LOX-2 metabolites induce apoptosis in K-562 cells

Both phase-contrast and DAPI-DNA binding fluorescent microscopic studies manifested that 15-(*S*)-HPETE and 15-(*S*)-HETE trigger rapid cell death through induction of apoptosis in K-562 cells. The current findings demonstrating the rapid induction of apoptosis by 15-LOX metabolites gain importance as the half-life of these metabolites is quite less and as they get degraded rapidly by cellular detoxification systems *in vivo*. K-562 cells treated with 10 μM 15-(*S*)-HPETE or 40 μM 15-(*S*)-HETE, revealed membrane blebbing, chromatin condensation, and formation of apoptotic bodies, characteristic features of cells undergoing apoptosis. Flow cytometric analysis of treated cells showed a prominent sub G_0/G_1 peak, both 15-(*S*)-HPETE and 15-(*S*)-HETE showed increase in the percentage of sub G_0/G_1 cells. However, 15-(*S*)-HPETE and 15-(*S*)-HETE showed differential effects, while 15-(*S*)-HPETE at 10 μM by 3 h could induce 50 % of cell death, 15-(*S*)-HETE could exert similar effects only at much higher concentrations (40 μM) by 6 h. It appears that these metabolites need a threshold concentration to initiate the induction of apoptosis, as at lower concentrations these effects are not observed. Similar effects were observed with parent polyunsaturated fatty acids, which induce apoptosis in various cancer cell lines at a threshold

concentration (Jiang, 1998). However, these parent polyunsaturated fatty acids lost their cytotoxicity when coadministered with eicosatetraynoic acid (ETYA), a substrate analogue, which completely inhibits endogenous lipoxygenase activity (Maccarrone et al., 1999). This observation clearly suggests that fatty acids have to be converted into the corresponding hydro(pero)xides in order to become proapoptotic. DNA isolated from 15-(*S*)-HPETE and 15-(*S*)-HETE treated cells has clearly shown DNA ladder formation, a characteristic gel electrophoretic band pattern associated with apoptosis. DNA ladder, the biochemical hallmark of apoptosis, is the result of DNA degradation by endogenous DNases, activated during apoptosis induction, which cleave the internucleosomal regions into double-stranded DNA fragments of 180-200 base pairs.

5.3. 15-LOX-2 metabolites induce apoptosis through intrinsic death pathway

Mitochondria play a key role in the activation or amplification of the caspase cascade via the release of cytochrome *c* from the mitochondrial intermembrane space (Liu et al., 1996). Release of cytochrome *c* into the cytosol is one of the early events that initiate apoptosis. Consistent with these findings release of cytochrome *c* in early hours was found both in case of 15-(*S*)-HPETE and 15-(*S*)-HETE treatments that increased in a time dependent manner. The levels of cytochrome *c* in the cytosol were elevated within 1 h after treatment with 15-(*S*)-HPETE and the levels were increased further at later time periods (2 h & 3 h). In case of 15-(*S*)-HETE treatment, same time dependent increase in the cytosolic level of cytochrome *c* in the cytosol compared to control was observed. Once released into the cytosol, in the

presence of dATP, cytochrome *c* participates in a protein-protein interaction with Apaf-1, which leads to the sequential activation of pro-caspases-9 and pro-caspase-3 (Li et al., 1997). In the current study, the release of cytochrome *c* is followed by a clear time dependent activation of caspase-3 that was evident from Western blot analysis carried out with antibodies specific to cleaved caspase-3, which showed clear time dependent activation of caspase-3 in cells treated with 15-(*S*)-HPETE and 15-(*S*)-HETE. Results obtained in a fluorometric assay with caspase-3 specific substrate Ac-DEVD-AFC, showed a 5 fold and approximately 4 fold increase in caspase-3 activity in cells treated with 10 μM 15-(*S*)-HPETE by 2 h and 40 μM 15-(*S*)-HETE by 4 h respectively compared to control. Z-VAD-FMK, a broad-spectrum caspase inhibitor has completely abrogated 15-LOX-2 metabolite-induced apoptosis. These results clearly suggest that apoptosis induced by 15-LOX-2 metabolites involve intrinsic death pathway mediators, caspase-9 and caspase-3. Activated caspase-3 cleaves off target substrates like poly (ADP-ribose) polymerase (PARP), a nuclear enzyme that senses DNA nicks and catalyzes the ADP ribosylation of histones and other nuclear proteins in order to facilitate DNA repair (Lazebnik et al., 1994). PARP cleavage observed in the current study provides a conclusive and definitive evidence for caspase-3 activation and the apoptosis induced thereafter by 15-LOX-2 metabolite treatments. With these findings, it is clearly demonstrated that 15-LOX-2 metabolites induce apoptosis by activating the intrinsic death pathway through a series of events involving the cytochrome *c* release, caspase-3 activation, PARP cleavage and DNA fragmentation.

5.4. ROS mediates 15-LOX-2 metabolite-induced apoptosis in K-562 cells

Association between cytochrome *c* leakage, mitochondrial permeability transition perturbations and reactive oxygen species generation (ROS) (Tan, et al., 1998; Chandra et al., 2000; Martindale and Holbrook, 2002) or intracellular Ca^{2+} release (McConkey and Orrenius 1996; Ermak and Davies, 2001) has been well documented. Even LOX product mediated apoptosis has earlier been linked to rapid intracellular Ca^{2+} influx (Maccarrone et al., 2000). ROS generation has been linked to rapid induction of apoptosis in many cases (Ling et al., 2003). In the current study, the possible involvement of ROS generation was examined through DCFH-DA analysis. The results clearly indicate a 6 to 9 fold increase in ROS generation in 15-(*S*)-HPETE treated cells with in an hour compared to control and the magnitude of ROS generation incase of 15-(*S*)-HETE is less compared to 15-(*S*)-HPETE treatment but still significantly higher compared to the control. The differential induction of ROS generation by 15-(*S*)-HPETE and 15-(*S*)-HETE might be responsible for their differential abilities to induce apoptosis. The ROS generation is associated with drastic depletion of cellular glutathione levels, a cellular anti-oxidant defense system. The depletion in the cellular glutathione levels was found to parallel 15-LOX-2 metabolite-induced apoptosis. The depletion in cellular glutathione levels is mainly because of the drop in reduced glutathione (GSH) levels rather than the increase in oxidized glutathione (GSSG) levels. This drop in GSH levels without changes in GSSG levels might be because of the inhibition of GSH synthesis or an increased rate of GSH efflux. Decrease in intracellular GSH levels in a similar model of

oxidative stress mediated Fas induced apoptosis was attributed to increased rate of GSH efflux (van den Dobbelsteen et al., 1996). N-Acetyl cysteine (NAC), a glutathione precursor and reduced glutathione (GSH) pretreatments have diminished the ROS production resulted from 15-LOX-2 metabolite treatment and subsequent activation of caspase-3 and induction of apoptosis. NAC (50 μM) pretreatment reduced apoptotic induction by 63.2% and 47% incase of 15-(*S*)-HPETE and 15-(*S*)-HETE respectively. Apoptosis induced by 10 μM 15-(*S*)-HPETE and 40 μM 15-(*S*)-HETE was reduced by 66.8% and 55% when the cells were pretreated directly with 200 μM GSH, corroborating the association between induction of ROS and depletion of reduced glutathione in 15-LOX-2 metabolite-induced apoptosis. These antioxidants indeed inhibit the activation of caspase-3 and thereby abrogating the subsequent induction of apoptosis. The ability of NAC compared to GSH to inhibit 15-LOX-2 metabolite-induced apoptosis at much lower concentrations may be attributed to the difference in their membrane permeability.

5.5. NADPH Oxidase mediates ROS generation in K-562 cells exposed to 15-LOX-2 metabolites

Diphenyl iodonium (DPI), an NADPH oxidase inhibitor, has reduced ROS produced by both 15-(*S*)-HPETE and 15-(*S*)-HETE and abrogated the activation of caspase-3 and subsequent induction of apoptosis. Pretreatment of K-562 cells with DPI (10 μM) for 1 h reduced intracellular ROS levels by 85% in case of 15-(*S*)-HPETE and by 76% incase of 15-(*S*)-HETE treatments, and inhibited the induction of apoptosis approximately by 70 % in both the cases. These results clearly indicate that ROS generated through the activation

of NADPH oxidase is an upstream event responsible for cytochrome *c* release and caspase activation in the 15-LOX-2 metabolite-induced apoptosis. Several independent studies have shown that NADPH oxidase generated ROS are critical triggers of apoptosis (Coxon et al., 1996; 2003; Zhang et al., 2003). The current study has relied on the pharmacological inhibition of the NADPH oxidase with DPI that reacts with the heme and FAD prosthetic redox groups of the membrane-bound flavocytochrome *b* of the NADPH oxidase (Doussiere et al., 1999 a & b; Jones et al., 1991). DPI also inhibits other flavoprotein-using enzymes, which would include the nitric-oxide synthase (Stuehr et al., 1991). However, L-NMMA, a more specific inhibitor of nitric oxide synthase, had no significant effect on 15-LOX-2 metabolite-induced apoptosis. These results clearly demonstrate that nitric oxide or reactive nitrogen intermediates are not essential for 15-LOX-2 metabolite-induced apoptosis and further supports the role of NADPH oxidase induced ROS generation in the 15-LOX-2 metabolite-induced apoptosis.

5.6. Calcium plays a key role in 15-LOX-2 metabolite-induced apoptosis

Inhibition of 15-LOX-2 metabolite-induced apoptosis by verapamil, an L-type voltage dependent calcium channel blocker shows that calcium influx plays a role in the induction of apoptosis but this effect might be secondary or additive effect to the ROS generation as verapamil could not inhibit ROS generated by 15-LOX-2 metabolites. These results were in agreement with the earlier studies wherein apoptosis induced by 25-hydroxycholesterol in human aortic smooth muscle cells and by cadmium in human lymphoma U937 cells through Ca^{2+} activation was significantly inhibited by verapamil (Ares et al.,

1997; Li et al., 2000). Inability of lanthanum chloride and ruthenium red to inhibit the apoptotic induction shows that either store operated calcium channels or endoplasmic reticulum channels operated through ryanodyne receptor activation might not play a role in 15-LOX-2 metabolite-induced apoptosis. However, the possibility of release of Ca^{2+} from endoplasmic reticulum stores through the activation of inositol triphosphate receptor, the other class of Ca^{2+} receptors present on endoplasmic reticulum, cannot be ruled out.

5.7. Catalase and ERK signaling in 15-LOX-2 metabolite-induced apoptosis in K-562 cells

Catalase, an antioxidant enzyme inhibited to a greater extent the apoptosis induced by 15-(*S*)-HPETE and partially that of 15-(*S*)-HETE and this result is in accordance with the differential inhibition of catalase activity by 15-(*S*)-HPETE and 15-(*S*)-HETE observed in the present study. The fact that 15-LOX-2 metabolite-induced apoptosis was inhibited by catalase, suggests the possible accumulation of H_2O_2 and its involvement in the induction of apoptosis. Rapid phosphorylation of extra cellular signal regulated kinase (ERK) and down stream activation of transcription factor, activator protein-1 (AP-1) were found to be associated with H_2O_2 induced apoptosis in cultured glomerular mesangial cells. Inhibition of phosphorylation of ERK by PD09809, a MEK inhibitor, is known to suppress the induction of c-*fos,* a component of AP-1, leading to attenuation of AP-1 activation and further inhibition of H_2O_2 induced apoptosis (Ishikawa et al., 1997; Ishikawa et al., 2000). In congruence with the above findings, the

current study showed that PD184352, a MEK inhibitor, inhibited 15-LOX-2 metabolite-induced apoptosis significantly, suggesting the activation of ERK. Consistent to the activation of ERK, electrophoretic mobility shift analysis of AP-1 in K-562 cells treated with 15-LOX-2 metabolites showed activation of AP-1 and preliminary data showed that the activation of AP-1 was attenuated by PD184352 alleviating further induction of apoptosis. However, 15-LOX-2 metabolite-induced apoptosis was not found to be associated with the activation of another redox sensitive transcription factor, nuclear factor-κB (NF-κB).

5.8. Cellular Peroxidase is critical in 15-LOX-2 metabolite-induced cell death

Glutathione peroxidase (GPx) levels across the cell lines were examined to see its effect on 15-LOX-2 metabolite-induced apoptosis, as it is the principal enzyme in reducing hydroperoxy metabolites to less toxic hydroxy metabolites (Kuhn et al., 2002). Interestingly, the levels of GPx were found to be varying across the leukemia cell lines (K-562, Jurkat, HL-60 and U-937) and its direct relevance to the antiproliferative effects of 15-LOX-2 metabolites was studied. These studies revealed high levels of GPx activity in U-937 & HL-60 cell lines compared to Jurkat and K-562. Surprisingly, not only the hydroperoxy metabolite (15-(*S*)-HPETE), but even the hydroxy metabolite, 15-(*S*)-HETE has shown diminished antiproliferative effects in cells (U-937 and HL-60) with high peroxidase activity.

5.9. A hypothesis in making

The requirement of higher concentrations of 15-(*S*)-HETE compared to 15-(*S*)-HPETE to induce apoptosis, the inability of 13-(*S*)-HODE to induce apoptosis, the differential antiproliferative effects exerted by 15-(*S*)-HETE across the cell lines with varying levels of GPx and execution of apoptosis by 15-(*S*)-HETE through similar mechanism as that of 15-(*S*)-HPETE made us to presume and propose a hypothesis. According to this hypothesis, 15-(*S*)-HETE be undergoing further changes like oxygenations after entering the K-562 cells, which render it to induce apoptosis (Fig.31). Our hypothesis draws support from earlier observations that 15-(*S*)-HETE which has got additional doubly allelic methylene groups can undergo further oxygenation once entered into the cell (Chavis et al., 1996). 15-(*S*)-HETE gets converted to a hydroperoxy, hydroxy metabolite like 5-hydroperoxy15-(*S*)-HETE or 8 hydroperoxy-15- (*S*)-HETE depending on the type of LOX present in the cell. These hydroperoxy, hydroxy metabolites of 15-(*S*)-HETE might in turn generate ROS and lead to the induction of apoptosis. In agreement with this hypothesis, chronic myeloid leukemia cells have been shown to contain other lipoxygenase enzymes like 5-LOX (Maccarrone et al., 1998; Maccarrone et al., 1999). 13-(*S*)-HODE, however, lacks the divinyl methyl groups to undergo further oxygenation and hence unable to generate ROS and induce apoptosis.

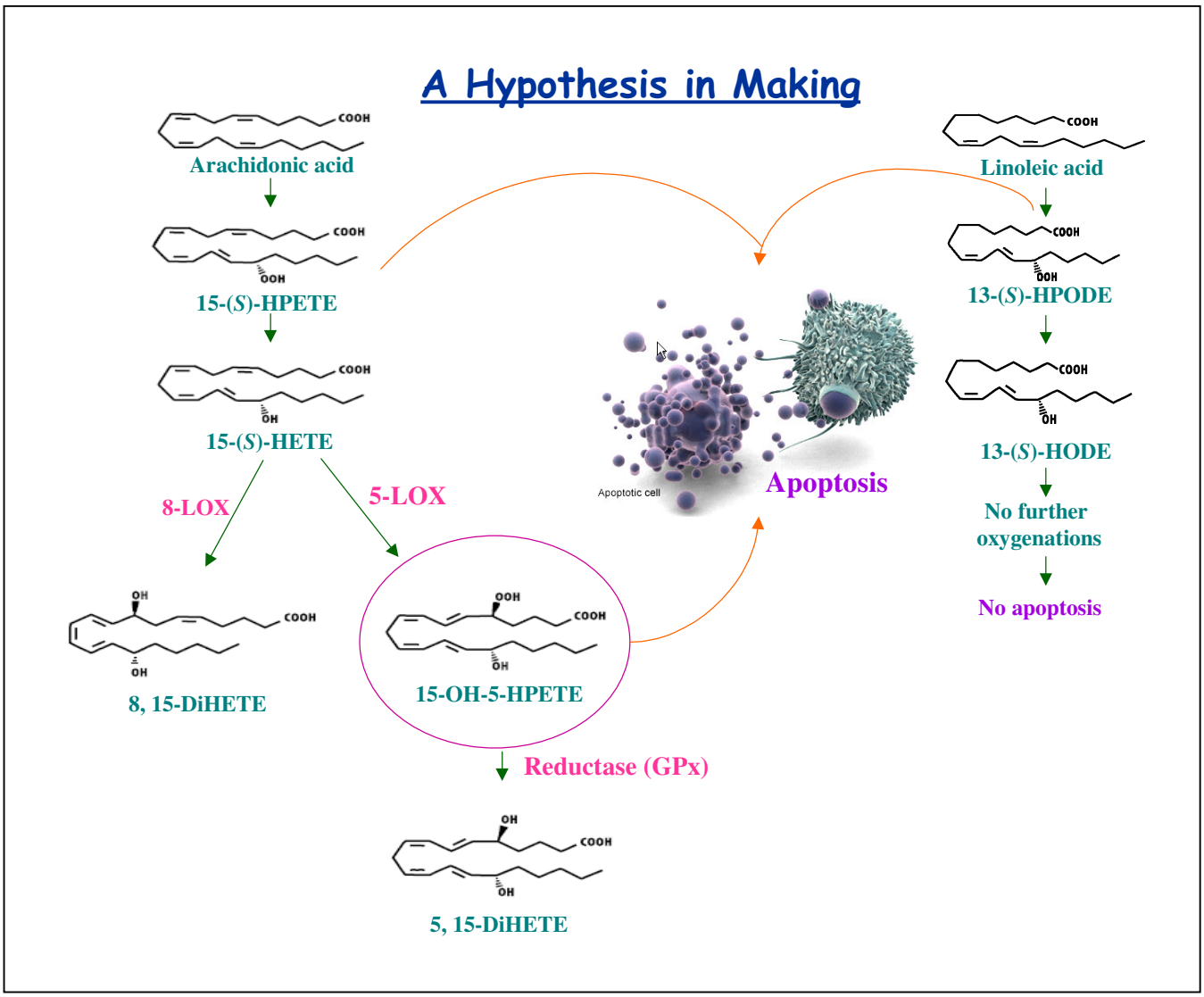

Fig. 31. A hypothesis in making

The current study was aimed at delineating the pathway of apoptotic induction by 15-LOX-2 metabolites and the molecular mechanisms associated with it. The results clearly indicate that the apoptosis induced by 15-LOX-2 metabolites is associated with the release of cytochrome *c*, activation of caspase-3, PARP cleavage and DNA fragmentation, the key events in the intrinsic death pathway of apoptosis. For the first time, the current study shows that ROS produced by NADPH oxidase activation is responsible for the

15-LOX-2 metabolite-induced apoptosis through intrinsic death pathway. In the present study, a hypothesis has been proposed which could atleast partially answer the discrepancies existing between the differential effects shown by the two 15-LOX (15-LOX-1 and 15-LOX-2) isoforms and their hydroperoxy (13 -(*S*)-HPODE and 15-(*S*)-HPETE) and hydroxy (13-(*S*)-HODE and 15-(S)-HETE) metabolites.

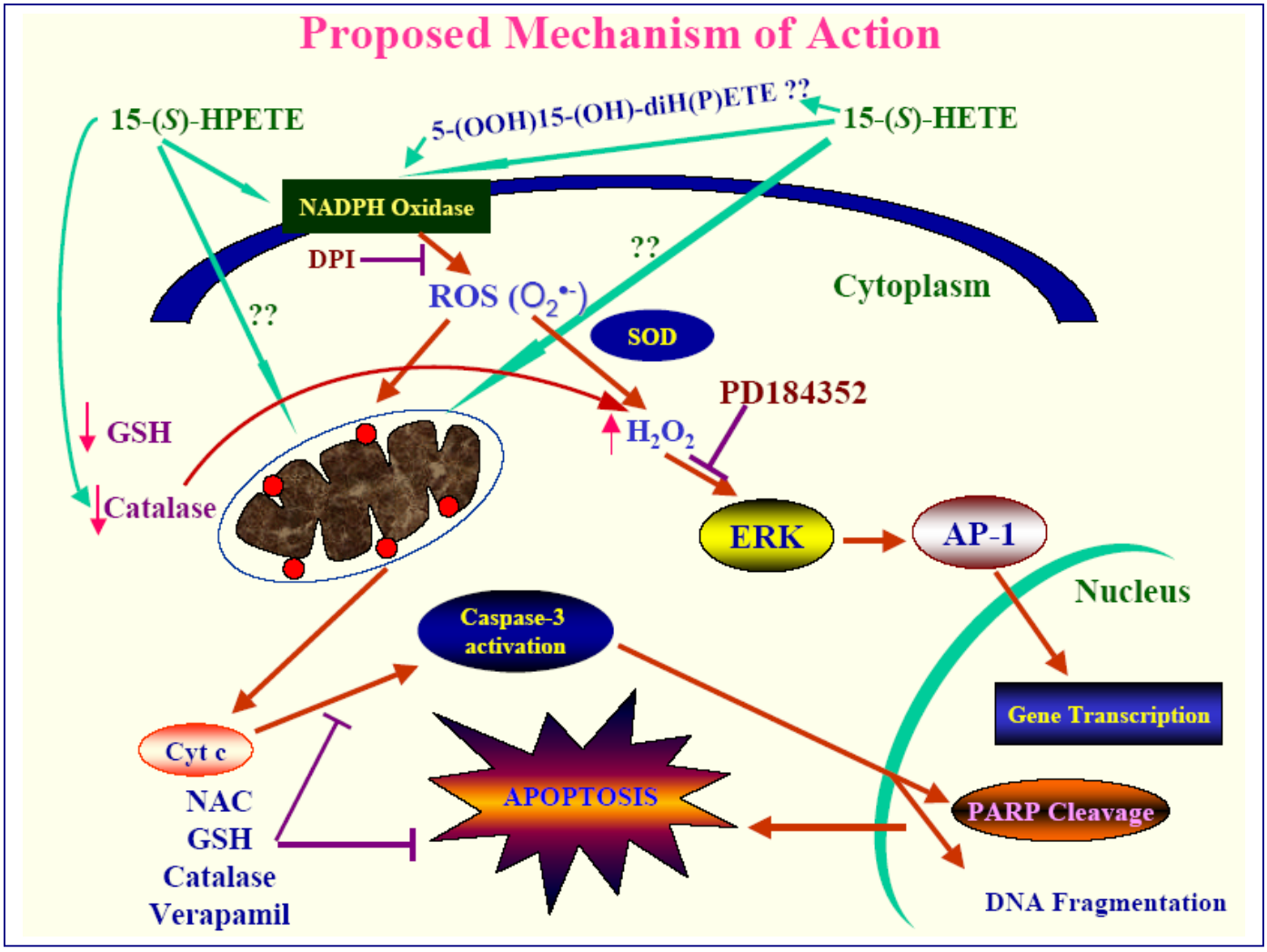

Fig. 32. Proposed mechanism of action of 15-LOX-2 metabolite-induced apoptosis in chronic myeloid leukemia cell line - K-562

Summary

Summary

There is a long debated relationship between diet and the incidence of cancer and among the important dietary components, lipids have raised considerable interest. Polyunsaturated fatty acids (PUFAs), a class of lipids, play important physiological roles acting as building blocks of membranes, metabolic fuel and also produce various secondary signal molecules. The physiological roles of PUFAs are well illustrated in a condition known as essential fatty acid deficiency (EFAD). Induction of EFAD by dietary manipulation results in dermatitis and delayed wound healing, both of which are reversed by restoring essential fatty acids (EFAs) in diet. Abnormalities of PUFAs and EFAs are also associated with heart and other vascular conditions. Over the past two decades, the role of PUFAs in cancer has particularly drawn attention. The relationship between dietary lipid uptake and arthritis, psoriasis, bronchial asthma, cancer has perhaps been best demonstrated in Eskimos who consume ω-3 polyunsaturated fatty acid (PUFA) rich diets and enjoy a low incidence of the above disorders. Of late strong *in vitro* evidence emerged showing the toxic effects of EFAs on malignant cells.

Early tumorigenesis studies in animals showed that dietary fats enhance carcinogenesis through a structure containing polyunsaturated bonds and the ω-6 function (*e.g.,* arachidonic and linoleic through conversion to arachidonic acids) promote tumorigenesis, whereas, ω-3 polyunsaturated fatty acids (*e.g.,* those found in fish oil) have antitumorigenic effects in animal models. Later tumorigenesis studies demonstrated that polyunsaturated fatty acids must undergo oxidative metabolism to enhance tumorigenesis. The

lipoxygenases (LOXs) and cyclooxygenases (COXs) mediate the oxidative metabolism of linoleic and arachidonic acids forming an array of biologically active metabolites, such as HODEs, HETEs, and prostaglandins. LOX products have been linked to tumorigenesis *in vitro* and *in vivo* in various experimental models, and the modulation of LOX metabolism has anticarcinogenic effects in these models.

The relationship between carcinogenesis and lipoxygenases is very well established and recent studies show that various LOX pathways exist in a dynamic balance that shifts during carcinogenesis towards 5-, 8-, and 12-LOX and away from 15-LOX. Even though the role of 15-LOX was well studied in relation with carcinogensis, there are antithetical reports regarding the role of 15-LOX-1, an isoform of 15-LOX, in controlling carcinogenesis. On the other hand, 15-LOX-2 in several studies has been shown to negatively regulate cell proliferation. Even though the role of 15-LOX in mediating anti-carcinogenic effects was very well established, the mechanisms behind these effects are still unclear. Further more the intricate details of the apoptotic cascades mediated by 15-LOXs and their metabolites are not very well explored. Therefore, the current study is designed to understand the molecular mechanisms mediating 15-LOX metabolite-induced apoptosis, taking a human chronic myeloid leukemia cell line - K-562 as a model cell line.

15-LOX-1 and 15-LOX-2 are two isoenzymes of 15-LOX, 15-LOX-1 preferentially acts on linoleic acid (18:2, ω-6) and converts it primarily to 13-hydroperoxyoctadecadienoic acid (13-(*S*)-HPODE), which will eventually be reduced to 13-hydroxyoctadecadienoic acid (13-(*S*)-HODE). In contrast,

Summary

15-LOX-2 preferentially acts on arachidonic acid (20:4, ω-6) to convert it to 15-hydroperoxyeicosatetraenoic acid (15-(*S*)-HPETE) that will be subsequently reduced to stable 15-hydroxyeicosatetraenoic acid (15-(*S*)-HETE). In the current study metabolites of both 15-LOX-1 [13-(*S*)-HPODE & 13-(*S*)-HODE] and 15-LOX-2 [15-(*S*)-HPETE & 15-(*S*)-HETE] were prepared *in vitro*, separated on HPLC and charecterised on LC-MS. These metabolites were employed to study their effects on a cancer cell line, chronic myeloid leukemia (CML) - K-562. These studies revealed that hydroperoxy [15-(*S*)-HPETE & 13-(*S*)-HPODE] metabolites of both isoforms of 15-LOX [15-LOX-1 & 15-LOX-2] and hydroxy metabolite of 15-LOX-2 (15-(*S*)-HETE) show potent growth inhibitory effects on K-562 cell line. However the hydroxy metabolite of 15-LOX-1 (13-(*S*)-HODE) did not show any significant effect on CML cells. 15-HPETE at 10 μM (IC_{50}) by 3 h inhibited the growth of CML cells approximately by 50% where as 15-HETE inhibited the growth of CML cells appoximately by 50% at 40 μM (IC_{50}) concentration by 6 h. These studies thus reveal that 15-(*S*)-HPETE is more potent in the inhibition of the growth of K-562 cells compared to 15-(*S*)-HETE. In view of the significant effects seen with 15-LOX-2 metabolites, further studies were undertaken only with 15-(*S*)-HPETE and 15-(*S*)-HETE.

Phase contrast and fluorescence microscopic studies of 15-LOX-2 metabolite treated cells have shown typical morphological features of cells undergoing apoptosis. Phase contrast studies revealed the membrane blebs and apoptotic bodies and fluorescence microscopic analysis by DAPI have shown the fragmented, marginalised and condensed DNA, typical of cells

undergoing apoptosis. Flow cytometric analysis of 15-LOX-2 metabolites treated cells upon staining with Propidium Iodide (PI) has shown distinct subG0/G1 peak charecteristic of cells undergoiong apoptosis.

Release of cytochrome *c* from the mitochondrial intermembrane space into the cytosol is one of the early events that initiate apoptosis. Consistent with these findings, release of cytochrome *c* in early hours was found both in case of 15-(*S*)-HPETE and 15-(*S*)-HETE treatment, that increased in a time dependent manner. In the current study, the release of cytochrome *c* is followed by a clear time dependent activation of casspase-3, suggesting that apoptosis induced by 15-LOX-2 metabolites involves activation of intrinsic death pathway mediators, caspase-9 and caspase-3. Activated caspase-3 cleaves off target substrates like poly(ADP-ribose) polymerase (PARP), a nuclear DNA damage repair enzyme and PARP cleavage observed in the present study in K-562 cells exposed to 15-(*S*)-HPETE and 15-(*S*)-HETE provides a conclusive and definitive evidence for caspase-3 activation and the induction of apoptosis through intrinsic death pathway. DNA isolated from 15-(*S*)-HPETE and 15-(*S*)-HETE treated cells, has clearly shown DNA ladder formation, a characteristic gel electrophoretic band pattern associated with apoptosis. These findings clearly demonstrate that 15-LOX-2 metabolites induce apoptosis by activating the intrinsic death pathway through a series of events involving the release of cytochrome *c*, caspase-3 activation, PARP cleavage and DNA fragmentation.

ROS generation has been linked to rapid induction of apoptosis in many cases. In the current study, the possible involvement of ROS generation

was studied through a flow cytometry based DCFH-DA analysis. These studies revealed a clear induction of ROS within minutes after treating with 15-LOX-2 metabolites. This increase in ROS generation coincided with a clear decrease in the GSH/GSSG ratio, in K-562 cells treated with 15-LOX-2 metabolites.

N-acetyl cysteine (NAC), a glutathione precursor was used to test whether ROS generated can be inhibited in the presence of NAC. NAC indeed reduced the levels of ROS induced by both 15-LOX-2 metabolites. 15-LOX-2 metabolite induced apoptosis and caspase-3 activation were inhibited when the cells were pretreated with NAC and GSH. Pretreatment of the cells with diphenylene iodonium (DPI), an NADPH oxidase inhibitor, has drastically reduced the ROS generation by both 15-HPETE and 15-HETE and thus demonstrating that ROS generated by 15-LOX-2 metabolites is NADPH oxidase dependent. DPI has almost completely abrogated caspase-3 activation and 15-LOX-2 metabolite-induced apoptosis, further supporting the activation of NADPH oxidase in response to 15-LOX-2 metabolite treatments.

15-(*S*)-HPETE has drastically inhibited catalase activity where as 15-(*S*)-HETE did not significantly inhibit catalase activity showing that H_2O_2 is rapidly accumulated in 15-(*S*)-HPETE treated K-562 cells. Other antioxidant enzymes, superoxide dismutase and glutathione peroxidase, were unaffected by 15-LOX-2 metabolites.

The differential effects observed in the present study with 15-(*S*)-HPETE and 15-(*S*)-HETE on K-562 cells, suggest a possible role for cellular peroxidase activity. In order to test this hypothesis, leukemia cell lines with

varying levels of peroxidase activity were exposed to 15-LOX-2 metabolites and analyzed for growth inhibitory effects. The anti-proliferative studies carried out on U-937 cells and Jurkat cells with 15-LOX-2 metabolites have shown that U-937 cells with high GPx activity, are more resistant to 15-LOX-2 metabolite-induced cell death and the Jurkat cells with less GPx activity are more sensitive and the growth inhibitory effects were comparable between Jurkat and K-562 cells. These results have clearly shown that glutathione peroxidase levels have significant effect on 15-LOX-2 metabolite-induced apoptosis. 15-LOX-2 metabolite-induced apoptosis was shown to be associated with the activation of redox sensitive transcription factor, activator protein-1 (AP-1). However, nuclear factor-κB, another redox sensitive transcription factor was not found to be activated.

References

References

Alimonti, J. B., Shi, L., Baijal, P. K., and Greenberg, A. H. Granzyme B induces BID-mediated cytochrome c release and mitochondrial permeability transition. J. Biol. Chem. 276: 6974–6982, 2001.

Anderson, K. M., Seed, T., Vos, M., Mulshine, J., Meng, J., Alrefai, W., Ou, D., and Harris, J. E. 5-Lipoxygenase inhibitors reduce PC-3 cell proliferation and initiate nonnecrotic cell death. Prostate 37: 161–173, 1998.

Ares, M. P., Porn-Ares, M. I., Thyberg, J., Juntti-Berggren, L., Berggren, P. O., Diczfalusy, U., Kallin, B., Bjorkhem, I., Orrenius, S., and Nilsson, J. Ca2+ channel blockers verapamil and nifedipine inhibit apoptosis induced by 25-hydroxycholesterol in human aortic smooth muscle cells. J. Lipid Res. 38: 2049-2061, 1997.

Avis, I. M., Jett, M., Boyle, T., Vos, M. D., Moody, T., Treston, A. M., Martinez, A., and Mulshine, J. L. Growth control of lung cancer by interruption of 5-lipoxygenase-mediated growth factor signaling. J. Clin. Investig. 97: 806–813, 1996.

Baer, A. N., Costello, P. B., and Green, F. A. In vivo activation of an ω-6 oxygenase in human skin. Biochem. Biophys. Res. Commun. 180: 98–104, 1991.

Bai, J., Rodriguez, A.M., Melendez, J.A., Cederbaum, A.I. Overexpression of catalase in cytosolic or mitochondrial compartment protects HepG2 cells against oxidative injury. J. Biol. Chem. 274: 26217-24, 1999.

Bailie, M. B., Standiford, T. J., Laichalk, L. L., Coffey, M. J., Strieter, R., and Peters-Golden, M. Leukotriene-deficient mice manifest enhanced lethality from Klebsiella pneumonia in association with decreased alveolar macrophage phagocytic and bactericidal activities. J. Immunol. 157: 5221-5224, 1996.

Bass, D. A., Parce, J. W., Dechatelet, L. R., Szejda, P., Seeds, M. C., and Thomas, M. Flow cytometric studies of oxidative product formation by neutrophils: a graded response to membrane stimulation. J. Immunol. 130: 1910–1917, 1983.

Bauer, M. K. A., Vogt, M., Los, M., Siegel, J., Wesselborg, S., and Schulze-Osthoff, K. Role of reactive oxygen intermediates in activation-induced CD95 (APO-1/Fas) ligand expression. J. Biol. Chem. 273: 8048–8055, 1998.

Beauchamp, C., and Fridovich, I. Superoxide dismutase: improved assays and an assay applicable to acrylamide gels. Anal. Biochem. 44: 276-287, 1971.

Beers, R. F. Jr., and Sizer, I. W. A. Spectrophotometric method for measuring the breakdown of hydrogen peroxide by catalase. J. Biol. Chem. 195: 133-140, 1952.

Belkner, J., Stender, H., and Kühn, H. The rabbit 15-lipoxygenase preferentially oxygenates LDL cholesterol esters, and this reaction does not require Vitamin E. J. Biol. Chem. 273: 23225–23232, 1998.

Beyer, R. E. An analysis of the role of coenzyme Q in free radical generation and as an antioxidant. Biochem. Cell. Biol. 70: 390-403, 1992.

Bigby, T. D., Levy, B. D., and Serhan, C. N. Cell biology of the 5-lipoxygenase pathway: amplification and generation of leukotrienes and novel eicosanoids by transcellular biosynthesis, in Five Lipoxygenase Products in Asthma. (Drazen JM, Dahlen SE and Lee T eds) pp 125-173, 1998, Marcel Dekker, Inc, New York.

Boado, R. J., Pardridge, W. M., Vinters, H. V., and Black, K. L. Differential expression of arachidonate 5-lipoxygenase transcripts in human brain tumors – evidence for the expression of a multitranscript family. Proc. Natl. Acad. Sci. U. S.A. 89: 9044–9048, 1992.

Boeglin, W. E., Kim, R. B., and Brash, A. R. A 12R-lipoxygenase in human skin: Mechanistic evidence, molecular cloning, and expression. Proc. Natl. Acad. Sci. U. S. A 95: 6744-6749, 1998.

Bortuzzo, C., Hanif, R., Kashfi, K., Staiano-Coico, L., Shiff, S. J., and Rigas, B. The effect of leukotrienes B and selected HETEs on the proliferation of colon cancer cells. Biochim. Biophys. Acta. 1300: 240–246, 1996.

Boyington, J. C., Gaffney, B. J., and Amzel, L. M. The three-dimensional structure of an arachidonic acid 15-lipoxygenase. Science. 260: 1482-1486, 1993.

Bradford, M. M. A rapid and sensitive method for the quantitation of microgram quantities of protein utilizing the principle of protein-dye binding. Anal. Biochem. 72: 248-254, 1976.

Brash, A. R. Lipoxygenases: occurrence, functions, catalysis and acquisition of substrate. J. Biol. Chem. 274: 23679-23682, 1999.

Brash, A. R., Boeglin, W. E., and Chang, M. S. Discovery of a second 15-S-lipoxygenase in humans. Proc. Natl. Acad. Sci. U. S. A. 94: 6148–6152, 1997.

Brash, A. R., Boeglin, W. E., Chang, M. S., and Shieh, B. H. Purification and molecular cloning of an 8R-lipoxygenase from the coral Plexaura homomalla

reveal the related primary structures of R- and S-lipoxygenases. J. Biol. Chem. 271: 20949-20957, 1996.

Brinckmann, R., Schnurr, K., Heydeck, D., Rosenbach, T., Kolde, G., and Kühn, H. Membrane translocation of 15-lipoxygenase in hematopoietic cells is calcium dependent and activates the oxygenase activity of the enzyme. Blood 91: 64–74, 1998.

Brinckmann, R., Topp, MS., Zalan, I., Heydeck, D., Ludwig, P., and Kuhn, H. Regulation of 15-lipoxygenase expression in lung epithelial cells by interleukin-4. Biochem. J. 318: 305–312, 1996.

Broitman, S. A., Vitale, J. J., Vavrousek-Jakuba, E., and Gottlieb, L. S. Polyunsaturated fat, cholesterol and large bowel tumorigenesis. Cancer (Phila.). 40: 2455– 2463, 1977.

Bronstein, J. C., and Bull, A. W. The correlation between 13-hydroxyoctadecadienoic acid dehydrogenase (13-HODE dehydrogenase) and intestinal cell differentiation. Prostaglandins. 46: 387-395, 1993.

Bryant, R. W., Bailey, J. M., Schewe, T., and Rapoport, S. M. Positional specificity of a reticulocyte lipoxygenase: Conversion of arachidonic acid to 15-S-hydroperoxy-eicosatetraenoic acid. J. Biol. Chem. 257: 6050–6055, 1980.

Bull, A. W., Earls, S. M., and Blackburn, M. L. Regulation of the induction of ornithine decarboxylase in short-term rat colon organ culture by dexamethasone and 13-hydroxyoctadecadienoic acid (13-HODE). Life Sci. 53: 377–385, 1993.

Bull, A. W., Nigro, N. D., Golembieski, W. A., Crissman, J. D., and Marnett, L. J. In vivo stimulation of DNA synthesis and induction of ornithine decarboxylase in rat colon by fatty acid hydroperoxides, autoxidation products of unsaturated fatty acids. Cancer Res. 44: 4924–4928, 1984.

Buttke, T. M., and Sandstrom, P .A. Oxidative stress as a mediator of apoptosis. Immunol. Today 15: 7– 10, 1994.

Cabaner, C., Gajate, C., Macho, A., Munoz, E., Modolell, M., and Mollinedo, F. Induction of apoptosis in human mitogen-activated peripheral blood T-lymphocytes by the ether phospholipid ET-18-OCH3: involvement of the Fas receptor/ligand system. Br. J. Pharmacol. 127: 813– 825, 1999.

Casciola-Rosen, L., Nicholson, D. W., Chong, T., Rowan, K.R., Thornberry, N. A., Miller, D. K., and Rosen, A. Apopain/CPP32 cleaves proteins that are essential for cellular repair: a fundamental principle of apoptotic death. J. Exp Med., 183: 1957-1964, 1996.

Cathcart, R., Schwiers, E., and Ames, B. N. Detection of picomole levels of hydroperoxides using a fluorescent dichlorofluorescein assay. Anal. Biochem. 134: 111–116, 1983.

Chandra, J., Samali, A., and Orrenius, S. Triggering and modulation of apoptosis by oxidative stress. Free Radic. Biol. Med. 29: 323–333, 2000.

Chang, W. L., Chapkin, R. S., and Lupton, J. R. Fish oil blocks azoxymethaneinduced rat colon tumorigenesis by increasing cell differentiation and apoptosis rather than decreasing cell proliferation. J. Nutr. 128: 491–497, 1998.

Chaturvedi, M. M., Kumar, A., Darnay, B. G., Chainy, G, B., Agarwal, S., Aggarwal, B. B. Sanguinarine (pseudochelerythrine) is a potent inhibitor of NF-kappaB activation, IkappaBalpha phosphorylation, and degradation. J. Biol. Chem. 272: 30129-34, 1997.

Chavis, C., Vachier, I., Chanez, P., Bousquet, J., and Godard, P. 5(S),15(S)-dihydroxyeicosatetraenoic acid and lipoxin generation in human polymorphonuclear cells: dual specificity of 5-lipoxygenase towards endogenous and exogenous precursors. J. Exp. Med. 183(4): 1633-1643, 1996.

Chen, X, S., Kurre, U., Jenkins, N. A., Copeland, N. G., and Funk, C. D. cDNA cloning, expression, mutagenesis of C-terminal isoleucine, genomic structure, and chromosomal localizations of murine 12-lipoxygenases. J. Biol. Chem. 269: 13979–13987, 1994

Chopra, H., Timar, J., Chen, Y. Q., Rong, X. H., Grossi, I. M., Fitzgerald, L. A., Taylor, J. D., and Honn, K. V. The lipoxygenase metabolite 12(S)-HETE induces a cytoskeleton-dependent increase in surface expression of integrin α IIb β 3 on melanoma cells. Int. J. Cancer. 49: 774-786, 1991.

Conrad, D. J., and Lu, M. Regulation of human 12/15-lipoxygenase by Stat6-dependent transcription. Am. J. Respir. Cell Mol .Biol. 22: 226–234, 2000.

Conrad, D. J. The arachidonate 12/15 lipoxygenases. A review of tissue expression and biologic function. Clin. Rev. Allergy Immunol. 17: 71–89, 1999.

Coxon, A., Rieu, P., Barkalow, F. J., Askari, S., Sharpe, A. H., von Andrian, U. H., Arnaout, M. A., and Mayadas, T. N. A novel role for the beta 2 integrin CD11b/CD18 in neutrophil apoptosis: a homeostatic mechanism in inflammation. Immunity 5: 653-666, 1996.

Creagh, E. M., Carmody, R. J., and Cotter, T.G. Heat shock protein 70 inhibits caspase-dependent and -independent apoptosis in Jurkat T cells. Exp. Cell Res. 257: 58-66, 2000.

Daret, D., Blin, P., and Larrue, J. Synthesis of hydroxy fatty acids from linoleic acid by human blood platelets. Prostaglandins 38: 203–214, 1989.

De Groot, J. J. M. C., Veldink, G. A., Vliegenthart, J. F. G., and Boldingh, J. On the interaction of soybean lipoxygenase-1 and 13-L-hydroperoxylinoleic acid, involving yellow and purple coloured enzyme species, involving yellow and purple coloured enzyme species. FEBS Lett. 56: 50–54, 1975.

De Petrocellis, L., and Di Marzo, V. Aquatic invertebrates open up new perspectives in eicosanoid research: biosynthesis and bioactivity Prostaglandins Leukot. Essent. Fatty Acids. 51: 215-229, 1994.

DeLong, M. J. Apoptosis: a modulator of cellular homeostasis and disease states. Ann. N.Y. Acad. Sci. 842: 82–90, 1998.

Desplat, V., Dulery, C., Praloran, V., and Denizot, Y. Incorporation and effect of arachidonic acid on the growth of human myeloma cell lines. Mediat. Inflamm. 8: 115–118, 1999.

Dixon, R. A., Diehl, R. E., Opas, E., Rands, E., Vickers, P. J., Evans, J. F., Gillard, J. W., and Miller, D. K. Requirement of a 5-lipoxygenase-activating protein for leukotriene synthesis. Nature (Lond) 343: 282-284, 1990.

Donoiwitz, M. Arachidonic acid metabolites and their role in inflammatory bowel disease. Gastroenterology 88: 580–587, 1985.

Doussiere, J., Bouzidi, F., Poinas, A., Gaillard, J., and Vignais, P. V. Kinetic study of the activation of the neutrophil NADPH oxidase by arachidonic acid. Antagonistic effects of arachidonic acid and phenylarsine oxide . Biochemistry 38: 16394-16406, 1999 a.

Doussiere, J., Gaillard, J., and Vignais, P. V. The heme component of the neutrophil NADPH oxidase complex is a target for aryliodonium compounds . Biochemistry 38: 3694-3703, 1999 b.

Drazen, J. M. Pharmacology of leukotriene receptor antagonists and 5-lipoxygenase inhibitors in the management of asthma. Pharmacotherapy 17: 22S–30S, 1997.

Dumont, A., Hehner, S. P., Hofmann, T. G., Ueffing, M., Droge, W., and Schmitz, M. L. Hydrogen peroxide-induced apoptosis is CD95-independent, requires the release of mitochondria-derived reactive oxygen species and the activation of NF-kappaB. Oncogene 18: 747–757, 1999.

Egmond, M, R., Veldink, G. A., Vliegenthart, J. F., and Boldingh, J. C-11 H-Abstraction from linoleic acid, the rate-limiting step in lipoxygenase catalysis. Biochem. Biophys. Res .Commun 54: 1178-1184. 1973.

Ermak, G., and Davies, K. J. A. Calcium and oxidative stress: from cell signaling to cell death. Mol. Immunol. 38: 713–721, 2001.

Finkel, T., and Holbrook, N. J. Oxidants, oxidative stress and the biology of ageing. Nature 408: 239-247, 2000.

Fischer, S. M., Baldwin, J. K., Jasheway, D. W., Patrick, K. E., and Cameron, G. S. Phorbol ester induction of 8-lipoxygenase in inbred SENCAR (SSIN) but not C57BL/6J mice correlated with hyperplasia, edema, and oxidant generation but not ornithine decarboxylase induction. Cancer Res. 48: 658-664. 1988.

Funk, C. D. Prostaglandins and leukotrienes: advances in eicosanoid biology. Science 294: 1871-1875, 2001.

Funk, C. D. The molecular biology of mammalian lipoxygenases and the quest for eicosanoid functions using lipoxygenase-deficient mice. Biochim. Biophys. Acta. 1304: 65–84, 1996.

Furstenberger, G., Hagedorn, H., Jacobi, T., Besemfelder, E., Stephan, M., and Lehmann, W.D. Characterization of an 8-lipoxygenase activity induced by the phorbol ester tumor promoter 12-Otetradecanoylphorbol-13-acetate in mouse skin *in vivo*. J. Biol. Chem. 266: 15738-15745. 1991.

Gan, Q. F., Witkop, G. L., Sloane, D. L., Straub, K. M., and Sigal, E. Identification of a specific methionine in mammalian 15-lipoxygenase which is oxygenated by the enzyme product 13-HPODE: dissociation of sulfoxide formation from self-inactivation. Biochemistry 34: 7069–7079. 1995.

Gao, X., Grignon, D. J., Chbihi, T., Zacharek, A., Chen, Y. Q., Sakr, W., Porter, A. T., Crissman, J. D., Pontes, J. E., Powell, I. J., and Honn, K. V. Elevated 12-lipoxygenase mRNA expression correlates with advanced stage and poor differentiation of human prostate cancer. Urology 46: 227–237. 1995.

Gerwick, W. H., and Bernart, M. W. in Marine Bio/Technology, Volume I: Pharmaceutical and Bioactive Natural Products (Attaway, D. H., and Zaborsky, O. R., eds) pp. 101–152, Plenum Publishing Corp., New York, 1993.

Gerwick, W. H. Structure and biosynthesis of marine algal oxylipinz.. Biochem. Biophys. Acta. 1211: 243-255, 1994.

Ghosh, J., and Myers, C. E. Arachidonic acid stimulates prostate cancer cell growth: critical role of 5-lipoxygenase. Biochem. Biophys. Res. Commun. 235: 418–423. 1997.

Ghosh, J., and Myers, C. E. Inhibition of arachidonate 5-lipoxygenase triggers massive apoptosis in human prostate cancer cells. Proc. Natl. Acad. Sci. USA. 95: 13182–13187, 1998.

Gillmor, S. A., Villasenor, A., Fletterick, R., Sigal, E., and Browner, M. F. The structure of mammalian 15-lipoxygenase reveals similarity to the lipases and the determinants of substrate specificity. Nat. Struct. Biol. 4: 1003-1009, 1997.

Glasgow, W. C., and Eling, T. E. Epidermal growth factor stimulates linoleic acid metabolism in BALB/c 3T3 fibroblasts. Mol. Pharmacol. 38: 503–510. 1990.

Glasgow, W. C., and Everhart, A. L. The role of linoleic acid metabolism in the proliferative response of cells overexpressing the erbB-2/HER2 oncogene. Adv. Exp. Med. Biol. 407: 393–397, 1997.

Glasgow, W. C., Afshari, C. A., Barrett, J. C., and Eling, T. E. Modulation of the epidermal growth factor mitogenic response by metabolites of linoleic and arachidonic acid in Syrian hamster embryo fibroblasts. Differential effects in tumor suppressor gene (+) and (-) phenotypes. J. Biol. Chem. 267: 10771–10779, 1992.

Gores, G. J., Herman, B., and Lemasters, J. J. Plasma membrane bleb formation and rupture: a common feature of hepatocellular injury. Hepatology 11: 690–698, 1990.

Grechkin, A. Recent developments in biochemistry of the plant lipoxygenase pathway . Prog. Lipid Res. 37: 317-352 , 1998.

Grullich, C., Duvoisin, R. M., Wiedmann, M., and van Leyen, K. Inhibition of 15-lipoxygenase leads to delayed organelle degradation in the reticulocyte. FEBS Lett. 489: 51–54, 2001.

Gupta, S., Srivastava, M., Ahmad, N., Sakamoto, K., Bostwick, D. G., and Mukhtar, H. Lipoxygenase-5 is overexpressed in prostate adenocarcinoma Cancer (Phila.). 91: 737–743, 2001.

Hamberg, M., and Samuelsson, B. Prostaglandin endoperoxides. Novel transformations of arachidonic acid in human platelets. Proc. Natl. Acad. Sci. U. S. A. 71: 3400–3404, 1974.

Hampton, M. B., and Orrenius, S. Dual regulation of caspase activity by hydrogen peroxide: implications for apoptosis. FEBS Lett. 414: 552–556, 1997.

Harats, D., Kurihara, H., Belloni, P., Oakley, H., Zoiber, A., Ackley, D., *et al*. Targeting gene expression to the vascular wall in transgenic mice using the murine preproendothelin-1 Promotor. J. Clin. Invest. 95: 1335–1344, 1995.

Harats, D., Shaish, A., George, J., Mulkins, M., Kurihara, H., Levkovitz, H., et al. Overexpression of 15-lipoxygenase in vascular endothelium accelerates early atherosclerosis in LDL receptor-deficient mice. Arterioscler. Thromb. Vasc. Biol . 20: 2100–2105, 2000.

Haslett, C. Resolution of acute inflammation and the role of apoptosis in the tissue fate of granulocytes. Clin. Sci. (Colch.) 83: 639– 648, 1992.

Heidt, M., Fürstenberger, G., Vogel, S., Marks, F., and Krieg, P. Diversity of mouse lipoxygenases: identification of a subfamily of epidermal isozymes exhibiting a differentiation-dependent mRNA expression pattern. Lipids 35: 701-707, 2000.

Henricks, P. A., Engels, F., van der Vliet, H., and Nijkamp, F. P. 9- and 13-hydroxy-linoleic acid possess chemotactic activity for bovine and human polymorphonuclear leukocytes. Prostaglandins 41: 21–27, 1991.

Henriksson, P., Hamberg, M., and Diczfalusy, U. Formation of 15-HETE as a major hydroxeicosatetraenoic acid in the atherosclerotic vessel wall. Biochim. Biophys. Acta. 834: 272–274, 1985.

Herlin, T., Fogh, K., Hansen, E. S., Andreasen, A., Knudsen, V., Henriksen, T. B., *et al.* 15-HETE inhibits leukotriene B4 formation and synovial cell proliferation in experimental arthritis. Agents Actions 29: 52–53, 1990.

Hermann, M., Lorenz, H. M., Voll, R., Grunke, M., Woith, W., and Kalden, J. R. A rapid and simple method for the isolation of apoptotic DNA fragments. Nucleic Acids Res. 22: 5506-5507, 1994.

Herrmann, J. L., Menter, D. G., Beham, A., von Eschenbach, A., and McDonnell, T. J. Regulation of lipid signaling pathways for cell survival and apoptosis by bcl-2 in prostate carcinoma cells. Exp. Cell Res. 234: 442–451, 1997.

Higgs, G. A., Salmon, J. A., and Spayne, J. A. The inflammatory effects of hydroperoxy and hydroxy acid products of arachidonate lipoxygenase in rabbit skin. Br. J. Pharmacol. 74: 429–433, 1981.

Hill, E. M., Eling, T., and Nettesheim, P. Differentiation dependency of eicosanoid enzyme expression in human tracheobronchial cells. Toxicol. Lett. 96: 239–244, 1998.

Hiltunen, T., Luoma, J., Nikkari, T. and Ylä-Herttuala, S. Induction of 15-lipoxygenase mRNA and protein in early atherosclerotic lesions. Circulation 92: 3297–3303 1995.

His, L.C., Xi, X., Lotan, R., Shureiqi, I., and Lippman, S. M. The histone deacetylase inhibitor suberoylanilide hydroxamic acid induces apoptosis via induction of 15-lipoxygenase-1 in colorectal cancer cells. Cancer Res. 68778-68781, 2004.

Hohn, K. V., Nelson, K. K., Renaud, C., Bazaz, R., Diglio, C. A., and Timar, J. Fatty acid modulation of tumor cell adhesion to microvessel endothelium and experimental metastasis. Prostaglandins 44: 413–429, 1992.

Holtzman, M. J. Arachionic acid metabolism in airway epithelial cells Annu. Rev. Physiol. 54: 303–329, 1992.

Holtzman, M. J., Zhang, V., Hussain, H., Roswit, W. T., and Wilson, J. D. Prostaglandin H synthase and lipoxygenase gene families in the epithelial cell barrier. Ann. NY. Acad. Sci. 744: 58–77, 1994.

Holzhutter, H. G., Wiesner, R., Rathman, J., Stößer, R., and Kühn, H. Kinetic studies on the interaction of nitric oxide with a mammalian lipoxygenases. Eur. J. Biochem. 245: 608–616, 1997.

Huang, M. T., Lysz, T., Ferraro, T., Abidi, T. F., Laskin, J. D., and Conney, A. H. Inhibitory effects of curcumin on in vitro lipoxygenase and cyclooxygenase activities in mouse epidermis. Cancer Res. 51: 813–819, 1991.

Hubbard, N. E., Lim, D., and Erickson, K. L. Alteration of murine mammary tumorigenesis by dietary enrichment with n-3 fatty acids in fish oil. Cancer Lett. 124: 1–7, 1998.

Hugou, I., Blin, P., Henri, J., Daret, D., and Larrue, J. 15-Lipoxygenase expression in smooth muscle cells from atherosclerotic rabbit aorta. Atherosclerosis 113: 189–195, 1995.

Hui, R., Everhart, A. L., and Glasgow, W. C. Epidermal growth factor-stimulated production of sterified 13(S)-hydroxyoctadecadienoic acid is associated with tumor suppressor phenotype in Syrian hamster embryo fibroblasts. J. Lipid Res. 38: 46–60, 1997.

Hunter, J. A., Finkbeiner, W. E., Nadel, J. A., Goetzl, E. J., and Holtzman, M. J. Predominant generation of 15-lipoxygenase metabolites of arachidonic acid

by airway epithelial cells from human trachea. Proc .Natl. Acad .Sci. U. S. A. 82: 4633–4637, 1985.

Hussey, H. J., and Tisdale, M. J. Novel anti-tumor activity of 2,3,5-trimethyl-6-(3- pyridylmethyl)-1,4-benzoquinone (CV-6504) against established murine adenocarcinomas (MAC). Br. J. Cancer. 73: 1187–1192, 1996.

Ikawa, H., Kamitani, H., Calvo, B. F., Foley, J. F., and Eling, T. E. Expression of 15-lipoxygenase-1 in human colorectal cancer. Cancer Res. 59: 360-366, 1999.

Ikawa, H., Kamitani, H., Calvo, B., Foley, J., and Eling, T. Expression of 15-lipoxygenase-1 in human colorectal cancer. Int. J. Cancer 49: 774–786, 1999.

Ishikawa, Y., and Kitamura, M. Anti-apoptotic effect of quercitin: intervention in the JNK- and ERK- mediated apoptotic pathways. Kidney Int. 58: 1078-1087, 2000.

Ishikawa, Y., Yokoo, T., and Kitamur, M. c-Jun/AP-1, but not NF-κB, is a mediator for oxidant-initiated apoptosis in glomerular mesangial cells. Biochem. Biophys. Res. Commun. 240: 496-501, 1997.

Jack, G. S., Brash, A. R., Olson, S. J., Manning, S., Coffey, C. S., Smith, J. A. Jr., and Shappell, S. B. Reduced 15-lipoxygenase-2 immunostaining in prostate adenocarcinoma: correlation with grade and expression in high-grade prostatic intraepithelial neoplasia. Hum. Pathol. 31: 1146-1154, 2000.

Jacobson, M. D. Reactive oxygen species and programmed cell death. Trends Biochem. Sci. 21: 83–86, 1996.

Jiang, W. G., Bryce, R. P., and Horrobin, D. F. Essential fatty acids: molecular and cellular basis of their anti-cancer action and clinical implications. Criti. Rev. in Oncol. Hematol. 27: 179–209, 1998.

Jisaka, M., Kim, R. B., Boeglin, W. E., Nanney, L. B., and Brash, A. R. Molecular cloning and functional expression of a phorbol ester-inducible 8S-lipoxygenase from mouse skin. J. Biol. Chem. 272: 24410-24416, 1997.

Jones, O.T., Cross, A. R., Hancock, J. T., Henderson, L M., and O'Donnell, V. B. Inhibitors of NADPH oxidase as guides to its mechanism. Biochem. Soc. Trans. 19: 70-72, 1991.

Kamitani, H., Kameda, H., Kelavkar, U. P., and Eling, T. E. A GATA binding site is involved in the regulation of 15-lipoxygenase-1 expression in human colorectal carcinoma cell line, caco-2. FEBS Lett. 467: 341–347, 2000.

Kang, L. T., and Vanderhoek, J. Y. Characterization of specific subcellular 15-hydroxyeicosatetraenoic acid (15-HETE) binding sites on rat basophilic leukemia cells. Biochim. Biophys. Acta. 1256: 297–304, 1995.

Kelavkar, U. P., Cohen, C., Kamitani, H., Eling, T. E., and Badr, K. F. Concordant induction of 15-lipoxygenase-1 and mutant p53 expression in human prostate adenocarcinoma: correlation with Gleason staging. Carcinogenesis. 21: 1777-1787, 2000.

Kerr, J. F., Wyllie, A. H., and Currie, A. R. Apoptosis: a basic biological phenomenon with wide-ranging implications in tissue kinetics. Br. J. Cancer 26: 239– 257, 1972.

Kiran Kumar, Y.V., Raghunathan, A., Sailesh, S., Prasad, M., Vemuri, M. C., and Reddanna, P. Differential effects of 15-HPETE and 15-HETE on BHK-21 cell proliferation and macromolecular composition. Biochim. Biophys. Acta. 1167: 102-108, 1993.

Kishimoto, K., Nakamura, M., Suzuki, H., Yoshimoto, T., Yamamoto, S., Takao, T., et al. Suicide inactivation of porcine leukocyte 12-lipoxygenase associated with its incorporation of 15-hydroperoxy- 5,8,11,13-eicosatetraenoic acid derivative. Biochim. Biophys. Acta. 1300: 56–62, 1996.

Kitamura M, Ishikawa Y, Moreno-Manzano V, Xu Q, Konta T, Lucio-Cazana J, Furusu A, Nakayama K. Intervention by retinoic acid in oxidative stress-induced apoptosis. Nephrol Dial Transplant. 7: 84-7, 2002.

Krieg, P., Kinzig, A., Heidt, M., Marks, F., and Fürstenberger, G. cDNA cloning of an 8-lipoxygenase and a novel epidermis-type lipoxygenase from phorbol ester-treated mouse skin. Biochim. Biophys. Acta 1391: 7-12, 1998.

Kuhn, H., Schewe, T., and Rapoport, S. M. The stereochemistry of the reactions of lipoxygenases and their metabolites. Proposed nomenclature of lipoxygenases and related enzymes Adv. Enzymol.Relat. Areas Mol. Biol. 58: 273 –311, 1986.

Kuhn, H., and Brash, A. R. Occurrence of lipoxygenase products in membranes of rabbit reticulocytes, Evidence for a role of the reticulocyte lipoxygenase in the maturation of red cells. J. Biol. Chem. 265: 1454–1458, 1990.

Kuhn, H., Belkner, J., Suzuki, H., and Yamamoto, S. Oxidative modification of human lipoproteins by lipoxygenases of different positional specificities. J. Lipid Res. 35: 1749–1759, 1994.

Kuhn, H., Belkner, J., Wiesner, R., and Brash, A. R. Oxygenation of biological membranes by the pure reticulocyte lipoxygenase. J. Biol. Chem 265: 18351–18361, 1990.

Kuhn, H., Heydeck, D., Brinckman, R., and Trebus, F. Regulation of cellular 15-lipoxygenase activity on pre-translational, translational and post-translational levels. Lipids 34: S273–S279, 1999.

Kuhn, H., Walther, M., and Kuban, R. J. Mammalian arachidonate 15-lipoxygenases structure, function, and biological implications. Prostaglandins Other Lipid Mediat. 68-69: 263-290, 2002.

Lai, C. K., Phillips, G. D., Jenkins, J. R., and Holgate, S. T. The effect of inhaled 15(S)-hydroxyeicosatetraenoic acid (15-HETE) on airway calibre and non-specific responsiveness in normal and asthmatic human subjects. Eur. Respir. J. 3: 38–45, 1990 a.

Lai, C. K., Polosa, R., and Holgate, S. T. Effect of 15-(s)-hydroxyeicosatetraenoic acid on allergen-induced asthmatic response. Am. Rev. Respir. Dis. 141: 1423–1427, 1990 b.

Lazebnik Y. A., Kaufmann S. H., Desnoyers S., Poirier G. G., Earnshaw W. C. Cleavage of poly(ADP-ribose) polymerase by a proteinase with properties like ICE. Nature 371: 346-7, 1994.

Levy, B. D., Romano, M., Chapman, H. A., Reilly, J. J., Drazen, J., and Serhan, C. N. Human alveolar macrophages have 15-lipoxygenase and generate 15(S)-hydroxy-5, 8,11-cis-13-trans-eicosatetraenoic acid and lipoxins. J. Clin. Invest. 92: 1572–1579, 1993.

Li, M., Kondo, T., Zhao, Q. L., Li, F. J., Tanabe, K., Arai, Y., Zhou, Z. C., and Kasuya, M. Apoptosis induced by cadmium in human lymphoma U937 cells through Ca2+-calpain and caspase-mitochondria- dependent pathways. J. Biol. Chem. 275: 39702-39709, 2000.

Li, P., Nijhawan, D., Budihardjo, I., Srinivasula, S. M., Ahmad, M., Alnemri, E. S., and Wang, X. Cytochrome c and dATP-dependent formation of Apaf-1/caspase-9 complex initiates an apoptotic proteasecascade. Cell 91: 479-489, 1997.

Ling, Y. H., Liebes, L., Zou, Y., and Perez-Soler, R. Reactive oxygen species generation and mitochondrial dysfunction in the apoptotic response to Bortezomib, a novel proteasome inhibitor, in human H460 non-small cell lung cancer cells. J. Biol. Chem. 278: 33714-33723, 2003.

Lee, Y. S., Nam, D. H., Kim, J. A. Induction of apoptosis by capsaicin in A172 human glioblastoma cells. Cancer Lett. 161: 121-30, 2000.

Liu, B., Khan, W. A., Hannun, Y. A., Timar, J. D., Taylor, J., Lundy, S., Butovich, I., and Honn, K. V. 12(S)-hydroxyeicostetraenoic acid and 13(S)-hydroxyoctadecadienoic acid regulation of protein kinase C-α in melanoma cells: role of receptormediated hydrolysis of inositol phospholipids. Proc. Natl. Acad. Sci. USA. 92: 9323–9327, 1995.

Liu, X., Kim, C. N., Yang, J., Jemmerson, R., and Wang, X. Induction of apoptotic program in cell-free extracts: requirement for dATP and cytochrome *c*. Cell 86: 147-157, 1996.

Liu, X., Li, P., Widlak, P., Zou, H., Luo, X., Garrard, W. T., and Wang, X. The 40-kDa subunit of DNA fragmentation factor induces DNA fragmentation and chromatin condensation during apoptosis. Proc. Natl. Acad. Sci. U. S. A. 95: 8461–8466, 1998.

Luo, X., Budihardjo, I., Zou, H., Slaughter, C., and Wang, X. Bid, a Bcl2 interacting protein, mediates cytochrome *c* release from mitochondria in response to activation of cell surface death receptors. Cell 94: 481– 490, 1998.

Maas, R. L., and Brash, A. R. Evidence for a lipoxygenase mechanism in the biosynthesis of epoxide and dihydroxy leukotrienes from 15(S)-hydroperoxyicosatetraenoic acid by human platelets and porcine leukocytes. Proc. Natl. Acad. Sci. U. S. A 80: 2884-2888, 1983.

MacCarrone, M., Lorenzon, .T., Guerrieri, P., and Agro, A F. Resveratrol prevents apoptosis in K562 cells by inhibiting lipoxygenase and cyclooxygenase activity. Eur. J. Biochem. 265: 27-34, 1999.

Maccarrone, M., Putti, S., Finazzi Agro, A. Altered gravity modulates 5-lipoxygenase in human erythroleukemia K562 cells. J. Gravit. Physiol. 5: P97-P98, 1998.

Maccarrone, M., Ranalli, M., Bellincampi, L., Salucci, M. L., Sabatini, S., Melino, G., and Finazzi-Agro, A. Activation of different lipoxygenase isozymes induces apoptosis in human erythroleukemia and neuroblastoma cells. Biochem. Biophys. Res. Commun. 272: 345-350, 2000.

Maccarrone M, Melino G, Finazzi-Agro A. Lipoxygenases and their involvement in programmed cell death. Cell Death Differ. 8: 776-84, 2001.

Macho, A., Hirsch, T., Marzo, I., Marchetti, P., Dallaporta, B., Susin, S.A., Zamzami, N., and Kroemer, G. Glutathione depletion is an early and calcium elevation is a late event of thymocyte apoptosis. J. Immunol. 158: 4612–4619, 1997.

Martindale, J. L., and Holbrook, N. J. Cellular Response to Oxidative Stress: Signaling for Suicide and Survival. J. Cell Physiol. 192: 1–15, 2002.

Martinou, J. C., Desagher, S., and Antonsson, B. Cytochrome c release from mitochondria: all or nothing. Nat. Cell Biol. 2: E41-E43, 2000.

Matsura, T., Kai, M., Fujii, Y., Ito, H., Yamada, K. Hydrogen peroxide-induced apoptosis in HL-60 cells requires caspase-3 activation. Free Radic. Res. 30: 73– 83, 1999.

McConkey, D. J., and Orrenius, S. The role of calcium in the regulation of apoptosis. J. Leukoc. Biol. 59: 775–783, 1996.

Michiels, C., Raes, M., Toussaint, O., Remacle, J. Importance of Se-glutathione peroxidase, catalase, and Cu/Zn-SOD for cell survival against oxidative stress. Free Radic. Biol Med. 17: 235-48, 1994.

Miller, C. C., and Ziboh, V. A. Induction of epidermal hyperproliferation by topical n-3 polyunsaturated fatty acids on guinea pig skin linked to decreased levels of 13-hydroxyoctadecadienoic acid (13-HODE). J. Investig. Dermatol. 94: 354–358, 1990.

Miller, Y. I., Chang, M. K., Funk, C. D., Feramisco, J. R., and Witztum, J. L. 12/15-Lipoxygenase translocation enhances site-specific actin polymerization in macrophages phagocytosing apoptotic cells. J. Biol. Chem. 276: 19431–19439, 2001.

Minor, W., Steczko, J., Stec, B., Otwinowski, Z., Bolin, J. T., Walter, R., and Axelrod, B. Biochemistry 35, 10687–10701, 1996.

Montero, A., Uda, S., Munger, K. A., and Badr, K. F. LTA4 hydrolase expression during glomerular inflammation: correlation of immunohistochemical localization with cytokine regulation. Adv. Exp. Med. Biol. 469: 449–454, 1999.

Morel, Y., and Barouki, R. Repression of gene expression by oxidative stress. Biochem J. 342: 481-96, 1999.

Mosmann, T. Rapid colorimetric assay for cellular growth and survival: application to proliferation and cytotoxicity assays. J. Immunol. Methods 65: 55-63, 1983.

Muga, S. J., Thuillier, P., Pavone, A., Rundhaug, J. E., Boeglin, W. E., Jisaka, M., et al.,. 8(S)-Lipoxygenase products activate peroxisome proliferator-activated receptor alpha and induce differentiation in murine keratinocytes Cell Growth & Differentiation 11: 447-454, 2000.

Nair, J., Furstenberger, G., Burger, F., Marks, F., and Bartsch, H. Promutagenic etheno-DNA adducts in multistage mouse skin carcinogenesis: correlation with lipoxygenase-catalyzed arachidonic acid metabolism. Chem. Res. Toxicol. 13: 703-709, 2000.

Nathan, C. Inducible nitric oxide synthase: what difference does it make? J. Clin. Invest. 100: 2417-2423, 1997.

Neuzil, J., Upston, J. M., Witting, P. K., Scott, K. F., and Stocker, R. Secretory phospholipase A2 and lipoprotein lipase enhance 15-lipoxygenase-induced enzymic and nonenzymic lipid peroxidation in low-density lipoproteins. Biochemistry 37: 9203-9210, 1998.

Nicholson, D. W., and Thornberry, N. A. Caspases: killer proteases Trends Biochem. Sci. 22: 299-306, 1997.

Nie, D., Hillman, G. G., Geddes, T., Tang, K., Pierson, C., Grignon, D. J., and Honn, K. V. Platelet-type 12-lipoxygenase in a human prostate carcinoma stimulates angiogenesis and tumor growth. Cancer Res. 58: 4047–4051, 1998.

Nixon, J. B., Kim, K. S., Lamb, P. W., Bottone, F. G., and Eling TE. 15-Lipoxygenase-1 has anti-tumorigenic effects in colorectal cancer. Prostaglandins Leukot. Essent. Fatty Acids. 70: 7-15, 2004.

Nugteren, D. H. Arachidonate lipoxygenase in blood platelets. Biochim. Biophys. Acta. 380: 299–307, 1975.

Oda, T., Sadakata, N., Komatsu, N., and Muramatsu, T. Specific efflux of glutathione from the basolateral membrane domain in polarized MDCK cells during ricin-induced apoptosis. J. Biol. Chem. 126: 715– 721, 1999.

Ostareck-Lederer, A., Ostareck, D. H., Standart, N., and Thiele, B. J. Translation of 15-lipoxygenase is inhibited by a protein that binds to a repeated sequence in the 3' untranslated region. EMBO J. 13: 1476–1481, 1994.

Paglia, D. E., and Valentine, W. N. Studies on the quantitative and qualitative characterization of erythrocyte glutathione peroxidase. J. Lab. Clin. Med. 70: 158-169, 1967.

Peter, M. E., and Krammer, P. H. Mechanisms of CD95 (APO-1/Fas)-mediated apoptosis. Curr. Opin. Immunol. 10: 545-51, 1998.

Pidgeon, G. P., Kandouz, M., Meram, A., and Honn, K.V. Mechanisms controlling cell cycle arrest and induction of apoptosis after 12-lipoxygenase inhibition in prostate cancer cells. Cancer Res. 62: 2721-2727, 2002.

Pinkus, R., Weiner, L. M., and Daniel, V. Role of oxidants and antioxidants in the induction of AP-1, NF-kappaB, and glutathione S-transferase gene expression. J. Biol. Chem. 271: 13422– 13429, 1996.

Prigge, S. T., Boyington, J. C., Gaffney, B. J., and Amzel, L. M. Structure conservation in lipoxygenases: structural analysis of soybean lipoxygenase-1 and modeling of human lipoxygenases. Protein Struct. Funct. Genet. 24: 275–291, 1996.

Profita, A., Sala, A., Riccobono, L., Pace, E., Paterno, A., and Zarini, S., et al., 15(S)-HETE modulates LTB(4) production in neutrophil chemotaxis in chronic bronchitis. Am. J. Physiol. Cell Physiol. 279: 1249–1258, 2000.

Profita, M., Vignola, A. M., Sala, A., Mirabella, A., Siena, L., and Pace, E., *et al.* Interleukin-4 enhances 15-lipoxygenase activity and incorporation of 5(S)-HETE into cellular phospholipids in cultured pulmonary epithelial cells. Am. J. Respir. Cell Mol. Biol. 20: 61–68, 1999.

Radmark, O. Arachidonate 5-lipoxygenase. Prostaglandins & other Lipid Mediators. 68–69: 211–234, 2002.

Ragab, A., Durand, J., Bitsch, C., Chap, H., and Rigaud, M. The lipoxygenase pathway of arachidonic acid metabolism in reproductive tissues of the firebrat, *Thermobia domestica* (Thysanura). Insect Biochem. 21: 321–326, 1991.

Rao, C. V., Rivenson, A., Simi, B., and Reddy, B. S. Chemoprevention of colon carcinogenesis by dietary curcumin, a naturally occurring plant phenolic compound. Cancer Res. 55: 259–266, 1995.

Rapoport, S, M., Schewe, T., Wiesner, R., Halangk, W., Ludwig, P., Janicke-Höhne M., et. al.,. The lipoxygenase of reticulocytes. Purification, characterization and biological dynamics of the lipoxygenase; its identity with the respiratory inhibitors of the reticulocyte. Eur. J. Biochem. 96: 545–561, 1979.

Rapoport, S. M., Schewe, T., Thiele, B., and Dubiel, W. The role of lipoxygenase and ATP-dependent proteolysis in the maturation of the reticulocyte. Prog. Clin. Biol. Res . 102: 47–58, 1982.

Rapoport, S., Hartel, B., and Hausdorf, G. Methionine sulfoxide formation: the cause of self-inactivation of reticulocyte. Eur. J. Biochem. 139: 573–576, 1984.

Reddanna, P., Sandeep Prabhu, K., Whelan, J., and Channa Reddy, C. Carboxypeptidase A-catalyzed direct conversion of leukotriene C_4 to Leukotriene F_4. Arch. Biochem. Biophys. 413: 158-163, 2003.

Reddy, M. C., Subhashini, J., Mahipal, S. V., Bhat, V. B., Srinivas Reddy, P., Kiranmai, G., Madyastha, K. M., Reddanna, P. C-Phycocyanin, a selective cyclooxygenase-2 inhibitor, induces apoptosis in lipopolysaccharide-stimulated RAW 264.7 macrophages. Biochem. Biophys. Res. Commun. 304: 385-92, 2003.

Reddy, R., Reddanna, P., Reddy, C. C., and Curtis, W. R. 11-hydroperoxyeicosatetraenoic acid is the major dioxygenation product of lipoxygenase isolated from hairy root cultures of Solanum tuberosum. Biochem . Biophys. Res. Commun. 189: 1349-1352, 1992.

Reed, D. J. Glutathione: toxicological implications. Annu. Rev. Pharmacol. Toxicol. 30: 603-31, 1990.

Rickert, K. W., and Klinman, J. P. Nature of hydrogen transfer in soybean lipoxygenase 1: separation of primary and secondary isotope effects. Bochemistry 38:12218-28, 1999.

Sah, N. K., Taneja, T. K., Pathak, N., Begum, R., Athar, M. and Hasnain, S. E. The baculovirus anti-apoptotic p35 gene also functions via an oxidant-dependent pathway . Proc. Natl. Acad. Sci. U. S. A. 96: 4838–4843, 1999.

Sailesh, S., Kumar, Y. V., Prasad, M., and Reddanna P. Sheep uterus dual lipoxygenase in the synthesis of 14,15-leukotrienes. Arch. Biochem. Biophys. 315: 362-368, 1994.

Sakahira, H., Enari, M., and Nagata, S. Cleavage of CAD inhibitor in CAD activation and DNA degradation during apoptosis. Nature 391: 96– 99, 1998.

Salari, H., and Schellenberg, R. R. Stimulation of human airway epithelial cells by platelet activating factor (PAF) and arachidonic acid produces 15-hydroxyeicosatetraenoic acid (15-HETE) capable of contracting bronchial smooth muscle cells. Pulm. Pharmacol. 4:1–7, 1991.

Saleh, A., Srinivasula, S. M., Acharya, S., Fishel, R. and Alnemri, E. S. Cytochrome *C* and dATP-mediated oligomerization of Apaf-1 is a prerequisite for procaspase-9 activation. J. Biol. Chem. 274: 17941– 17945, 1999.

Sambrook, J., Frotsch, C. F., and Maniatis, T. Molecular cloning. Plain view: Coldspring Harbour, 1989.

Samuelsson B. From studies of biochemical mechanism to novel biological mediators: prostaglandin endoperoxides, thromboxanes, and leukotrienes. Biosci. Rep. 3: 791-813, 1983.

Sandstrom, P. A., Pardi, D., Tebbey, P. W., Dudek, R. W., Terrian, D. M., Folks, T. M., and Buttke, T. M. Lipid hydroperoxide-induced apoptosis: lack of inhibition by Bcl-2 over-expression. FEBS Lett. 365: 66–70, 1995.

Schewe, T., Rapoport, S. M., and Kuhn, H. Enzymology and physiology of reticulocyte lipoxygenase. Comparison with other lipoxygenases. Adv. Enzymol. 58: 191–271, 1986.

Schwenk, U., Morita, E., and Schroder, J. M. Identification of 5-oxo-15-hydroxy-6,8,11,13-eicosatetraenoic acid as a novel and potent human eosinophil chemotactic eicosanoid . J. Biol. Chem. 267: 12482–12488, 1992.

Setty, B. N., Dubowy, R. L. and Stuart, M. J. Endothelial cell proliferation may be mediated via the production of endogenous lipoxygenase metabolites. Biochem. Biophys. Res. Commun. 144: 345–351, 1987.

Shappell, S. B., Boeglin, W. E., Olson, S. J., Kasper, S., and Brash, A.R. 15-Lipoxygenase-2 (15-LOX-2) Is Expressed in Benign Prostatic Epithelium and Reduced in Prostate Adenocarcinoma. Am. J. Path. 155, 235-245, 1999.

Shappell, S. B., Gupta, R. A., Manning, S., Whitehead, R., Boeglin, W. E., Schneider, C., Case, T., Price, J., Jack, G. S., Wheeler, T. M., Matusik, R. J., Brash, A. R., and Dubois, R. N. 15S-Hydroxyeicosatetraenoic acid activates peroxisome proliferator-activated receptor gamma and inhibits proliferation in PC3 prostate carcinoma cells. Cancer Res. 61: 497-503, 2001.

Shen, J., Herderick, E., Cornhill, J. F., Zsigmond, E., Kim, H. S., Kühn, H., et al.,. Macrophage-mediated 15-lipoxygenase expression protects against atherosclerosis. J. Clin. Invest. 98: 2201–2208, 1996.

Shureiqi, I., and Lippman, S. M. Lipoxygenase modulation to reverse carcinogenesis. Cancer Res. 61: 6307-12. 2001.

Shureiqi, I., Chen, D., Lee, J. J., Yang, P., Newman, R. A., Brenner, D. E., Lotan, R., Fischer, S. M., and Lippman, S. M. 15-LOX-1: a novel molecular target of nonsteroidal anti-inflammatory drug-induced apoptosis in colorectal cancer cells. J. Natl. Cancer Inst. (Bethesda). 92: 1136–1142, 2000 a.

Shureiqi, I., Chen, D., Lotan, R., Yang, P., Newman, R. A., Fischer, S. M,. and Lippman, S. M. 15-Lipoxygenase-1 mediates nonsteroidal anti-inflammatory druginduced apoptosis independently of cyclooxygenase-2 in colon cancer cells . Cancer Res. 60: 6846–6850, 2000 b.

Shureiqi, I., Wojno, K. J., Poore, J. A., Reddy, R. G., Moussalli, M. J., Spindler, S. A., Greenson, J. K., Normolle, D., Hasan, A. A. K., Lawrence, T. S., and Brenner, D. E. Decreased 13-S-hydroxyoctadecadienoic acid levels

and 15-lipoxygenase-1 expression in human colon cancers. Carcinogenesis (Lond.) 20: 1985–1995, 1999.

Shureiqi, I., Xu, X., Chen, D., Lotan, R., Morris, J. S., Fischer, S. M., and Lippman, S. M. Nonsteroidal anti-inflammatory drugs induce apoptosis in esophageal cancer cells by restoring 15-lipoxygenase-1 expression. Cancer Res. 61: 4879–4884, 2001.

Sigal E., and Nadel, S. The airway epithelium and aracchidonic acid 15-lipoxygenase Am. Rev. Respir. Dis. 143: 71–74, 1991.

Sigal, E., Grunberger, D., Highland, E., Gross, C., Dixon, R., and Craik, C. Expression of cloned human reticulocyte 15-lipoxygenase and immunological evidence that 15-lipoxygenases of different cell types are related. J. Biol. Chem. 265: 5113–5120, 1990.

Singh, J., Hamid, R., and Reddy, B. S. Dietary fat and colon cancer: modulating effect of types and amount of dietary fat on ras-p21 function during promotion and progression stages of colon cancer. Cancer Res. 57: 253–258, 1997.

Skrzypczak-Jankun, E., Amzel, L. M., Kroa, B. A., and Funk, M. O. J. Structure of soybean lipoxygenase L3 and a comparison with its L1 isoenzyme. Proteins. 29: 15-31. 1997.

Smith, R. J., Justen, J. M., Nidy, E. G., Sam, L. M., and Bleasdale, J. E. Transmembrane signaling in human polymorphonuclear neutrophils: 15(S)-hydroxy- (5Z, 8Z, 11Z, 13E)-eicosatetraenoic acid modulates receptor agonist-triggered cell activation . Proc .Natl. Acad .Sci. U.S.A. 90: 7270–7274, 1993.

Smith, W. L., Garavito, R. M., and DeWitt, D. L. Prostaglandin endoperoxide H synthases (cyclooxygenases)-1 and –2. J. Biol. Chem. 271(52): 33157-33160, 1996.

Stamler, J. S., Singel, D. J., and Loscalzo, J. Biochemistry of nitric oxide and its redox-activated forms . Science 258: 1898-1902, 1992.

Steele, V. E., Holmes, C. A., Hawk, E. T., Kopelovich, L., Lubet, R. A., Crowell, J. A., Sigman, C. C., and Kelloff, G. J. Lipoxygenase inhibitors as potential cancer chemopreventives. Cancer Epidemiol. Biomarkers Prev. 8: 467–483, 1999.

Stridh, H., Kimland, M., Jones, D.P., Orrenius, S., and Hampton, M.B. Cytochrome c release and caspase activation in hydrogen peroxide- and tributyltin-induced apoptosis . FEBS Lett. 429: 351– 355, 1998.

Stuehr, D. J., Fasehun, O. A., Kwon, N. S., Gross, S. S., Gonzalez, J. A., Levi, R., and Nathan, C. F. Inhibition of macrophage and endothelial cell nitric oxide synthase by diphenylene iodonium and its analogs. FASEB J. 5: 98-103, 1991.

Sun, D., Elsea, S. H., Patel, P. I., and Funk, C. D. Cloning of a Human "Epidermal-Type" 12-Lipoxygenase-Related Gene and Chromosomal Localization to 17p13". Cytogenet. Cell Genet.81: 79-82, 1998.

Supinski G, Nethery D, Stofan D, DiMarco A. Extracellular calcium modulates generation of reactive oxygen species by the contracting diaphragm. J Appl Physiol. 87: 2177-85, 1999.

Takata, S., Matsubara, M., Allen, P. G., Janmey, P. A., Serhan, C. N., and Brady, H. R. Remodelling of neutrophil phospholipids with 15(S)-hydroxyeicosatetraenoic acid inhibits leukotriene B4-induced neutrophil migration across endothelium . J. Clin. Invest. 93: 499–508, 1994 a.

Takata, S., Papayianni, A., Matsubara, M., Jimenez, W., Pronovost, P. H., and Brady, H. R. 15-Hydroxyeicosatetraenoic acid inhibits neutrophil migration across cytokine-activated endothelium. Am. J .Pathol .145: 541–549, 1994 b.

Tammariello, S. P., Quinn, M. T., and Estus S. NADPH oxidase contributes directly to oxidative stress and apoptosis in nerve growth factor-deprived sympathetic neurons . J Neurosci. 20: RC53, 2000.

Tan, S., Sagara, Y., Liu, Y., Maher, P., and Schubert, D. The regulation of reactive oxygen species production during programmed cell death. J. Cell Biol. 141: 1423–1432, 1998.

Tang, D. G., Chen, Y. Q., and Honn, K. V. Arachidonate lipoxygenases as essential regulators of cell survival and apoptosis . Proc. Natl. Acad. Sci. U. S. A. 93: 5241–5246, 1996.

Tang, K., and Honn, K. V. 12(S)-HETE in cancer metastasis. Adv. Exp. Med. Biol. 447: 181–191, 1999.

Tang, S., Bhatia, B., Maldonado, C. J., Yang, P., Newman, R. A., Liu, J., Chandra, D., Traag, J., Klein, R. D., Fischer, S. M., Chopra, D., Shen, J., Zhau, H. E., Chung, L. W., and Tang D. G. Evidence that arachidonate 15-lipoxygenase 2 is a negative cell cycle regulator in normal prostate epithelial cells. Biol. Chem. 277: 16189-16201, 2002.

Thannickal, V. J., and Fanburg, B. L. Reactive oxygen species in cell signaling Am. J. Physiol. Lung Cell Mol. Physiol, 279: L-1005- L-1028, 2000.

Thiele, B. J., Andree, H., Höhne, M., and Rapoport, S. M. Lipoxygenase mRNA in rabbit reticulocytes. Its isolation, characterization and translational depression . Eur. J. Biochem. 129: 133–141, 1982.

Tietze, F. Enzymatic method for quantitative determination of nanogram amounts of total and oxidized glutathione: application to mammalian blood and other tissues. Anal. Biochem. 27: 502-522, 1969.

Timar, J., Chen, Y. Q., Liu, B., Bazaz, R., Taylor, J. D., and Honn, K. V. The lipoxygenase metabolite 12(S)-HETE promotes α IIb β 3 integrin-mediated tumor cell spreading on fibronectin. Int. J. Cancer. 52: 594–603, 1992.

Timar, J., Raso, E., Dome, B., Li, L., Grignon, D., Nie, D., Honn, K. V., and Hagmann, W. Expression, subcellular localization and putative function of platelettype 12-lipoxygenase in human prostate cancer cell lines of different metastatic potential. Int. J. Cancer. 87: 37–43, 2000.

Tome, M. E., Baker, A. F., Powis, G., Payne, C. M., and Briehl, M. M. Catalase-overexpressing thymocytes are resistant to glucocorticoid-induced apoptosis and exhibit increased net tumor growth. Cancer Res. 61: 2766-73, 2001.

Uberti, D., Yavin, E., Gil, S., Ayasola, K. R., Goldfinger, N., and Rotter, V. Hydrogen peroxide induces nuclear translocation of p53 and apoptosis in cells of oligodendroglia origin . Mol. Brain Res. 65: 167–175, 1999.

Van den Dobbelsteen, D. J., Nobel, C. S. I., Schlegel, J., Cotgreave, I.A., Orrenius, S., and Slater, A.F. Rapid and specific efflux of reduced glutathione during apoptosis induced by anti-Fas/APO-1 antibody. J. Biol. Chem. 271: 15420–15427, 1996.

Vanderhoek, J. Y., Bryant, R. W., and Bailey, J. M. Inhibition of leukotriene biosynthesis by the leukocyte product 15-hydroxy-5,8,11,13-eicosatetraenoic acid . J. Biol. Chem. 255: 10064–10066, 1980 a.

Vanderhoek, J. Y., Bryant, R. W., and Bailey, J. M. 15-hydroxy-5,8,11,13-eicosatetraenoic acid: a potent and selective inhibitor of platelet lipoxygenase. J. Biol. Chem. 255: 5996–5998, 1980 b.

Vanderhoek, J. Y., Karmin, M. T., and Ekborg, S. L. Endogenous hydroxyeicosatetraenoic acids stimulate the human polymorphonuclear leukocyte 15-lipoxygenase pathway. J. Biol. Chem. 260: 15482–15487, 1985.

Watanabe, K., Ishikawa, C., Ohtsuka, I., Kamata, M., Tomita, M., Yazawa, K., and Muramatsu, H. Lipid and fatty acid compositions of a novel docosahexaenoic acid-producing marine bacterium. Lipids. 32: 975-978, 1997.

Wiesner, R., Rathmann, J., Holzhütter, H. G., Stöber, R., Mäder, K., Nolting, H., *et al*. Nitric oxide oxidises ferrous mammalian lipoxygenases to a pre-activated ferric species . FEBS Lett. 389: 229–232, 1996.

Wong, B. C., Wang, W. P., Cho, C. H., Fan, X. M., Lin, M. C., Kung, H. F., and Lam, S.K. 12-Lipoxygenase inhibition induced apoptosis in human gastric cancer cells .Carcinogenesis 22: 1349-1354, 2001.

Wyllie, A. H., Kerr, J. F. and Currie, A. R. Cell death: the significance of apoptosis. Int. Rev. Cytol. 68: 251– 306, 1980.

Yamamoto, S. Mammalian lipoxygenases: molecular structures and functions Biochim. Biophys. Acta. 1128: 117-131, 1992.

Yamamoto, S., Suzuki, H. and Ueda, N. Arachidonate 12-lipoxygenases Prog. Lipid. Res. 36: 23-41, 1997.

Yang, X., Stennicke, H. R., Wang, B., Green, D. R., Janicke, R. U., Srinivasan, A., Seth, P., Salvesen, G. S. and Froelich, C. J. Granzyme B mimics apical caspases: description of a unified pathway for trans-activation of executioner caspase-3 and –7. J. Biol. Chem. 273: 34278– 34283. 1998.

Yla-Herttuala, S., Rosenfeld, M. E., Parthasarathy, S., Glass, C. K., Sigal, E., Witztum, J. T., *et al*. Colocalization of 15-lipoxygenase mRNA and protein with epitopes of oxidized low density lipoprotein in macrophage-rich areas of atherosclerotic lesions . Proc. Natl. Acad. Sci. U. S.A 87: 6959–6963, 1990.

Yoshimoto, T., and Takahashi, Y. Arachidonate 12-lipoxygenases, Prostaglandins Other Lipid Mediat. 68-69: 245-262, 2002.

Yu, K., Bayona, W., Kallen, C. B., Harding, H. P., Ravera, C. P., and McMahon, G. Differential activation of peroxisome proliferator-activated receptors by eicosanoids . J. Biol. Chem 270: 23975-23983, 1995.

Zamzami, N., Marchetti, P., Castedo, M., Decaudin, D., Macho, A., Hirsch, T., Susin, S.A., Petit, P.X., Mignotte, B., and Kroemer, G. Sequential reduction of mitochondrial transmembrane potential and generation of reactive oxygen species in early programmed cell death. J. Exp. Med. 182: 367–377, 1995.

Zeldin, D. C. Epoxygenase pathways of arachidonic acid metabolism. J. Biol. Chem. 276: 36059-36062, 2001.

Zhang, C., Yang, J., Jacobs, J. D., Jennings, L. K. Interaction of myeloperoxidase with vascular NAD(P)H oxidase-derived reactive oxygen species in vasculature: implications for vascular diseases. Am. J. Physiol. Heart . Circ. Physiol. 285: H2563-72, 2003.

Zijlstra, F. J., van Dijk, A. P., Garrelds, I. M., Ouwendijk, R. J. and Wilson, J. H. Species differences in the pattern of eicosanoids produced by inflamed and non-inflamed tissue (1991). Agents Actions C73–C75 [special issue].

Zimmerman, D. C., and Vick, B. A., Lipoxygenase in Chlorella pyrenoidosa. Lipids 8: 264-266, 1973.

Zou, H., Li, Y., Liu, X., Wang, X., An APAF-1.cytochrome c multimeric complex is a functional apoptosome that activates procaspase-9. J. Biol. Chem. 274: 11549– 11556, 1999.